Calhoun
Institutional Archive of the Naval Postgraduate School

Calhoun: The NPS Institutional Archive

Theses and Dissertations | Thesis Collection

1990-09

Radar target classification by natural resonances : system analysis

Reddy, Peter C.

Monterey California. Naval Postgraduate School

http://hdl.handle.net/10945/34927

DUDLEY KNOX LIBRARY

http://www.nps.edu/library

Calhoun is a project of the Dudley Knox Library at NPS, furthering the precepts and goals of open government and government transparency. All information contained herein has been approved for release by the NPS Public Affairs Officer.

Dudley Knox Library / Naval Postgraduate School
411 Dyer Road / 1 University Circle
Monterey, California USA 93943

NAVAL POSTGRADUATE SCHOOL
Monterey, California

AD-A241 170

DTIC
ELECTE
SEP 27 1991
S D

THESIS

RADAR TARGET CLASSIFICATION
BY NATURAL RESONANCES:
SYSTEM ANALYSIS

by

Peter C. Reddy

September 1990

Thesis Advisor: Michael A. Morgan

Approved for public release; distribution is unlimited.

91-11623

Unclassified

security classification of this page

REPORT DOCUMENTATION PAGE

1a Report Security Classification Unclassified			1b Restrictive Markings
2a Security Classification Authority			3 Distribution/Availability of Report: Approved for public release; distribution is unlimited.
2b Declassification Downgrading Schedule			
4 Performing Organization Report Number(s)			5 Monitoring Organization Report Number(s)
6a Name of Performing Organization: Naval Postgraduate School	6b Office Symbol (*if applicable*) 3A		7a Name of Monitoring Organization: Naval Postgraduate School
6c Address (*city, state, and ZIP code*): Monterey, CA 93943-5000			7b Address (*city, state, and ZIP code*): Monterey, CA 93943-5000
8a Name of Funding Sponsoring Organization	8b Office Symbol (*if applicable*)		9 Procurement Instrument Identification Number
8c Address (*city, state, and ZIP code*)			10 Source of Funding Numbers: Program-Element-No / Project No / Task No / Work Unit Accession No

11 Title (*include security classification*) RADAR TARGET CLASSIFICATION BY NATURAL RESONANCES: SYSTEM ANALYSIS

12 Personal Author(s) Peter C. Reddy

13a Type of Report	13b Time Covered From To	14 Date of Report (*year, month, day*)	15 Page Count
Master's Thesis		September 1990	148

16 Supplementary Notation The views expressed in this thesis are those of the author and do not reflect the official policy or position of the Department of Defense or the U.S. Government.

17 Cosati Codes			18 Subject Terms (*continue on reverse if necessary and identify by block number*)
Field	Group	Subgroup	Natural Resonances, Noncooperative Target Recognition, K-Pulse, Pole Extraction, Cadzow-Solomon

19 Abstract (*continue on reverse if necessary and identify by block number*) This thesis examines the system implementation considerations of a resonance-based radar target classification system. The basis of the system is the aspect and excitation independent property of electromagnetic scattering from a conducting body. Such a system consists of two components. pole extraction and annihilation filtering. The algorithms investigated here for these purposes are the Cadzow-Solomon pole extraction algorithm and the K-Pulse annihilation filter. Additionally, an aspect-dependent annihilation filter based on an inverse ARMA model is introduced. The procedures are applied to noise polluted synthetic data, as well as scattering data collected for a thin-wire and silver coated 1/72 scale model aircraft.

20 Distribution/Availability of Abstract	21 Abstract Security Classification	
☒ unclassified unlimited ☐ same as report ☐ DTIC users	Unclassified	
22a Name of Responsible Individual: M. A. Morgan	22b Telephone (*include Area code*): (408) 646-2677	22c Office Symbol: EC/Mw

DD FORM 1473,84 MAR

83 APR edition may be used until exhausted
All other editions are obsolete

security classification of this page

Unclassified

Approved for public release; distribution is unlimited.

Radar Target Classification by Natural Resonances: System Analysis

by

Peter C. Reddy
Captain, United States Marine Corps
B.S.A.E., University of Virginia, 1984

Submitted in partial fulfillment
of the requirements for the degree of

MASTER OF SCIENCE IN SYSTEMS ENGINEERING
(ELECTRONIC WARFARE)

from the

NAVAL POSTGRADUATE SCHOOL
September 1990

Author: [redacted]
Peter C. Reddy

Approved by: [redacted]
Michael A. Morgan, Thesis Advisor

[redacted]
Jeffrey B. Knorr, Second Reader

[redacted]
Joseph Sternberg, Chairman,
Electronic Warfare Academic Group

ABSTRACT

This thesis examines the system implementation considerations of a resonance-based radar target classification system. The basis of the system is the aspect and excitation independent property of electromagnetic scattering from a conducting body. Such a system consists of two components: pole extraction and annihilation filtering. The algorithms investigated here for these purposes are the Cadzow-Solomon pole extraction algorithm and the K-Pulse annihilation filter. Additionally, an aspect-dependent annihilation filter based on an inverse ARMA model is introduced. The procedures are applied to noise polluted synthetic data, as well as scattering data collected for a thin-wire and silver coated 1/72 scale model aircraft.

Accession For	
NTIS GRA&I	☑
DTIC TAB	☐
Unannounced	☐
Justification	
By	
Distribution/	
Availability Codes	
Dist	Avail and/or Special
A-1	

TABLE OF CONTENTS

LIST OF TABLES

LIST OF FIGURES

I. INTRODUCTION

Modern antiair warfare has, with the advent of radar in World War II, become a process of detecting aircraft and identifying them as friend or foe at sufficient ranges to allow engagement with appropriate weapon systems. Radar development has historically emphasized the first element of this process: detection. As modern air warfare has become more complex, dynamic, and lethal, identification has become as critical as detection.

In the past, identification has been facilitated by active measures on the part of friendly aircraft to distinguish them from enemy, i.e. IFF transponders, specific flight routes, etc. All these are subject to exploitation by an adversary. This has given rise to development of non-cooperative target recognition (NCTR), the ability to identify an enemy aircraft despite its efforts to deceive.

One approach to NCTR, as discussed in this thesis, is identification based on the natural complex resonances of the aircraft as a scatterer of incident electromagnetic (radar) energy. In 1971 Baum showed that an incident electromagnetic wave creates a current response on a body with certain complex natural resonances dependent on its physical configuration [Ref. 1]. Moffat and Mains proposed that a target scatters electromagnetic energy with resonances that are independent of incident polarization or angle [Ref. 2]. Morgan confirmed this through a rigorous theoretical description of induced currents and the

resultant scattered field [Ref. 3]. The problem, then, is to determine these complex poles for a target of interest and subsequently use them to identify this target.

The first step in using complex natural resonances for target identification is extraction of these poles from scattered responses of actual targets (either modeled or full size) [Ref. 4]. These poles are then used to create annihilation filters for each potentially observed target [Ref. 5]. A given filter will, in principle, produce a near null late-time response to its matched target's scattered signal, independent of aspect or polarization.

The objective of this thesis is to examine these processes in order to define the overall system characteristics and operational considerations of a radar target identification system based target natural resonsnces. This analysis will use the application of signal processing algorithms to both synthetic and actual electromagnetic scattering data. This thesis has been conducted in conjunction with research in pole extraction by Murphy [Ref. 6], whereby the data generated in that work was incorporated in the filters discussed in this effort.

A. BACKGROUND

The ability to extract poles and use them to identify a target is dependent on the nature of electromagnetic scattering from a conducting body. Consider a generalized electromagnetic pulse with electric and magnetic field components $E^i(r,t)$ and $H^i(r,t)$ respectively, travelling in a direction $\hat{p}$ and incident upon a finite-sized,

perfectly conducting body in free space. Currents are induced on the body which are described by the magnetic field integral equation [Ref. 7],

$$J(r,t) = 2\hat{n}\times H^i(r,t) + \iint_{S_{PV}} \tilde{K}(r,r',t)\cdot J(r',t-\frac{|r-r'|}{c})dS \qquad (1)$$

where $\hat{n}$ is the outward unit normal vector, J is the surface current density, and $\tilde{K}$ is a dyadic Green's function kernel. Here the surface integral is a principle-value type, excluding the point $r = r'$. The cross product term represents the physical optics contribution to the induced currents and the surface integral represents the feedback of currents on each point on the object due to the currents at all other points. This feedback mechanism forms the physical basis for natural resonances.

After the incident pulse leaves the target body, H^i in Equation (1) goes to zero; the source-free current modes that remain "ring" at the natural resonance frequencies of the object. These currents are described by the expression $J_n(r)\exp(s_n t)$, where $s_n = \sigma_n + j\omega_n$, are the frequencies which are dependent only on the physical properties of the scatterer. These complex frequencies are described in the Laplace domain by their damping constant, σ, in Nepers/sec, and their frequency, ω, in radians/sec. An infinite number of these resonant modes are inherent in any candidate scattering object, but only those in the bandwidth of the incident pulse are significantly excited. [Ref. 7]

The induced currents on the scattering body, J, give rise to a far-field distribution in the backscatter direction, $-\hat{p}$, (the direction of interest for monostatic radar applications) described by

$$H^S(-r\hat{p},t) = \frac{1}{4\pi cr}\frac{\partial}{\partial t}\iint_S \hat{p}\times J(r',t-\frac{|r-r'|}{c})dS'. \qquad (2)$$

This equation is applicable during the entire time the incident pulse is traversing the target in the direction $\hat{p}$ as well as after it has gone beyond it. When the specific current distribution described in Equation (1) is substituted here, the result is

$$H^S(-r\hat{p},t) = u(t-r/c)\left\{ H_{po}(-r\hat{p},t) + \sum_{\substack{n=-\infty \\ n\neq 0}}^{\infty} H_n(-r\hat{p},t)\exp(s_n t) \right\} \qquad (3)$$

where H_{po} is a physical optics term dependent on the incident direction, $\hat{p}$, relative to the object shape, and the summation term is due to the source-free currents behind the advancing wavefront. The field due to these currents resonates at the same frequencies as the currents themselves. However, during the time the pulse still resides somewhere on the target, the coefficients H_n are varying. After the pulse leaves, the aspect dependent physical optics term vanishes and the coefficients of the scattered resonant frequency modes become constant. This instant defines the transition from "early-time" to "late-time" in the scattered field. For backscattering this transition occurs after a time given by $T_o = 2D/c + \tau$, as measured from when

the pulse first impinges on the target, where D is the length of the object in the propagation direction, $\hat{p}$; c, the speed of light; and τ, the incident pulse width. [Ref. 7]

B. PROBLEM

Application of these characteristics to target identification involves two separate steps: pole extraction and annihilation filtering. The transfer function of an electromagnetic target contains a complicated set of poles that can be analytically predicted only for the simplest objects, e.g., a thin-wire or a sphere [Ref. 8]. Therefore, it will be necessary to extract the poles from complex targets, such as aircraft, through signal processing of their scattered response [Ref.4]. A number of algorithms have served as candidates for this process [Ref. 4], including the Kumaresan-Tufts and Cadzow-Solomon algorithms compared by Larison in [Ref. 9]. These will be discussed further in Chapter III.

After the poles are determined for the targets of interest, they will be incorporated in a bank of annihilation filters; each filter corresponding to a target. Scattering responses from unknown targets (radar returns in actual application) are passed to all the filters. The annihilation filter with the least output should correlate the unknown target to a previously cataloged response, thus identifying that target. This is the basis of the Resonance Annihilation Filter (RAF) concept discussed in [Ref. 7] and [Ref. 10]. Further analysis of this process and its implications for actual implementation are discussed in Chapter IV.

C. HISTORY

As stated, the initial work in the area of natural resonance response was derived from Baum's investigation of currents generated as a result of electromagnetic pulse (EMP) [Ref. 1]. Tesche developed the concept further into the specifics of the Singularity Expansion Method (SEM) applied to generating the time response of a thin wire scatterer analytically by examining its poles and residues [Ref. 11]. Morgan points out in [Ref. 3] and [Ref. 7] that the SEM description of the scattered signal is applicable only in late-time, the time after the incident pulse leaves the object. As a result of this limitation, earlier schemes for pole extraction based on Prony's method [Ref. 12] were limited by noise and clutter [Ref. 13].

Since that time, effort has been directed by many researchers into improved pole extraction algorithms. Chong incorporated the early-time in using a direct non-linear least-squares minimization [Ref. 14], but this approach is computationally intensive and requires much *a priori* knowledge of the signal [Ref. 4]. The Kumaresan-Tufts method of pole extraction is limited in applicability to the late-time only, but relieves some of the burden of *a priori* knowledge of the nature of the scattered response [Ref 15] and improves the noise handling capability of Prony's method. The Cadzow-Solo... n technique, a different extension of Prony's method, makes use of both the early and late-time, allowing it to use as much of the available energy as desired in the return signal. This algorithm, introduced in [Ref. 16] and applied to pole extraction in [Ref. 4], [Ref. 9] and [Ref. 6], does require input of the transmitted signal along with the return

scattering signal, but holds the most promise of the considered extraction methods in the presence of noise.

The annihilation filtering concept, as described above, has been attempted primarily with two basic algorithms. The K-Pulse algorithm, based on a difference equation representation of the filter, has been developed by Morgan [Ref. 7] and Dunavin [Ref. 17] from the original work of Kennaugh [Ref. 18]. The E-Pulse technique, developed by Simon [Ref. 19], uses integral operators to cancel the resonances in late-time. Simon compared these algorithms in [Ref. 10] and found similar results. This thesis will further investigate the K-Pulse annihilation filter, and will extend it to a recursive version which works on early-time energy as well.

II. EXPERIMENTAL SIGNALS

Both synthetic and actual signals were used to analyze the performance of pole extraction and annihilation filtering. Two types of synthetic signals were used. First, synthetic signals with predetermined complex poles were used to validate extraction and annihilation software and to gain insight into the mechanisms by which these algorithms worked. Secondly, poles were extracted from synthetically generated thin-wire scattering data generated by Morgan's thin-wire integral equation program [Ref. 20], and used in annihilation filters. For this set of data, the poles were not known in advance. After the software was tested on synthetic data, it was applied to actual scattering data, gathered by Walsh [Ref. 21]. This data was measured for a thin wire and several scale model aircraft using the NPS Transient Electromagnetic Scattering Laboratory (TESL). In the development of the first set of synthetic signals, as many parameters as possible were selected to match those anticipated in the TESL measured data.

A. ARMA SYNTHETIC SIGNALS

1. Scatterer Model

As discussed in the previous chapter, the scattered field consists of a physical optics term due to the driving incident wave and a feedback portion representing the complex natural resonances. These characteristics suggest an autoregressive moving average (ARMA) or recursive structure for modeling this

signal. Such a structure was realized with a recursive difference equation signal generator,

$$y(n) = \sum_{k=1}^{k=N} a_k y(n-k) + \sum_{k=0}^{k=L} b_k x(n-k) \qquad (4)$$

where $x(n)$ is the digital version of the incident pulse, $y(n)$ is the scatterer response and a_k and b_k are coefficients determined by the complex natural resonances and initial conditions, respectively [Ref. 22:pp. 81-84]. After selection of a sampling frequency for the synthetic signals, the coefficients were determined through conversion of a simple set of s-plane poles to the complex z-plane, followed by multiplication of rational polynomial terms representing each pole pair to arrive at an overall ratio of polynomials: the z-transform version of the scatterer's transfer function. The coefficients from the numerator and denominator appear in Equation (4) as b_k and a_k, respectively. Additional inputs were a complex coefficient of the z-plane poles to allow scaling or phase differences between poles. Program listings for the coefficient generator and the recursive signal generator appear in Appendices A and B.

The poles were selected in the s-plane to coincide generally in bandwidth with those obtainable by actual scattering measurements. As such, three sets of ten pole pairs each were selected, lying at integer values between 1 - 10 GHz. The three sets represent different levels of damping (Q factor) and are related in that they all

have the same modulus when plotted as vectors in the s-plane. For each set of poles, the frequency and damping coefficient, ω_p and σ_p, are related by a damping factor k_j,

$$\frac{\sigma_p}{\omega_p} = \frac{1}{2\pi}[\ln(k_j)] \tag{5}$$

where

k_1 = 0.5 (low Q/highly damped)

k_2 = 0.7 (medium Q/moderately damped)

k_3 = 0.8 (high Q/lightly damped) [Ref. 10].

These poles are plotted in the s and z-planes respectively in Figures 1 and 2 and are listed in Tables 1, 2 and 3. The units of f_p, σ_p and ω_p are GHz, GNp/sec and GRad/sec, respectively. The resulting ARMA coefficients, a_k and b_k, are in Table 4.

TABLE 1. LOW Q SYNTHETIC POLES

	POLES		RESIDUES	
f_p	σ_p	ω_p	A_p	φ_p
1	-0.6892	6.2474	1	0
2	-1.3784	12.4948	1	0
3	-2.0676	18.7422	1	0
4	-2.7568	24.9895	1	0
5	-3.4460	31.2369	1	0
6	-4.1352	37.4843	1	0
7	-4.8244	43.7317	1	0
8	-5.5136	49.9791	1	0
9	-6.2028	56.2264	1	0
10	-6.8919	62.4738	1	0

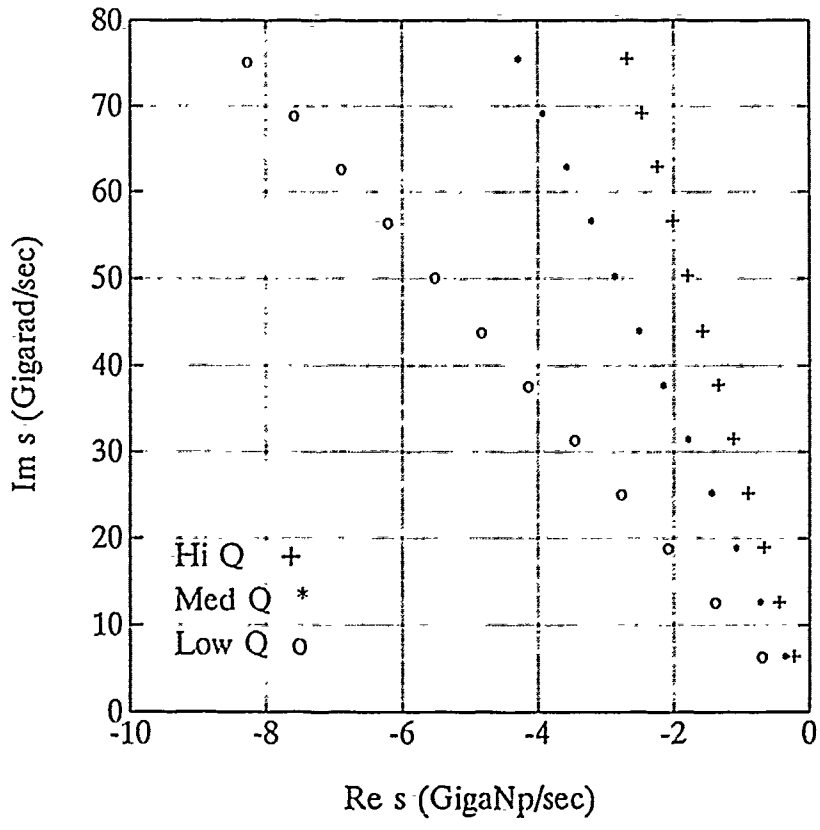

Figure 1. Synthetic poles, *s*-plane

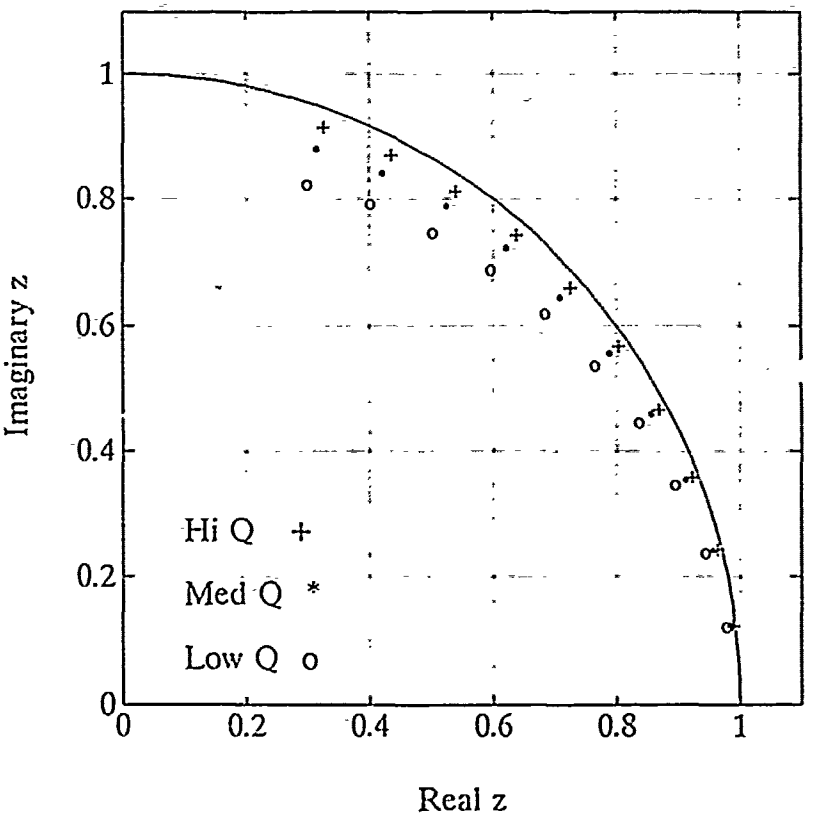

Figure 2. Synthetic poles, z-plane

TABLE 2. MEDIUM Q SYNTHETIC POLES

	POLES		RESIDUES	
f_p	σ_p	ω_p	A_p	φ_p
1	-0.3562	6.2752	1	0
2	-0.7124	12.5504	1	0
3	-1.0687	18.8256	1	0
4	-1.4249	25.1007	1	0
5	-1.7811	31.3759	1	0
6	-2.1373	37.6511	1	0
7	-2.4935	43.9263	1	0
8	-2.8498	50.2015	1	0
9	-3.2060	56.4767	1	0
10	-3.5622	62.7518	1	0

TABLE 3. HIGH Q SYNTHETIC POLES

	POLES		RESIDUES	
f_p	σ_p	ω_p	A_p	φ_p
1	-0.1625	6.2832	1	0
2	-0.3250	12.5664	1	0
3	-0.4876	18.8496	1	0
4	-0.6501	25.1327	1	0
5	-0.8126	31.4159	1	0
6	-0.9751	37.6991	1	0
7	-1.1376	43.9823	1	0
8	-1.3002	50.2655	1	0
9	-1.4626	56.5487	1	0
10	-1.6252	62.8319	1	0

The sampling frequency of 25.6 GHz, 512 samples in 20 nanoseconds, was used in the creation of the synthetic signals. This is the minimum "power-of-two"

TABLE 4. ARMA COEFFICIENTS FOR SYNTHETIC SCATTERING

	Low Q		Medium Q		High Q	
k	a_k	b_k	a_k	b_k	a_k	b_k
0	1.0	20.0	1.0	20.0	1.0	20.0
1	-3.77	-71.59	-3.54	-67.32	-3.46	-65.65
2	8.47	152.61	8.08	145.36	7.96	143.26
3	-14.27	-242.52	-14.09	-239.57	-14.14	-240.43
4	20.02	320.34	21.00	335.97	21.66	346.64
5	-24.51	-367.64	-27.61	-414.21	-29.40	-441.01
6	27.07	379.04	33.15	464.08	36.58	512.05
7	-27.40	-356.18	-36.69	-476.94	-42.03	-546.42
8	25.80	309.55	38.02	456.23	45.32	543.92
9	-22.70	-249.71	-36.96	-406.56	-45.90	-504.90
10	18.84	188.36	34.00	339.98	44.02	440.24
11	-14.72	-132.44	-29.50	-265.52	-39.85	-358.65
12	10.89	87.13	24.28	194.28	34.22	273.76
13	-7.58	-53.04	-18.80	-131.63	-27.64	-193.49
14	4.99	29.92	13.75	82.51	21.10	126.40
15	-3.04	-15.22	-9.33	-46.66	-14.89	-74.45
16	1.74	6.98	5.90	23.60	9.77	39.09
17	-0.89	-2.67	-3.33	-9.99	-5.72	-17.17
18	0.42	0.84	1.69	3.39	2.99	5.98
19	-0.15	-0.15	-0.67	-0.67	-1.21	-1.22
20	0.05	0.00	0.22	0.00	0.38	0.00

number of samples allowable in a 20 nanosecond collect time by the Nyquist requirement applied to the frequencies of interest, one to ten GHz. The requirement

to limit the sampling bandwidth as much as possible is derived from the use of the annihilation filter, discussed in Chapter IV.

2. Incident Pulse

After determination of the coefficients of the synthetic scatterer transfer function, these were used in the difference equation, Equation (4), above. The input waveform, x(n), was chosen to be a double Gaussian, in order to match that used in the actual scatterer data collection. The double Gaussian waveshape consists of a broad, slow Gaussian pulse subtracted from a narrow, rapid Gaussian pulse. The narrow pulse determines the high frequency roll-off; the broad pulse determines the low frequency roll-off. The incident pulse used here has ten percent narrow and wide pulse widths of 0.15 and 0.3 nanoseconds, respectively, and is pictured in Figure 3. The frequency domain representation is in Figure 4. The final results of the double Gaussian input to the ARMA model is shown for all three pole sets (high Q, medium Q, and low Q) in Figures 5, 6, and 7 and Figure 8 contains the spectrum of the medium Q target.

3. Noise Modeling

The synthetic signals were polluted by simulated Gaussian noise at various signal-to-noise ratio levels: 20 dB, 15 dB, 10 dB and 7 dB. The noise was introduced by a noise pollution routine, Appendix C, which uses a random number generation algorithm based on subroutines of the Fortran Scientific Library. This routine generates random numbers under a uniform distribution. The Central Limit

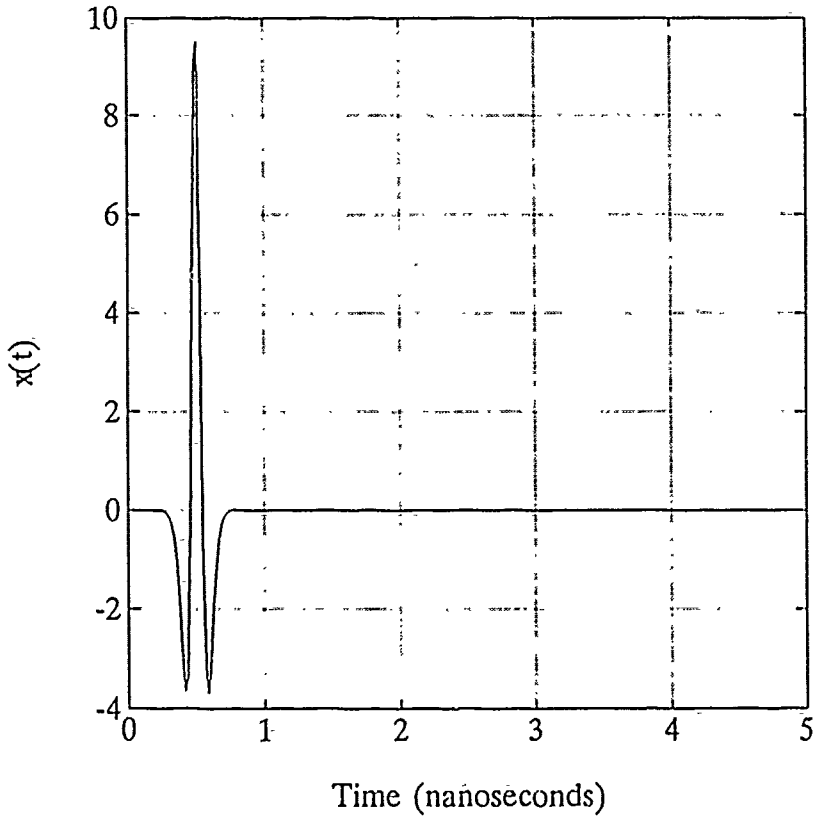

Figure 3. Incident double Gaussian pulse

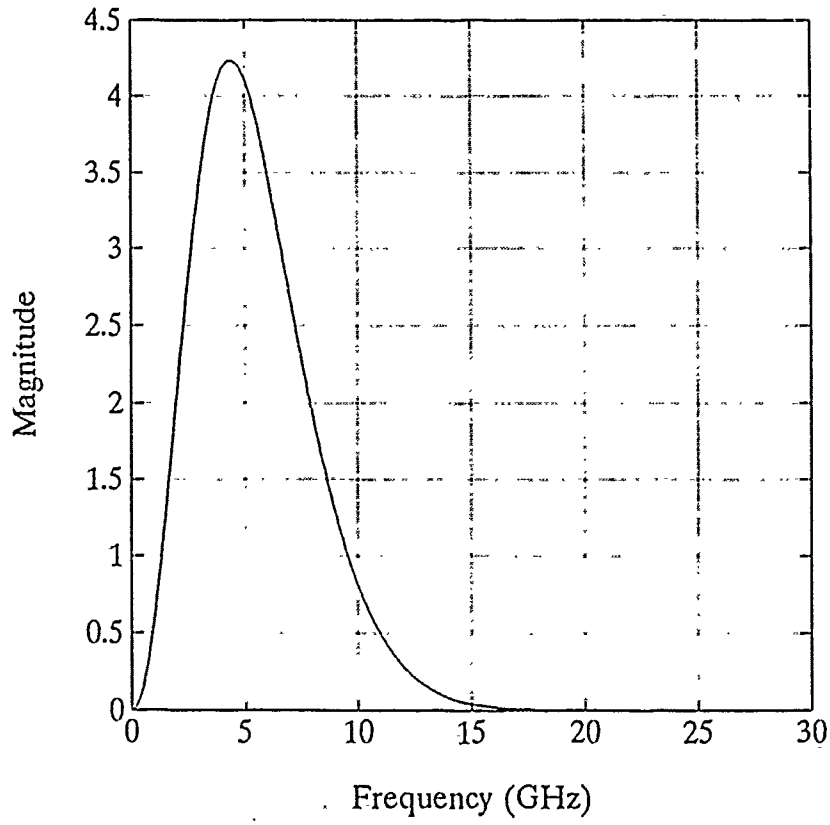

Figure 4. Frequency spectrum of double Gaussian

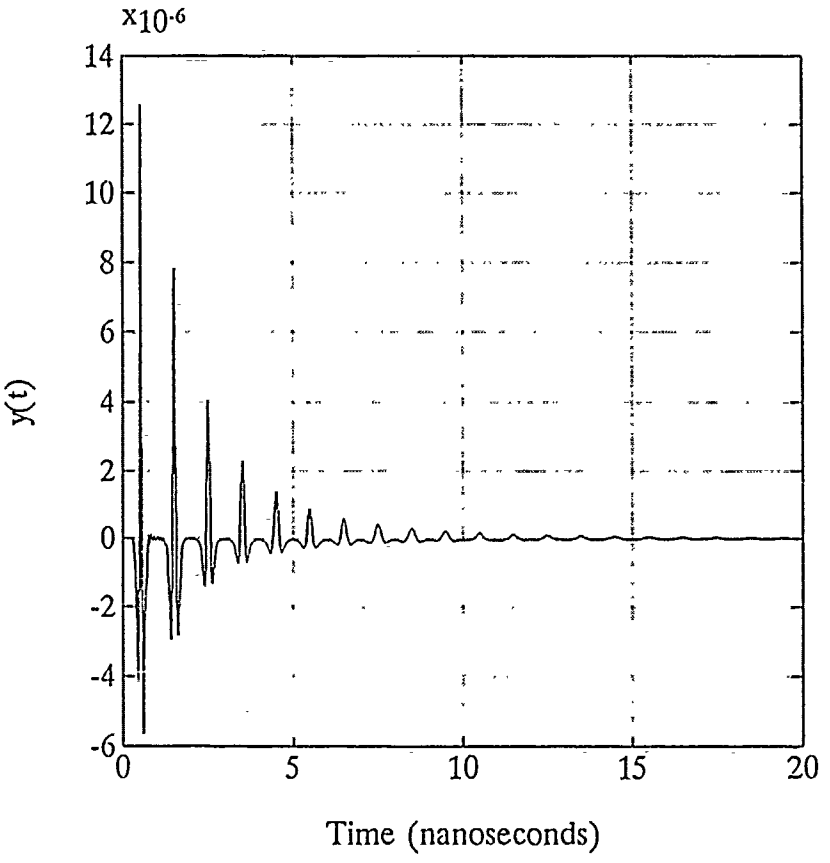

Figure 5. High Q synthetic scattering

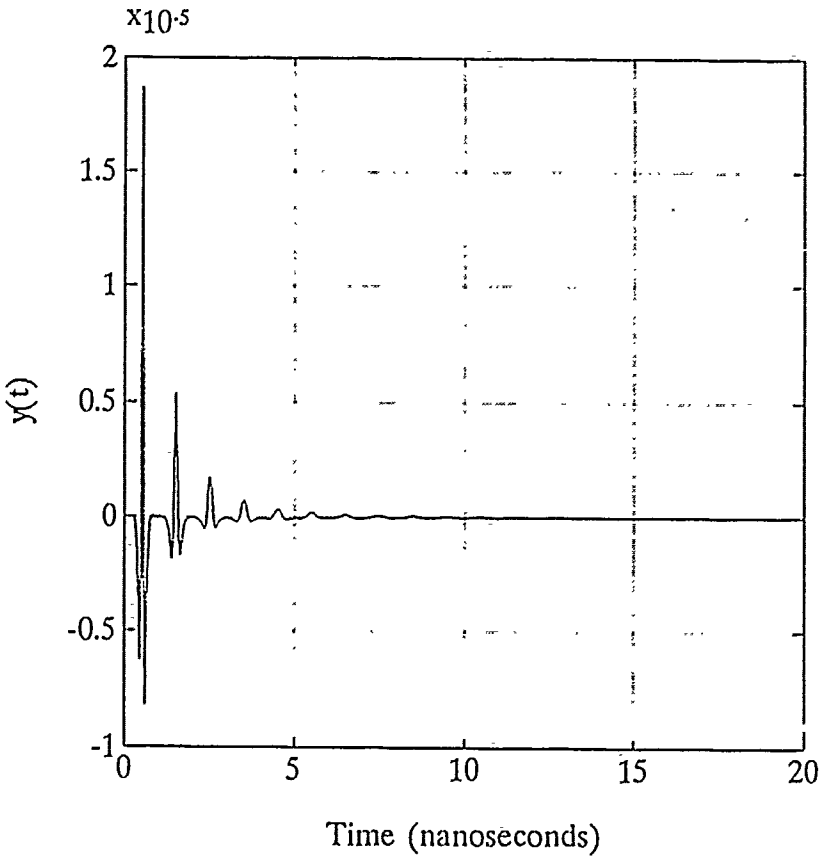

Figure 6. Medium Q synthetic scattering

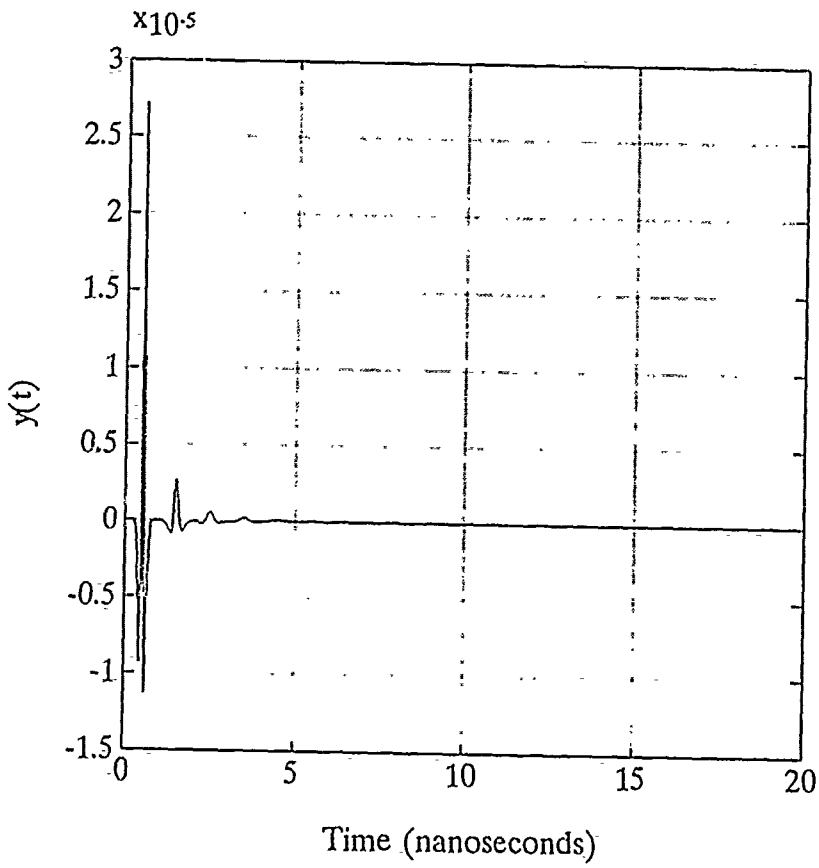

Figure 7. Low Q synthetic scattering

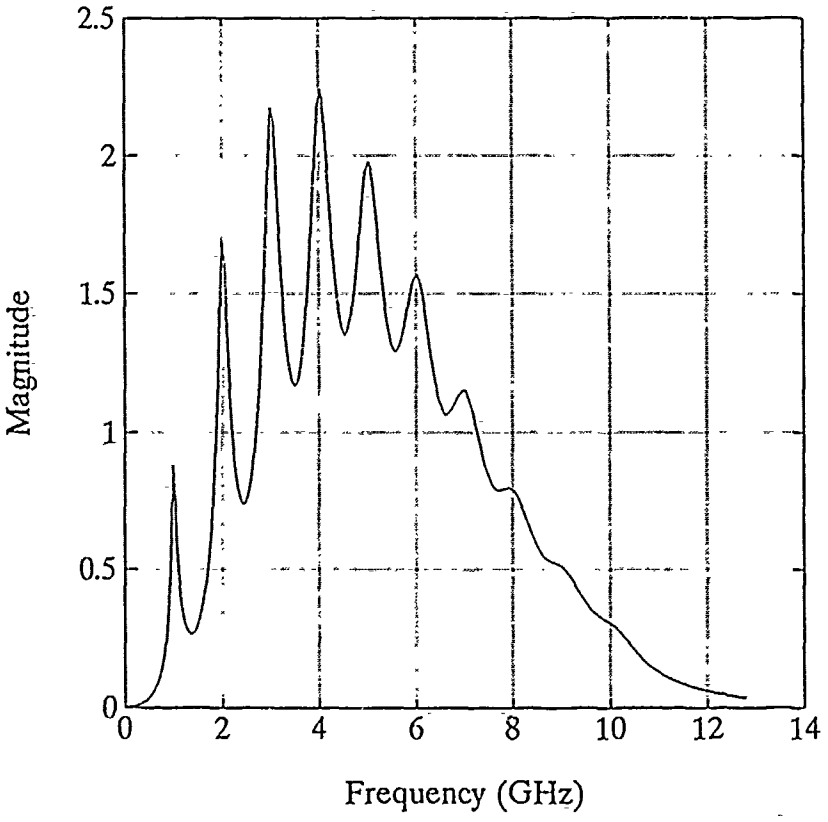

Figure 8. Frequency spectrum of medium Q synthetic target

Theorem was then invoked by calling this routine 1000 times for each additive noise point to ensure the resultant noise was Gaussian distributed. [Ref. 6] Figures 9 and 10 show the high Q waveform of Figure 5 with the addition of noise of 20 dB and 7 dB, respectively.

B. THIN-WIRE INTEGRAL EQUATION SIGNALS

The concept of extracting *unknown* poles and then incorporating them into filters was validated on the signals generated by the Time-Domain Integral Equation (TDIE) Thin-Wire Scattering Program, due to Morgan [Ref. 20]. This program uses a record length of 960 samples in a 20 nanosecond collect time. The scattering simulated excitation by the same double Gaussian pulse with approximately a 1-10 GHz bandwidth. The program generates wire scattering data for any combination of incident and reflection angles. Backscatter data, generated at angles of 175, 150, 110, and 90 degrees measured relative to the long axis of the wire, were used to effect a monostatic situation. This data was similarly noise polluted at the same signal-to-noise ratios. A representative case for the noiseless TDIE thin-wire data is in Figure 11 and its spectrum is in Figure 12.

C. LABORATORY SIGNALS

Actual scattering signals used for pole extraction and annihilation filtering were obtained from the NPS Transient Electromagnetic Scattering Laboratory. As stated, the parameters determined by the instrumentation of the laboratory were used throughout the experiments for both synthetic and actual signals as much as possible.

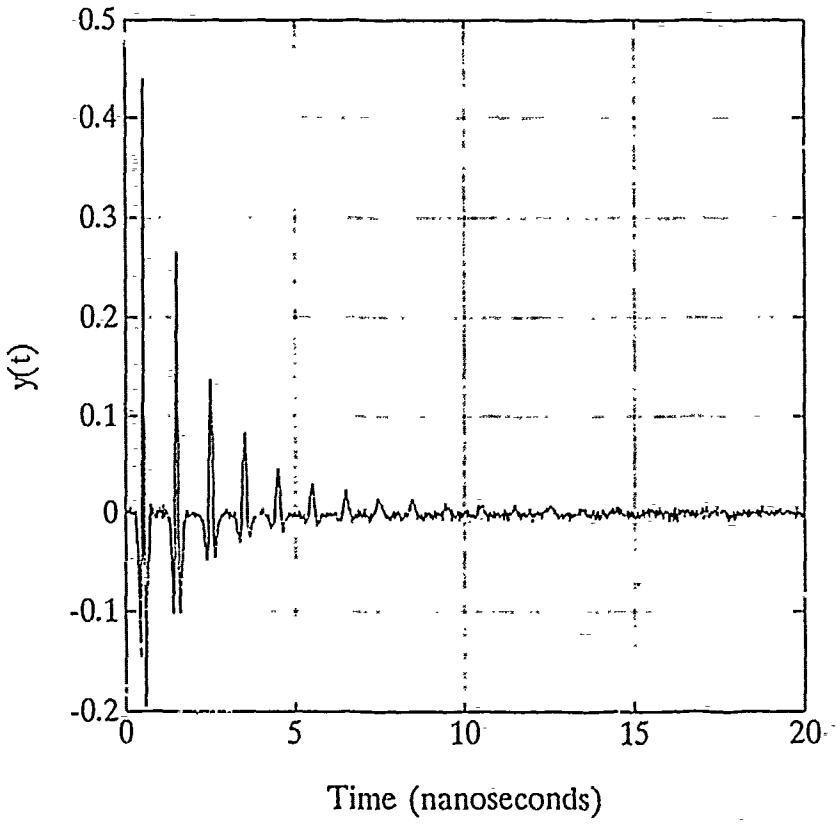

Figure 9. High Q synthetic scattering with 20 dB SNR

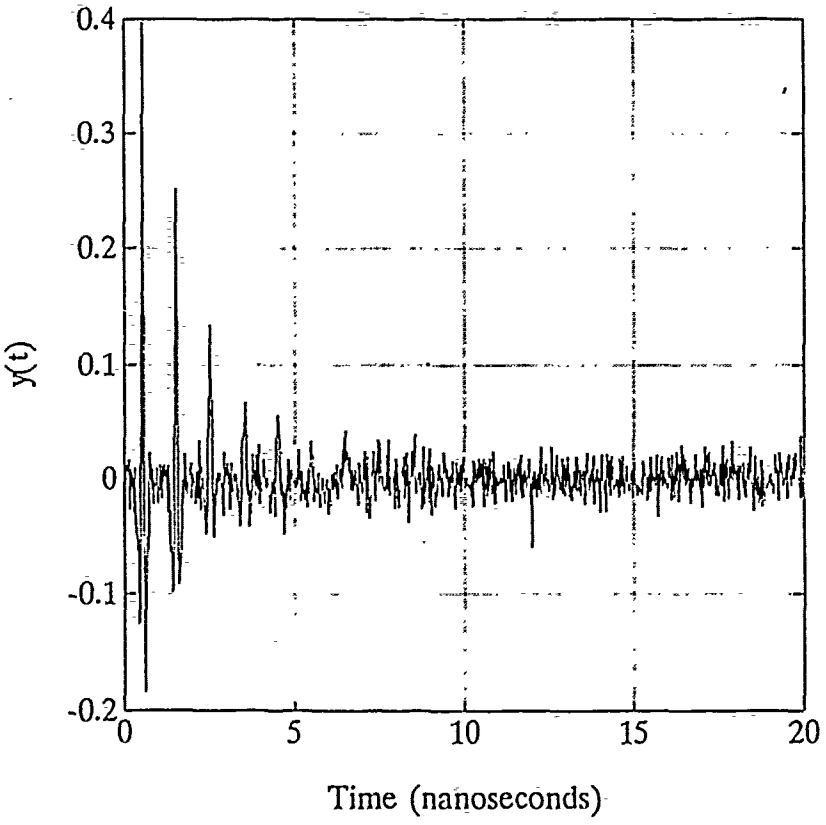

Figure 10. High Q synthetic scattering with 7 dB SNR

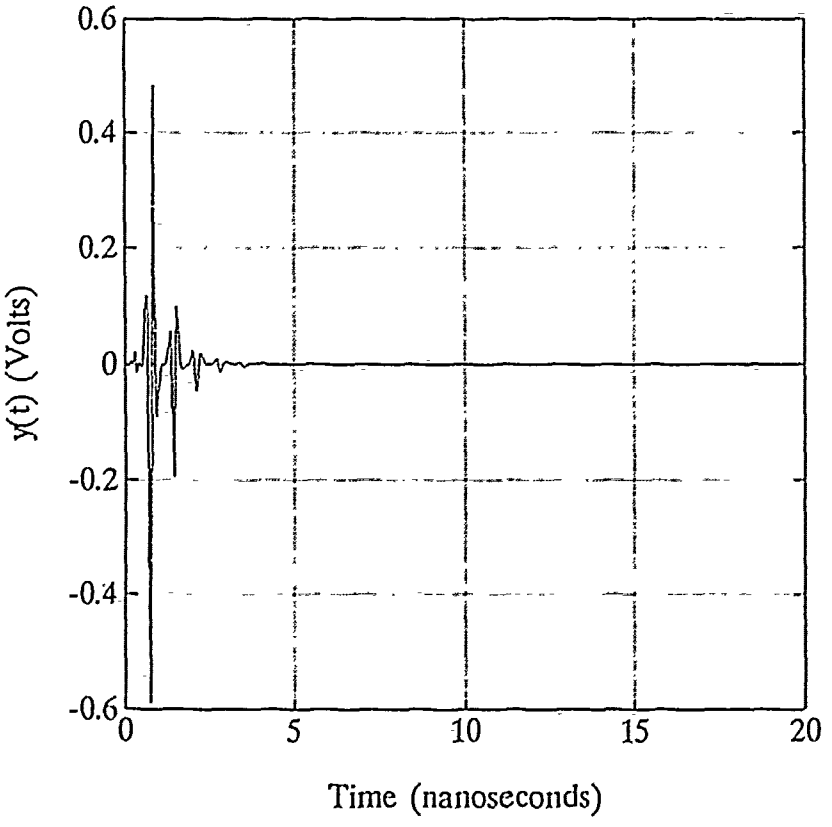

Figure 11. TDIE thin-wire scattering with 30° incidence, 150° reflection

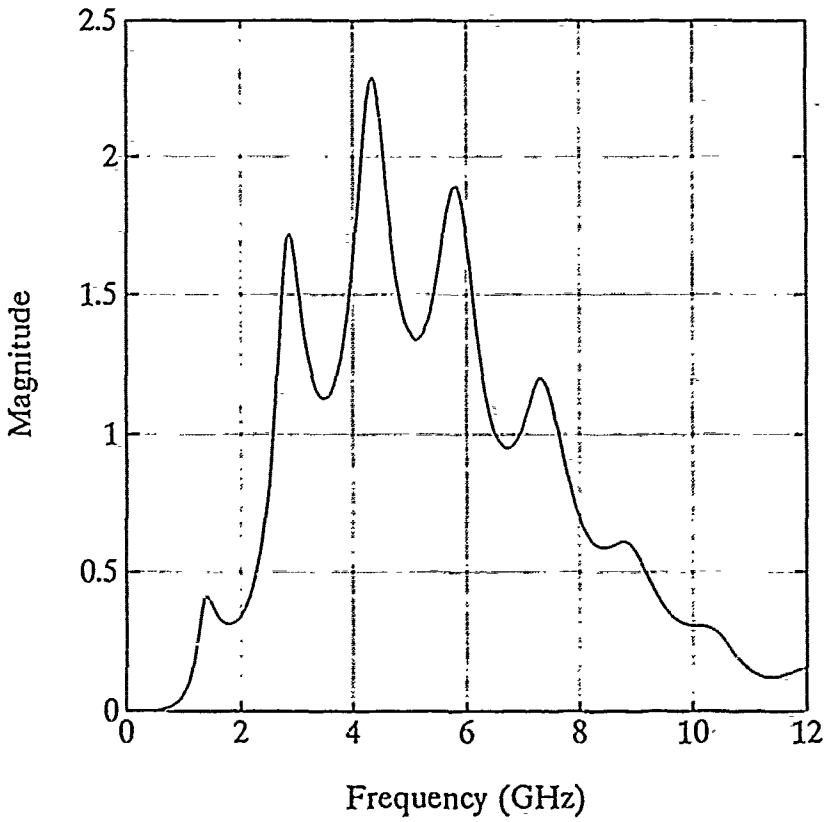

Figure 12. Spectrum of TDIE thin-wire 36°/150° data

This included the scattering collect time of 20 nanoseconds and the excitation bandwidth of 1-10 GHz due to the incident pulse double Gaussian waveshape. The sampling frequency serves as the notable exception to this matching. The TESL samples 1024 times in the 20 nanosecond collect time for a sampling frequency of 51.2 GHz. This twice oversampling, while allowing more flexibility in the use of the TESL, acted as a limiting factor for subsequent annihilation filtering. As a result, the collected scattering data from the lab was collapsed to the 25.6 GHz sampling frequency, mentioned above, by averaging each pair of points in the record before annihilation filtering. The TESL provides a nominal signal-to-noise ratio of approximately 26 dB [Ref. 21].

1. Deconvolution Postprocessing

The double Gaussian waveshape, as described above, is not actually transmitted in the TESL. Instead, a noise-like but highly repetitive signal, with approximately the same bandwidth is transmitted and the response of the target to the specific double Gaussian waveshape is estimated through deconvolution post-processing. This allows the target to be subjected to an analytically precise signal like the double Gaussian without requiring a tremendously sophisticated transmitter apparatus. Additionally, the free-space response of the target is more nearly obtained by removing the effects of the chamber and antennas. The details of this process are in [Ref. 21]. Targets used in the scattering experiments included a 0.1 meter thin-wire target and silver coated 1/72 scale model aircraft.

2. Measured Thin Wire Target

The transition to real-world scattering data was first made with scattering data collected in the TESL on a 0.1 meter long, 2.36 millimeter diameter thin metal wire [Ref. 21]. This wire data was collected monostatically at 30 degrees, 45 degrees and broadside to the wire. The time and frequency domain data for the 30 degree case are in Figures 13 and 14. Notice that the FFT of this target's scattering is much more complicated than for the synthetic TDIE thin wire. The spectrum in Figure 14 displays a significant resonance at approximately 3 GHz, with less excited poles at 1.5 and 4 GHz. As the apparent length of the wire, D, at this angle is 0.05 meters, so these resonances correspond roughly to modes at $\lambda \approx 2D$, $3D$, and $1.5D$, respectively. This demonstrates the complicated interaction between the excitation and resonances of the target.

3. Model Aircraft Targets

The bandwidth of the TESL, 1-12 GHz, is matched to the scaling factor of the model aircraft targets. Table 5 contains the significant dimensions, both actual and scaled, of the aircraft used to collect scattering data. Comparison of the scale model lengths to the wavelengths of the TESL excitation, 2.5 to 30 cm, indicate that large fractions of wavelengths can be contained in the dimensions of the aircraft models. This allows for the lowest order, i.e. the strongest available, modes to be excited in the model structure.

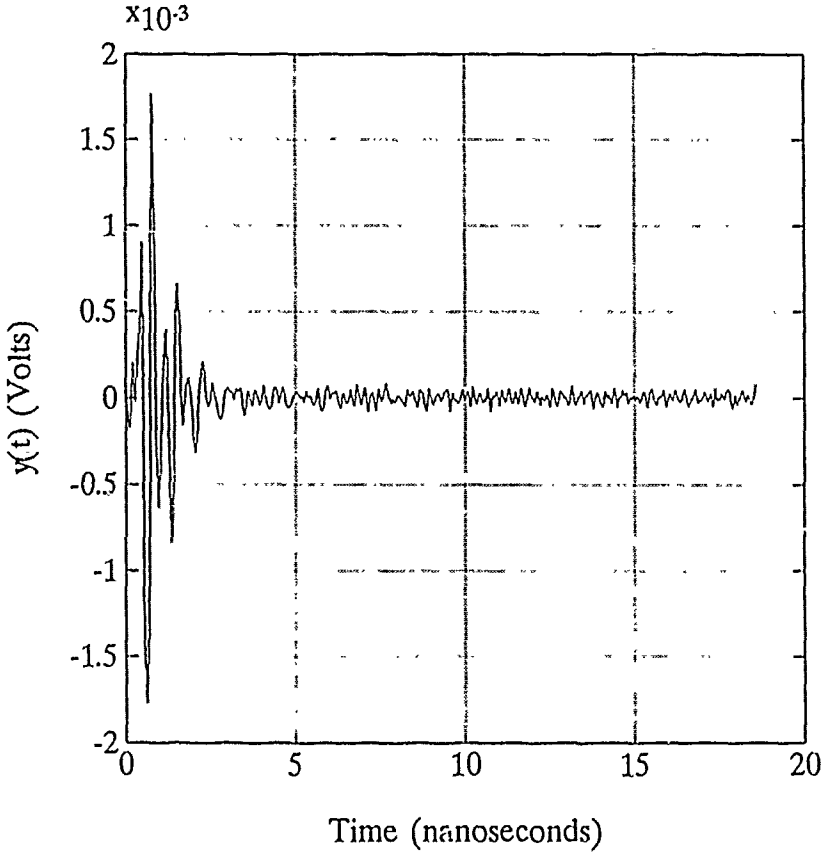

Figure 13. Measured thin-wire scattering at 30°/150°

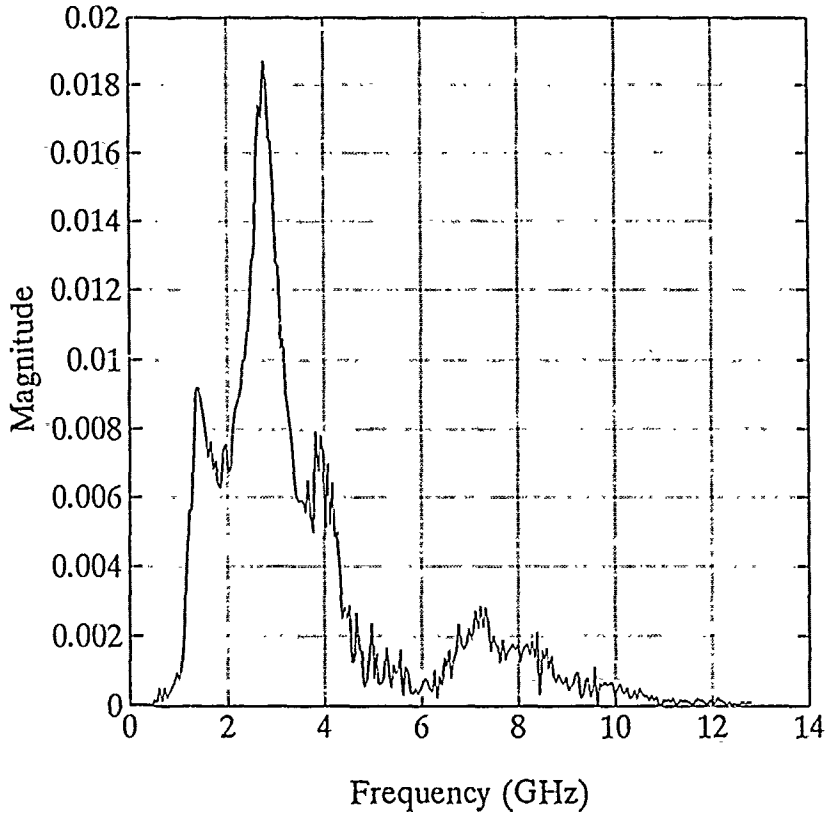

Figure 14. Spectrum of 30° measured thin-wire scattering

TABLE 5. DIMENSIONS OF AIRCRAFT TARGETS [Ref. 23, 24]

Target number		1	2	3	4	5
Overall length	actual (m)	19.43	15.03	17.07	12.20	15.88
	model (cm)	26.97	20.88	23.71	16.94	22.06
Wingspan	actual (m)	13.05	9.45	11.43	10.96	13.95
	model (cm)	18.13	13.13	15.88	15.22	19.38

The aircraft data was collected by Walsh at six different aspects: nose-on, tail-on, broadside, 30 degrees off the nose, and from above with both the fuselage and wingspan parallel to the incident electric field [Ref. 21]. Target No. 2 scattering data at thirty degrees aspect angle is in Figure 15 with its spectrum, Figure 16.

D. SUMMARY

Each of these target sets; the ARMA synthetic scatterer, the TDIE thin-wire scatterer, the actual thin wire, and the model aircraft; each represent an increasingly more complicated and challenging case for the pole extraction and annihilation filtering algorithms. This is especially evident when reviewing their various frequency response plots.

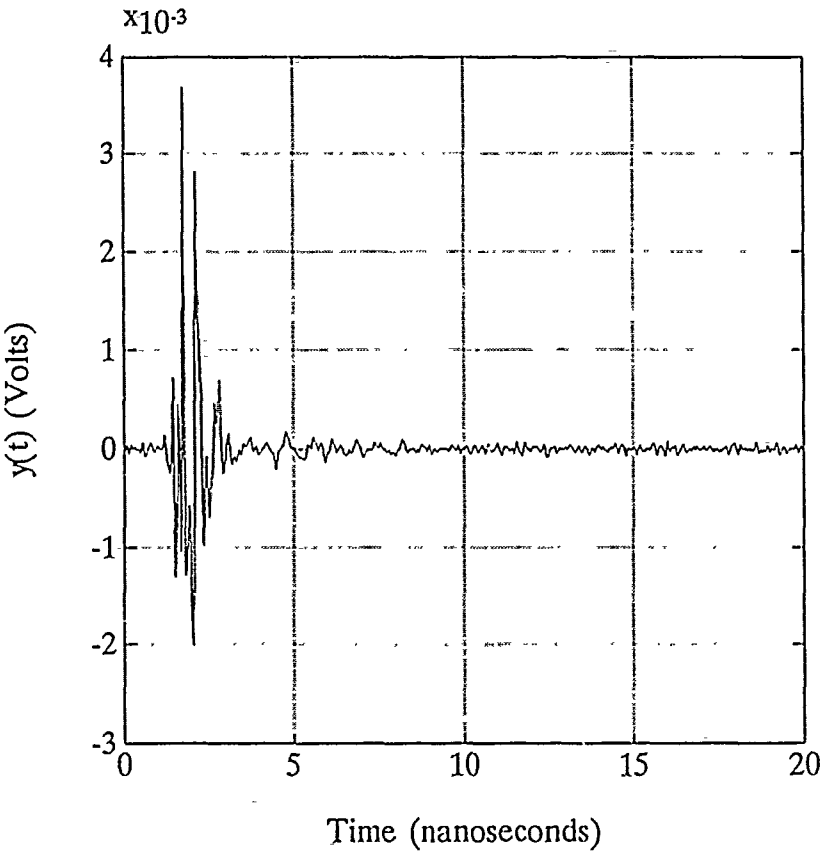

Figure 15. Scattering from aircraft target No. 2, 30° aspect

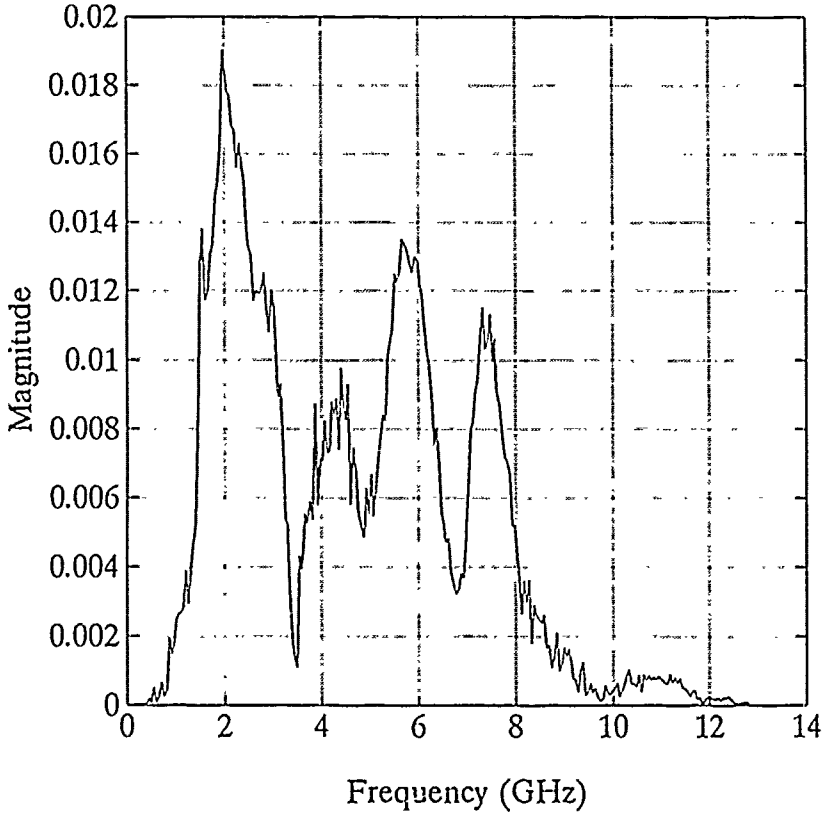

Figure 16. Spectrum of target No. 2, 30° aspect

III. POLE EXTRACTION

The pole extraction algorithm considered in this thesis is due to Cadzow and Solomon [Ref. 16]. Other algorithms have been used and are briefly discussed in Chapter I. More detailed analysis of the other algorithms can be found in [Ref. 4].

A. CADZOW-SOLOMON ALGORITHM

The scattered signal structure discussed in Chapter I and displayed in Chapter II consists of an early-time and late-time separated by the point where the incident signal ceases to excite the scatterer. In early-time, the resonances are just being initialized, so their amplitudes are small compared to the driver. However, the end of early-time marks the point where they have their largest instantaneous power. The Cadzow-Solomon algorithm takes advantage of this fact by attempting pole extraction from a data record containing both early and late-time data segments.

1. Applicability

The Cadzow-Solomon method seeks to identify the unknown coefficients a_k and b_k for an autoregressive moving average (ARMA) process given by Equation (4), which is repeated here,

$$y(n) = \sum_{k=1}^{k=N} a_k y(n-k) + \sum_{k=0}^{k=L} b_k x(n-k), \tag{6}$$

by analyzing the system input, $x(n)$ and output, $y(n)$ [Ref. 16]. Identification of these coefficients will allow for extraction of the poles and zeros of the transfer function which has been acted on by $x(n)$ to produce $y(n)$, specifically,

$$H(z) = \frac{b_0 + b_1 z^{-1} + \cdots + b_L z^{-L}}{1 + a_1 z^{-1} + \cdots + a_N z^{-N}}. \tag{7}$$

2. Methodology

The algorithm does not require specific knowledge of the system order, N and L in Equation (7), as it uses an "over-estimation" of this order to account for noise and extract the poles. Norton applied a technique used in the Kumaresan-Tufts algorithm, whereby the relationship in Equation (4) is written in reverse time order. This forces the desired poles to be extracted outside the unit circle on the z-plane, while the extraneous poles, introduced by "over-estimation" to allow for noise, are constrained to lie inside the unit circle [Ref. 4]. This reverse time, non-causal form of Equation (4) is

$$y(n) = \sum_{k=1}^{k=N} a_k y(N+n-k+1) + \sum_{k=0}^{k=L} b_k x(n-k). \tag{8}$$

The pole locations are then reflected through the unit circle resulting in the signal poles within, noise poles outside. This final presentation of the poles describes the actual scatterer: a stable, causal system.

For M segments of input-output data related by Equation (8), where

$M > N + L - 1$, the relationship is expanded to matrix form

$$\begin{bmatrix} y_{L+1} & \cdots & y_{L+N} & \vdots & x_0 & \cdots & x_L \\ \cdot & & \cdot & \vdots & \cdot & & \cdot \\ \cdot & & \cdot & \vdots & \cdot & & \cdot \\ \cdot & & \cdot & \vdots & \cdot & & \cdot \\ y_{L+M} & \cdots & y_{L+N+M-1} & \vdots & x_{M-1} & \cdots & x_{L+M-1} \end{bmatrix} \begin{bmatrix} a_N \\ \cdot \\ \cdot \\ \cdot \\ a_1 \\ \cdots\cdots \\ b_L \\ \cdot \\ \cdot \\ \cdot \\ b_0 \end{bmatrix} = \begin{bmatrix} y_L \\ \cdot \\ \cdot \\ \cdot \\ y_{L+M-1} \end{bmatrix} \tag{9}$$

where both parts of the $y|x$ data matrix are Toeplitz matrices in which each row introduces one new value and shifts all others one place to the right. Rewriting this equation in more compact notation yields

$$D_{yx} C_{ab} = y, \tag{10}$$

Extraction is accomplished by solving this matrix-vector equation for the ARMA parameter vector,

$$C_{ab}^{+} = D_{yx}^{+} y. \tag{11}$$

where C_{ab}^{+} is the minimum Euclidean norm solution vector for C_{ab} and D_{yx}^{+} is the psuedoinverse of the data matrix D_{yx}. The solution vector, C_{ab}^{+}, is the minimum length least-squares solution to the matrix-vector equation. [Refs. 4 and 9]

3. Singular Value Decomposition

The above solution relies on singular value decomposition (SVD) of the data matrix, D_{yx}, to derive its psuedoinverse, D_{yx}^{+}. This process separates D_{yx} into the product of three matrices,

$$D_{yx} = U\Sigma V^{T} \tag{12}$$

where U and V are both orthogonal matrices (that is, $U^{T}U=I$) and where V^{T} denotes the transpose of V. The columns of the matrices U (of size M by M) and V (N by N) are composed of the eigenvectors of $D_{yx}D_{yx}^{T}$ and $D_{yx}^{T}D_{yx}$ respectively. The singular values of the data matrix are the nonzero components of the M by N diagonal matrix, Σ. These singular values are the nonzero eigenvalues of both $D_{yx}D_{yx}^{T}$ and $D_{yx}^{T}D_{yx}$. Rearranging these components of the SVD of D_{yx} produces its psuedoinverse,

$$D_{yx}^{+} = V\Sigma^{+}U^{T}. \tag{13}$$

Here, the diagonal components of Σ^{+} are the inverse of the original singular values [Ref. 9].

The original singular values must be compensated for noise if it is present in the input/output data which comprises the data matrix. This compensation assumes the input and output noise variances to be equal. More detail on bias compensation is provided in [Refs. 4 and 9].

B. PERFORMANCE

The Cadzow-Solomon algorithm has demonstrated the ability to extract poles from scattering data. Larison [Ref. 9] applied the algorithm to synthetic target data, both measured and analytically predicted thin-wire scattering data, and aircraft model data. Murphy [Ref. 6] refined the process by further application to synthetic data sets as well as measured thin-wire and aircraft data as presented in Chapter II of this thesis.

1. Noise Tolerance

Murphy tested the synthetic scattering at various signals-to-noise ratios down to seven dB. Figure 17 shows that the algorithm remained relatively robust, as determined by observing the tightness of the clustering of the extracted poles, down to 20 dB [Ref. 6]. Below this level the poles would not cluster significantly to lend a high confidence to their location. Figure 17 presents fourteen extraction trials of medium Q data, each containing a different 20 dB noise sequence . Notice that the higher order poles (near $\pi/2$) are not extracted. Fewer poles are available with successively greater noise levels [Ref. 6].

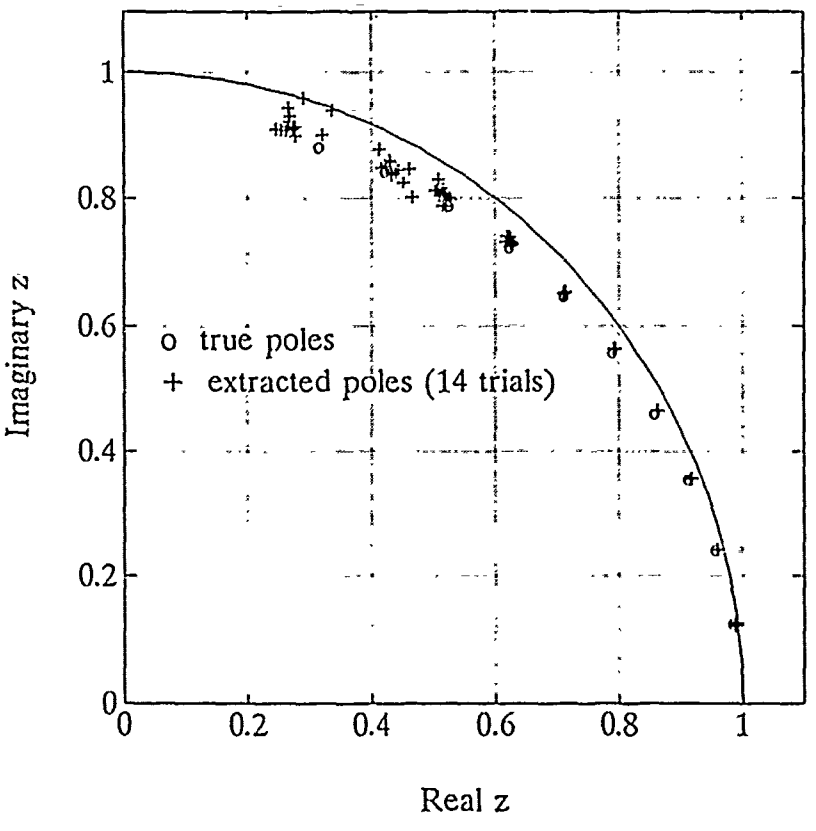

Figure 17. Extracted poles, medium Q synthetic data, 20 dB SNR [Ref. 6]

2. Accuracy Versus Precision

The adequacy of the extracted poles can be couched in terms of accuracy, the distance of the extracted poles to their true location; and precision, the tightness of a group of poles, regardless of its location. Figure 17 demonstrates some degradation in accuracy as the extracted poles are slightly biased toward the unit circle [Ref. 6].

The noiseless TDIE data yielded excellent results in producing very tightly grouped poles. This was to be expected because of the noise-free environment and the high quality resonator represented by the modeled thin wire.

For actual scattering data, accuracy can only be determined through evaluating the target discrimination effectiveness of the annihilation filters constructed from the extracted poles. Figure 18 shows a scatter plot of extracted poles from the measured thin-wire scatterer. The poles are represented by a scatter because their position can be perturbed by noise and is highly sensitive to the parameters used in the extraction algorithm. As such, the extracted poles from actual targets will represent some distribution about their true (unknown) location. Murphy used an averaging scheme on the extracted poles which lie in tight groups, after discarding outlying positions, for a given angle of incidence. These averages were then averaged over the available angles of incidence in an attempt to ameliorate any possible bias due to the parameters and to compensate for the changing relative excitation of one mode over another with incidence angle. [Ref. 6]

Some indication of the task before the algorithm can be seen be examining the frequency spectrum of that portion of the thin-wire data records used by the Cadzow-Solomon data matrix. Figure 19 shows these spectra for all three aspects available. Notice the varying levels of excitation of the modes. Notice also that the spectrum is rather complicated considering one expects frequencies based on just integer multiples of the half wavelength matched to the wire length: 1.5, 3.0, 4.5, 6.0 GHz, etc. This is due, in part, to the fact that some ten data points at the end of early-time are included to gain the most excited resonances. This early-time data is used by the algorithm to model the response of the feed-forward part of the target transfer function to the excitation waveform.

3. Aircraft Extracted Poles

The poles extracted from the model aircraft scattering data using the Cadzow-Solomon algorithm were much more highly sensitive to the input parameters and were less likely to group as well as the thin-wire data. The pole locations, used later in filtering, represent an average of the extracted location for various combinations of algorithm parameters and incidence angles. Individual extractions resulting in an outlying location from a cluster or outside the unit circle were ignored. The highly complex nature of the aircraft scatterer made difficult work for the algorithm. Figure 20 shows the frequency response of the portion of the data record processed for aircraft target two for the nose-on, tail-on, and thirty degree aspect. The spectrum is rich with closely spaced, strong frequency components at low frequencies which the Cadzow-Solomon algorithm must sort out. Figure 21 shows

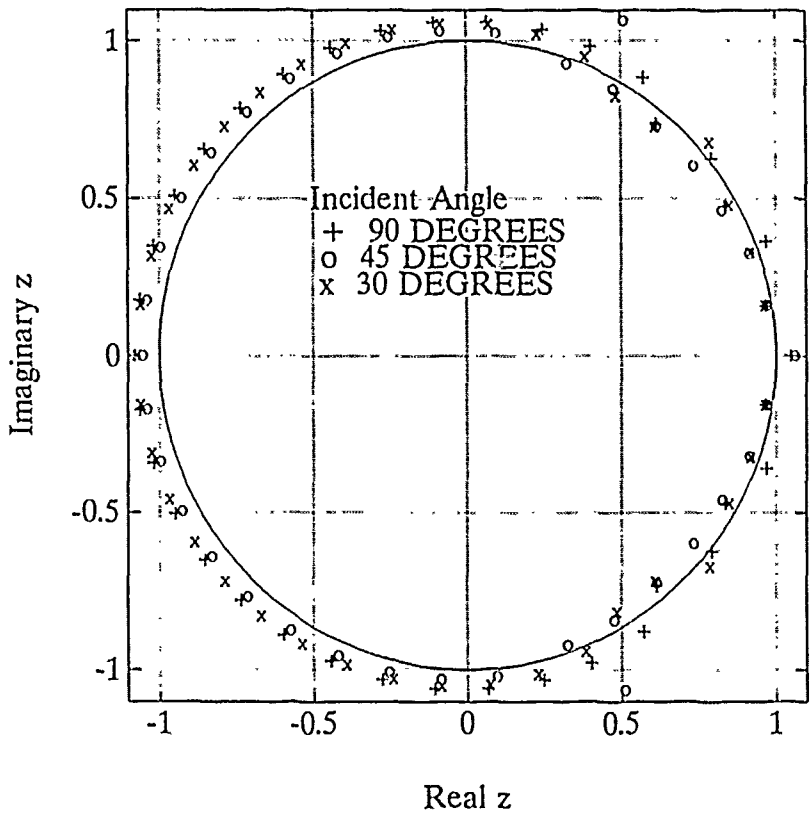

Figure 18. Extracted poles, measured thin-wire data [Ref. 6]

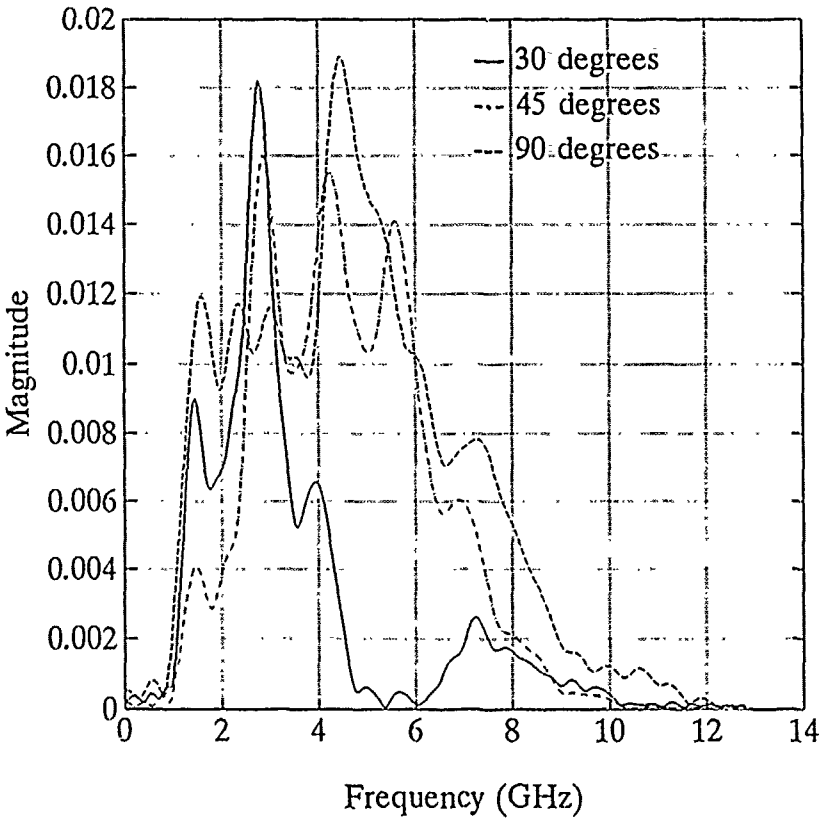

Figure 19. Spectra of measured thin-wire data processed for pole extraction

this same spectral information for target three. Notice that the low frequency content of both aircraft are similarly populated and complicated. This made the extraction/filtering discrimination problem very difficult, as all aircraft models tended to have a similar frequency spectrum, in terms of many significant components at lower frequencies. These lowest order poles would ideally be the ones used for target discrimination later in the filtering process because they have the most energy. [Ref. 6]

C. IMPLEMENTATION CONSIDERATIONS

Actual implementation of a transient pole extraction facility must address the questions of frequency-subject matching and subject accuracy, signal-to-noise ratio required, and post-extraction pole position processing.

1. Scattering Subject and Frequency

The scattering objects used for pole extraction must faithfully represent the actual targets of interest that will be encountered by the radar/annihilation filter system. This may only require more detailed scaled models than used above or may require full-scale targets. The two advantages of using scale models are the linear increase in frequency used (and linear decrease in size of antennas and components required) and the "reduced" availability of full scale targets — especially of aircraft of a potential adversary! However, scale models used must accurately represent the current distribution properties of the full scale targets. Validation of the modeling may be conducted on an aircraft available for both full-scale and model testing.

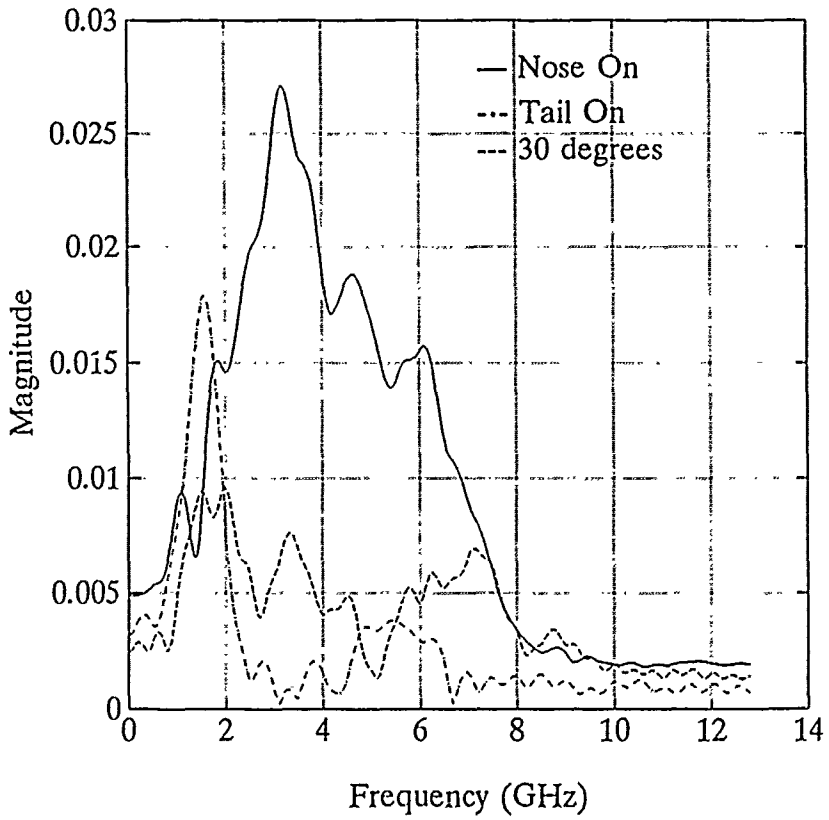

Figure 20. Spectra of target No. 2 data processed for pole extraction

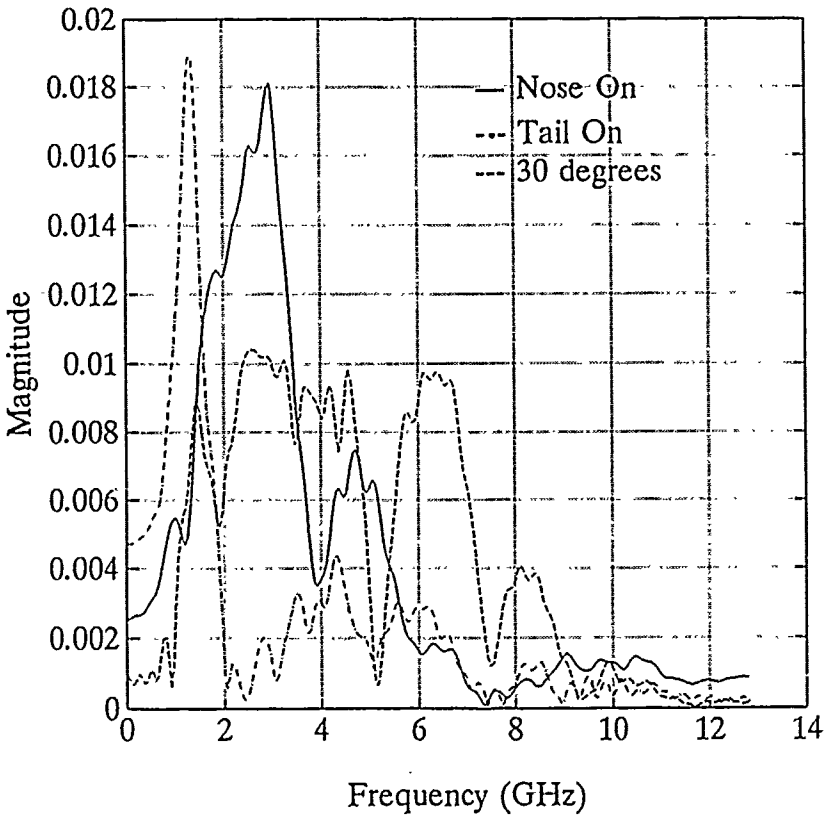

Figure 21. Spectra of target No. 3 data processed for pole extraction

Referring to the dimensions of the aircraft targets used in this thesis, Table 4, Chapter II, indicates the low order resonant frequencies of full scale targets lie in the 7 to 70 MHz region. This frequency range would be much more difficult to work in, not only due to the size of the antenna components, but also due to the requirement to create a broadband excitation pulse or swept frequency CW system in order to excite a number of the target's resonances. The ability to create a high power, short pulse to initiate the resonances is difficult at these low frequencies. The use of steady-state, stepped-frequency excitation may be a way to avoid this problem [Ref. 25]. Here, the target is excited by relatively long pulses or CW with narrow bandwidth subpulses, each centered on various frequencies in the resonance region. The scattered response is received coherently for each frequency and extruded from the fixed clutter, transmitter, and receiver response by deconvolution, in a similar manner to that done in the TESL (Chapter II, Section B). The target's broadband transient response is synthesized from the steady-state response at the various transmit frequencies by smoothing in the frequency domain and subsequently transforming back to the time domain. This also allows tailoring the bandwidth of the excitation to those frequencies of most interest, vice transmitting an indiscriminate broadband pulse [Ref. 26].

2. Signal-to-Noise Ratio

As stated above, the pole extraction process requires approximately 20 dB signal-to-noise ratio. The extraction process inherently requires higher SNR than more conventional RF imaging from ramp responses because of reduced integration

opportunity; the necessity to process mostly late-time, undriven responses; and the sensitivity of the system poles to perturbations [Ref. 27]. This requirement may dictate the choice between full or scale model targets. The frequency range of resonances of full scale targets of interest, generally 2 MHz to 1 GHz [Ref. 25], contains considerable man-made and atmospheric noise [Ref. 28:pp. 34.2-34.13], driving received noise levels well above the predominantly thermal noise region encountered for the resonant frequencies of scale model targets.

3. Post-Extraction Position Processing

As demonstrated with the model aircraft data, the extracted pole positions for a given set of data vary with the processing parameters chosen. Additionally, although the transfer function of the target is aspect independent, the relative excitation of the target's modes affects the extraction algorithm's output. The poles extracted by Murphy [Ref. 6], as discussed in the previous section, were gathered through a process of empirically optimizing a set of extraction parameters, then dithering them and averaging. The extracted pole positions are defined by some probabilistic distribution, therefore the "best" set of poles for a given target, relative to its actual, unknown poles, is not defined. Artificial intelligence or an expert system would be a logical choice to process and refine the position of extracted poles for a real world implementation. The expert system stage strapped to the output of the pole extraction algorithm could perform the sifting of extracted poles for outliers (performed by human eye for the poles above [Ref. 6]) and subsequent averaging. Possibly, a feedback path could be initiated to allow the smart processor to guide the

selection of extraction algorithm parameters to optimize the extracted positions. Additionally, this path could include the evaluation of the performance of the resultant annihilation filters to refine the poles.

IV. ANNIHILATION FILTERING

After extracting the necessary poles for the targets of interest, using the algorithm of the previous chapter, these poles were incorporated into the design of annihilation filters. The two alternatives for this process explored here are the K-Pulse resonance annihilation filter and the inverse ARMA filter.

A. RESONANCE ANNIHILATION FILTERING

The scattered response of a target, as discussed in Chapter I, consists of the early and late-time portions as well as any noise collected. Morgan describes the transition point, T_o, with unit step functions [Ref. 7],

$$y(t) = y_E(t)[u(t)-u(t-T_o)]+y_L(t)u(t-T_o)+N(t). \tag{14}$$

The early-time component is composed of excitation-dependent physical optics scattering and natural mode startups, while the late-time portion consists of the natural mode resonances. This late-time portion can be written as a sum of damped sinusoids,

$$y_L(t) = \sum_{p=1}^{\infty} A_p \exp(\sigma_p t) \cos(\omega_p t+\varphi_p) \tag{15}$$

where the amplitudes and phases (complex residues) of each mode, $A_p\exp(j\varphi_p)$, are aspect-dependent. The additive noise and clutter component, $N(t)$, is composed of atmospheric and thermal noise constituents, as well as other possible signal pollutants.

The resonance annihilation filter (RAF) concept employs a bank of filters, Figure 22, with the output of each being the result of convolution of the filter impulse response, h_m, and the scattered response, $y(t)$, from Equation (14) above,

$$w_m(t) = h_m(t) * y(t). \tag{16}$$

The decision criterion for deciding the type of target present is to match the filter output with the lowest average late-time energy,

$$\varepsilon_m = \frac{\int_{T_L}^{T_S} w_m^2(t)dt}{T_S - T_L} \tag{17}$$

with the resonances embodied in that filter. Here T_L is the start of late-time, picked late enough to ensure no early-time interaction remains, and T_S is the end of the integration time, which would ideally approach infinity for maximum discrimination, but must be time-limited to prevent noise from obliterating the resonant energy. This late-time start point is extended beyond the target late-time discussed in Chapter I, Section A, by the delay of the annihilation filter, τ_f. Here the input signal, y(t), is normalized by its late-time RMS energy and the filter response, h_m, is normalized by its RMS value over its record length [Ref. 10]. Morgan discusses the requisite features of the filters, h_m, in [Ref.7] and points out that using a finite impulse response (FIR) filter precludes the possibility of early-time energy being carried over into late-time and polluting the target discrimination process.

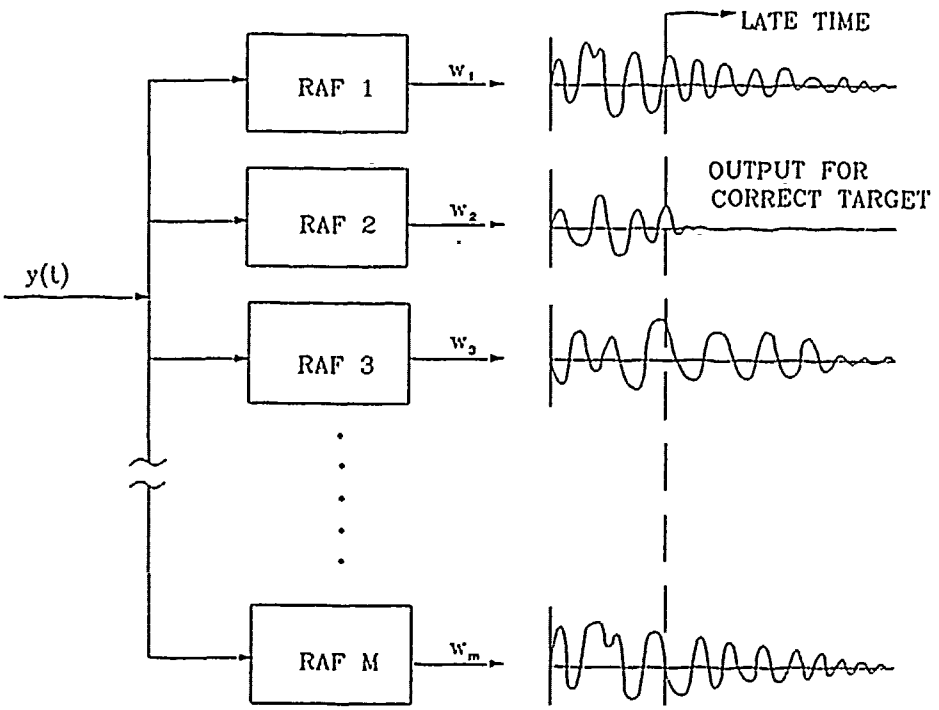

Figure 22. RAF identification process [Ref. 7]

B. THE K-PULSE FILTER

1. Methodology

In order to realize the annihilation filter processing with digital computers, the discrete time filter impulse response, h_m, must be solved for. The following derivation is due to Morgan [Ref. 29]. First the late-time response in Equation (15) is written in discrete time format, utilizing the complex z-transform operator to represent the sinusoidal poles,

$$y_L(n) = \sum_{\substack{p=-N \\ p\neq 0}}^{p=N} \alpha_p z_p{}^n, \tag{18}$$

where $z_p=\exp(s_p\Delta t)$, $z_{-p}=z_p^* =\exp(s_p^* \Delta t)$, s represents each pole in the Laplace domain, and α_p is the combination of the magnitude and residue terms which scale each pole's relative contribution to the scattering. Additional flexibility can be incorporated by allowing k integer delays between filter weights, after which the convolution process of Equation (16) is written as a difference equation

$$w(n) = \sum_{m=0}^{m=M} h_m y_L(n-km). \tag{19}$$

After substituting the late-time response of Equation (18) and rearranging the order of summation, the equation below is set to zero, indicating the annihilation action on the late-time energy,

$$w(n) = \sum_{\substack{p=-N \\ p\neq 0}}^{p=N} \alpha_p z_p^n \left(\sum_{m=0}^{m=M} h_m z_p^{-km} \right) = 0. \tag{20}$$

The coefficient, h_0, can be set to normalize the noise power passed through the filter, yielding the result

$$\sum_{m=1}^{m=M} h_m z_p^{-km} = h_0. \tag{21}$$

This result can be adjusted to represent a real linear system while reducing the dynamic range of the coefficients, which results in two sets of N equations

$$\sum_{m=1}^{m=M} h_m \left\{\exp(\sigma_p \Delta t)\right\}^{k\left(\frac{M}{2}-m\right)} \cos\left\{k\left(\frac{M}{2}-m\right)\omega_p \Delta t\right\} = -h_0 \cos\left\{k\left(\frac{M}{2}\right)\omega_p \Delta t\right\} \tag{22a}$$

$$\sum_{m=1}^{m=M} h_m \left\{\exp(\sigma_p \Delta t)\right\}^{k\left(\frac{M}{2}-m\right)} \sin\left\{k\left(\frac{M}{2}-m\right)\omega_p \Delta t\right\} = -h_0 \sin\left\{k\left(\frac{M}{2}\right)\omega_p \Delta t\right\} \tag{22b}$$

where $p = 1$ to N. To form a square matrix of equations which results in exact cancellation, M must equal $2N$. This derivation essentially places filter zeros upon the poles of the input signal to be annihilated.

Simon [Ref. 10] discusses a different approach to achieve an equivalent result. The coefficients, α_p and β_p, are solved for each mode by substituting the discrete time version of Equation (14) into a three-point difference equation

$$\alpha_p y_L[(n-1)\Delta t]+y_L[n\Delta t]+\beta_p y_L[(n+1)\Delta t] = 0. \quad (23)$$

This result yields an individual three point FIR filter for each mode. The z-transform derivation outlined above is equivalent to combining these in cascade and overlapping the leading and trailing points for each filter to form a single filter to handle all the target's modes.

The program to create the K-Pulse filter impulse response based on pole pair input is in Appendix D. Figure 23 contains an example K-Pulse filter impulse response created for the medium Q synthetic pole set; the other K-Pulse filters look similar.

2. Smoothing

The K-Pulse filter algorithm is difference equation based, which results in noise amplification through the filter. Notice that in Figure 24, which displays the spectrum of the filter of Figure 23, that the filter rises with frequency past the region where it performs the annihilation. In fact, the dynamic range of this plot precludes examining the structure of the filter's spectral magnitude at low frequencies. The frequency rise at the high frequency end of the spectrum, after the last zero, goes as f^{2N}, where N is the number of pole pair zeros incorporated in the filter [Ref. 29]. If the sampling bandwidth cannot be made small enough that the last zero is near the $f_s/2$ folding frequency, smoothing of the filter's impulse response must be accomplished before it can be used on data with noise. Simon convolved the K-Pulse filter impulse response with a double Gaussian smoothing function [Ref. 10].

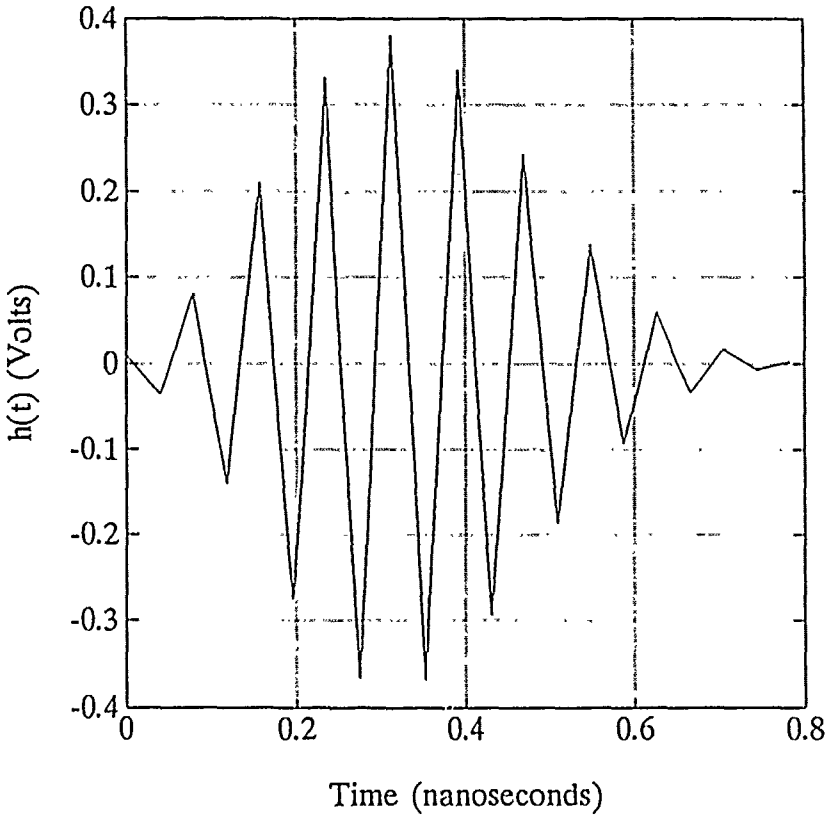

Figure 23. Medium Q synthetic data K-Pulse filter

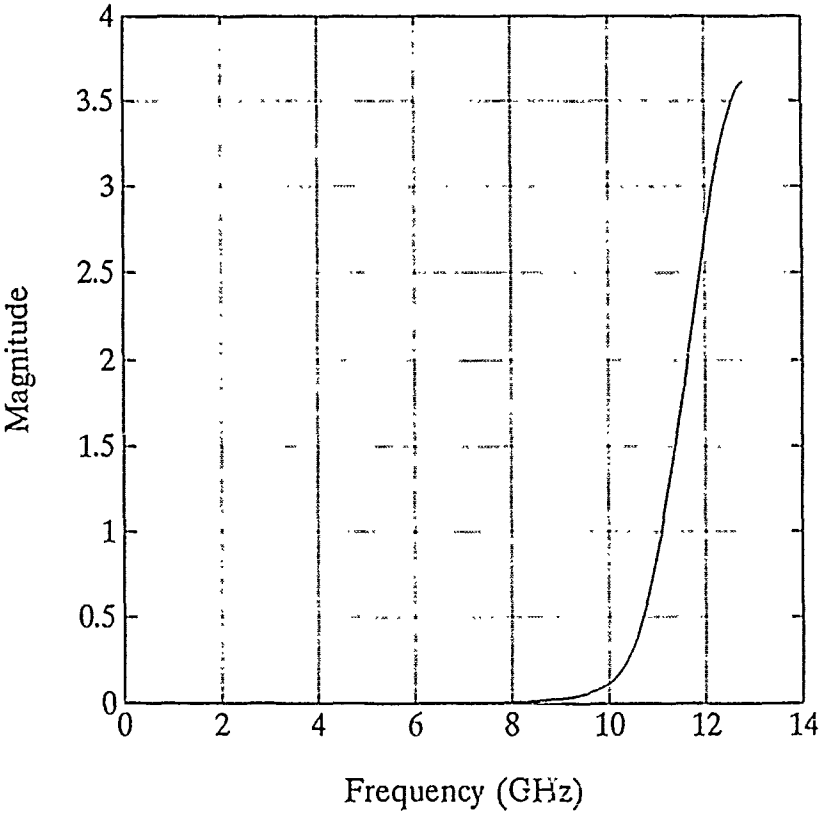

Figure 24. Spectrum of medium Q K-Pulse filter

Referring back to Figure 4, Chapter II, the spectrum of the double Gaussian is band-limited with the high and low frequency roll-offs determined by the width of the rapid and narrow Gaussian pulses used in its formation. The high frequency tail drops off as a Gaussian, that is $\exp(-\alpha f^2)$, where α is a coefficient determined by the relative widths of the pulses. This decaying exponential is used to overcome the polynomial growth of the K-Pulse filter. The programs used to create the smoothing functions and the smoothed K-Pulse filter are in Appendices E and F. The bandwidth of the smoothing functions used was determined by qualitatively examining the spectrum of the smoothed pulse. The desired filter frequency response would indicate the highest frequency zero with a definitive local minimum and then the spectrum would rapidly fall off, driven by the double Gaussian. The smoothed version of the ARMA medium Q synthetic data K-Pulse of Figure 23 is in Figure 25; its spectrum is Figure 26. Smoothed K-Pulse filters were used to test the annihilation filter concept on all the various signals discussed in Chapter II.

3. Performance

a. ARMA Synthetic Scattering

To evaluate the effectiveness of the K-Pulse filter, scattering data was created for the poles sets indicated in Chapter II, as well as for poles both five percent above and below the baseline sets, at infinite (no noise), 20, 15, 10 and 7 dB signal-to-noise ratio. These data records were convolved with the K-Pulse filters created for the "correct" pole pairs using the convolution routine in Appendix G. As

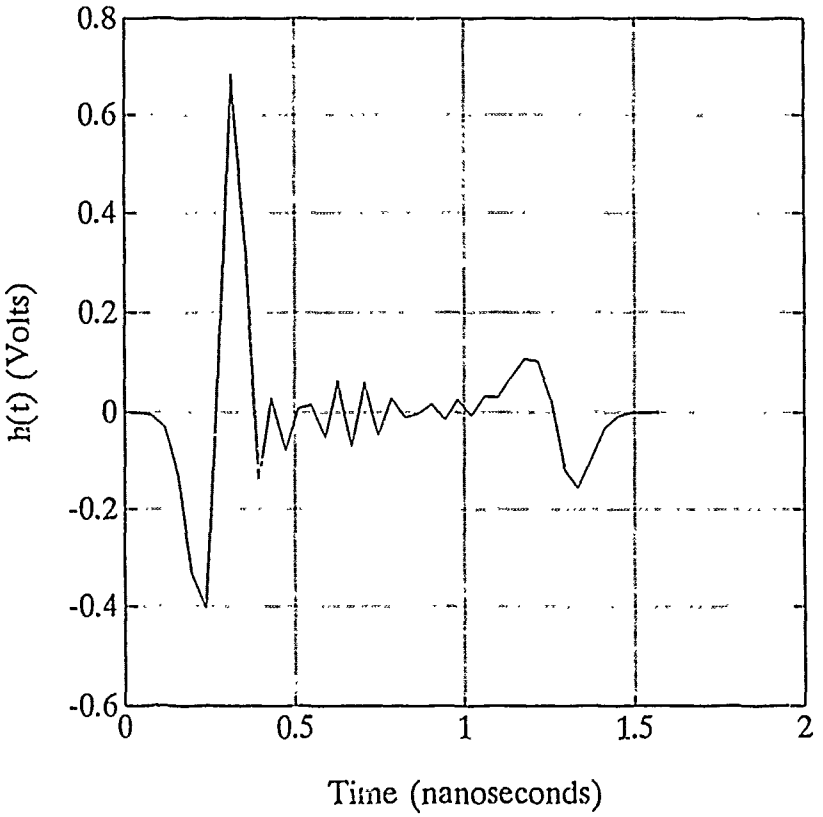

Figure 25. Smoothed medium Q K-Pulse filter

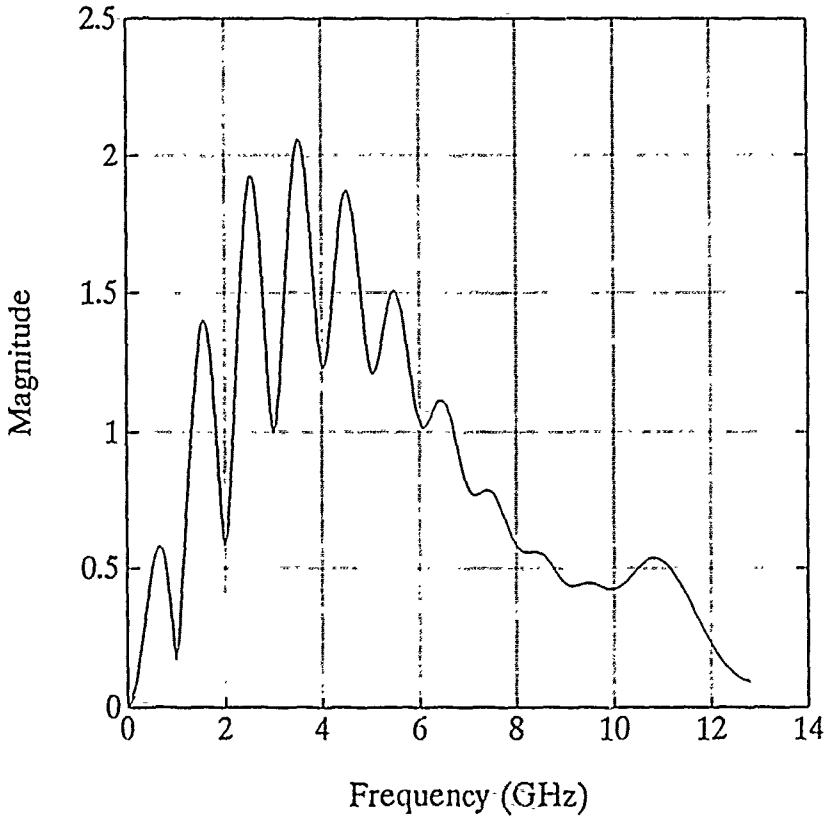

Figure 26. Spectrum of smoothed medium Q K-Pulse filter

a representative case, Figure 27 shows the output of the medium Q smoothed K-Pulse filter operating on the 20 dB correct pole scattering data. Figure 28 shows the same filter processing the 20 dB five percent above data and Figure 29 shows the same filter processing the correct data at 7 dB SNR. Table 6 shows the resulting ratios of average late-time energies between the correct and incorrect target/filter matching.

TABLE 6. RATIOS OF LATE-TIME ENERGIES: ARMA SYNTHETIC DATA

Test Signal	Signal to Filter Match	SNR				
		∞	20 dB	15 dB	10 dB	7 dB
High Q[1]	5 % above	28243	11.03	4.25	2.07	1.56
	5 % below	74442	26.80	8.53	3.59	2.29
Medium Q[2]	5 % above	20639	4.05	1.91	1.26	1.03
	5 % below	67721	11.79	4.4	2.07	1.53
Low Q[2]	5 % above	3568	0.98	0.98	0.99	0.99
	5 % below	8814	1.03	0.99	0.99	0.99

Note 1: Integration time = 5.14 ns
Note 2: Integration time = 1.64 ns

Late-time commences at T_0=2.86 nanoseconds for these trials. This includes the 0.3 nanosecond incident pulse width after a 0.2 nanosecond delay, approximately 0.78 nanoseconds resulting from 20 stages in the ARMA signal generator which represents the $2D/c$ propagation delay over the scatterer, and an additional 1.57 nanoseconds of "shadow-time" created by the delay of the smoothed K-Pulse filter. The length of the integration times beyond the start of late-time was determined by observing the result of the mismatched filter. The summation period

was terminated at a point just past where the significant signal structure remained in the output of an incorrectly matched filter to avoid noise "swamping out" discrimination. This was determined to be eight nanoseconds into the time record for the high Q data and 4.5 nanoseconds for the medium and low Q case; this resulted in integration periods of 5.14 and 1.64 nanoseconds, respectively. Ratios of 3 dB are still achievable down to 10 dB SNR for the medium Q five percent below target. This indicates the validity of the K-Pulse filtering discrimination for a simple target case in the presence of noise.

b. TDIE Thin-Wire Scattering

The synthetic thin-wire data was evaluated by creating a K-Pulse filter matched to the extracted poles, as well as filters derived from five percent variations in the extracted poles. Because of the lower inherent sampling frequency of the TDIE program which created these signals, 480 samples in 20 nanoseconds, and the fact that poles were extracted at sufficiently high enough frequencies, these kill pulses did not require smoothing. The correct filters were convolved with both correct and incorrect data at various signal-to-noise ratios. The results are summarized in Table 7. The late-time integration ran between 1.0 and 3.0 nanoseconds.

The results of the thin-wire data point to the aspect independence of the annihilation filter concept. Notice that the ratios are greatest for low aspect angles. This is due to the fact that a single late-time start value was used, when in fact, for the broadside (90 degree case) there is essentially no $2D/c$ contribution to late-time. Therefore, the latest late-time value selected, which is based on the longest

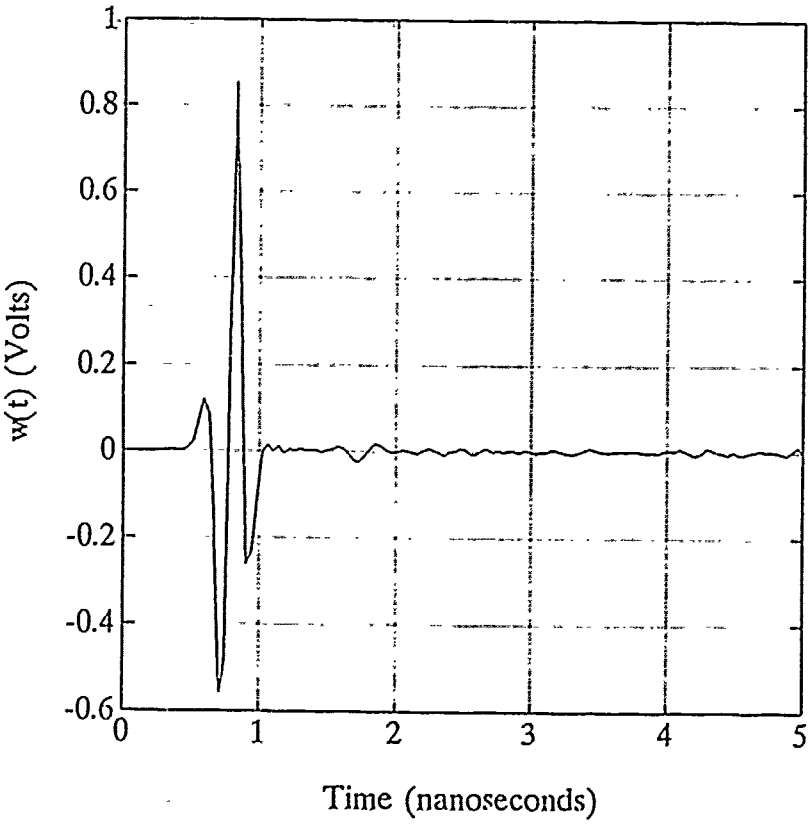

Figure 27. Filter output for correct, medium Q synthetic data, 20 dB SNR

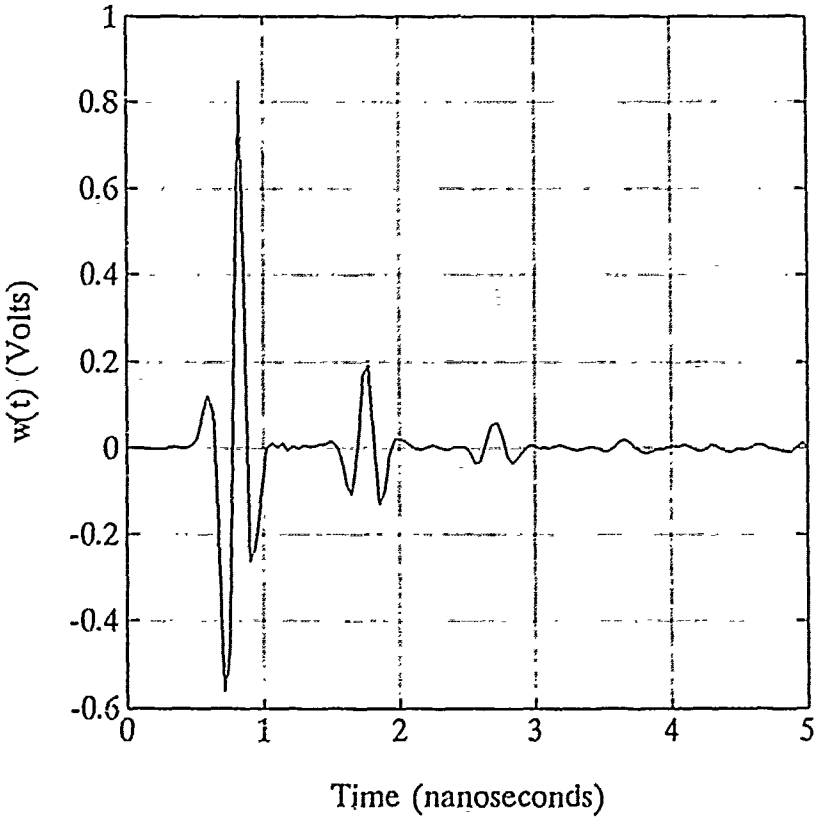

Figure 28. Filter output for five percent above, medium Q data, 20 dB SNR

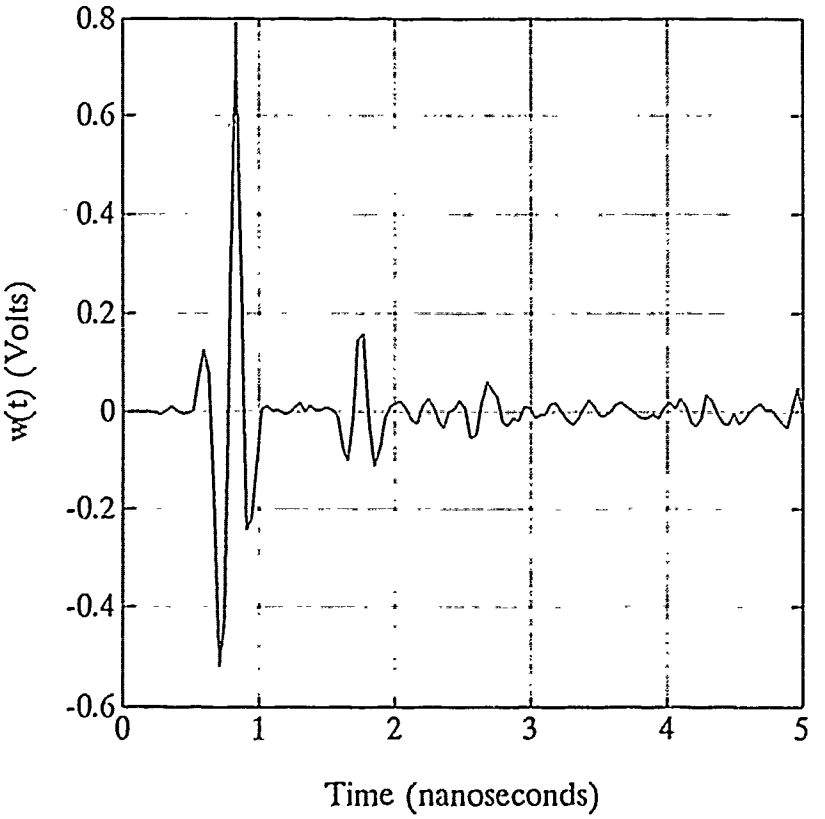

Figure 29. Filter output for five percent above, medium Q data, 7 dB SNR

TABLE 7. RATIOS OF LATE-TIME ENERGIES: TDIE THIN-WIRE DATA

Target Aspect (Degrees)	Filter to Target Match	SNR				
		∞	20	15	10	7
5	5% above	214.58	11.72	1.59	2.16	1.58
	5% below	462.50	24.46	3.10	3.68	2.42
30	5% above	50.92	12.52	5.68	2.73	1.94
	5% below	96.37	21.09	8.68	3.60	2.32
45	5% above	91.80	14.92	6.44	2.92	2.00
	5% below	132.90	19.94	8.04	3.30	2.13
70	5% above	5.31	4.56	3.60	2.39	1.82
	5% below	5.33	4.72	3.82	2.64	2.06
90	5% above	56.59	3.36	1.82	1.27	1.13
	5% below	49.94	2.48	1.42	1.12	1.07

target presentation aspect, starts much later than the significant late-time portion for the broadside case. Additionally, for the symmetric broadside aspect, only the odd modes are excited, further reducing the discrimination.

Figure 30 contains the correct and five percent above filter outputs for the 30 degree aspect case at 15 dB SNR. Notice the residual energy past one nanosecond for the incorrectly matched filter. Figure 31 shows the spectra for the late-time of these two output data records.

c. Measured Thin-Wire Scattering

The same five percent variation of all-aspect, averaged poles was incorporated into filters created for the measured thin-wire data. The input data records for all three aspects (30, 45 and 90 degrees) were passed to all three filters.

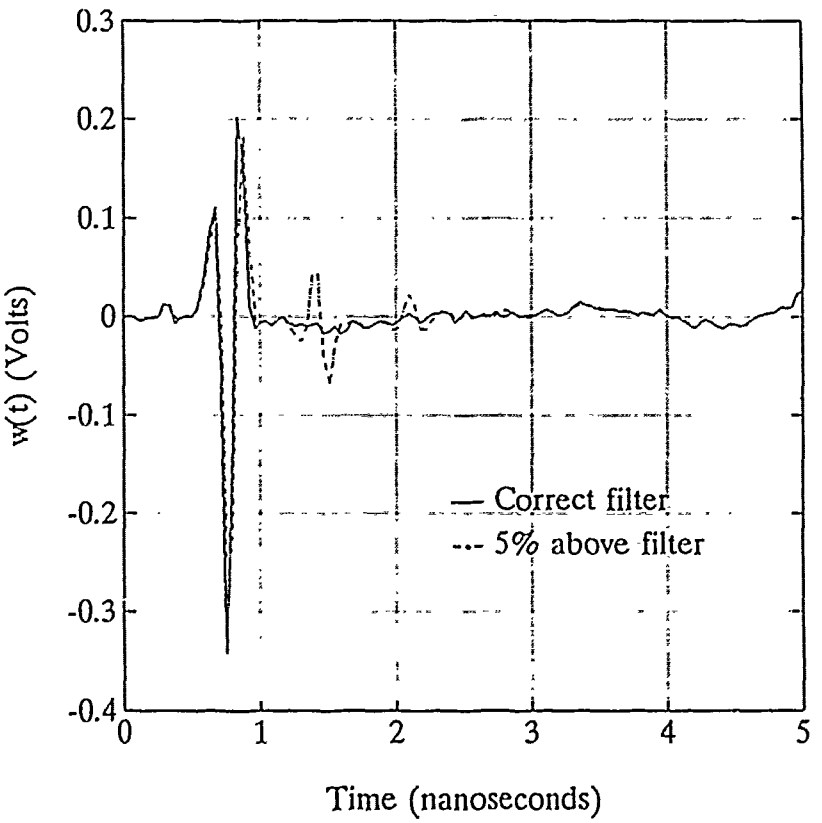

Figure 30. TDIE thin-wire filter output, 30°

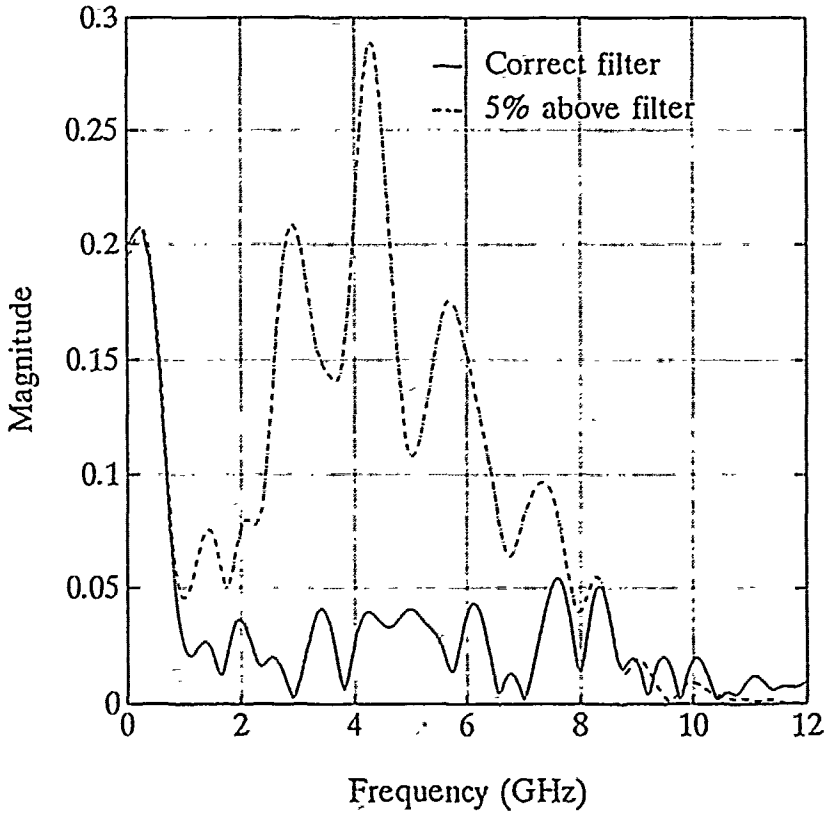

Figure 31. Spectrum of 30° TDIE thin-wire filter output

The resulting ratios of late-time energies are in Table 8.

The best case for this data was 30 degrees aspect, comparing the five percent below to the correct filter. The comparisons of the annihilation filter outputs in the time and frequency domains are in Figures 32 and 33, respectively. Notice that even the correct filter output still contains some frequency information. This is due to the biasing of the extracted poles from their true location in the Cadzow-Solomon extraction process. These relatively small inaccuracies, however, do not preclude proper identification of members of this simple class of targets.

TABLE 8. RATIOS OF LATE-TIME ENERGIES: MEASURED THIN-WIRE

Target Aspect (Degrees)	Filter to Target Match	Ratio
30	5% above	10.22
	5% below	12.68
45	5% above	4.81
	5% below	6.36
90	5% above	2.71
	5% below	2.28

d. Aircraft Scattering

The extracted poles for aircraft target No. 2 were incorporated into an annihilation filter, which was then smoothed. Scattering signals for various aspect angles of targets No. 2 and 3 were passed through the filter. Late-time energy summation was performed for two nanoseconds starting at the appropriate time, based on the late-time inherent in the scattering signal plus a processing "shadow-time" resulting from the K-Pulse filter. The smoothed K-Pulse filter for target No.

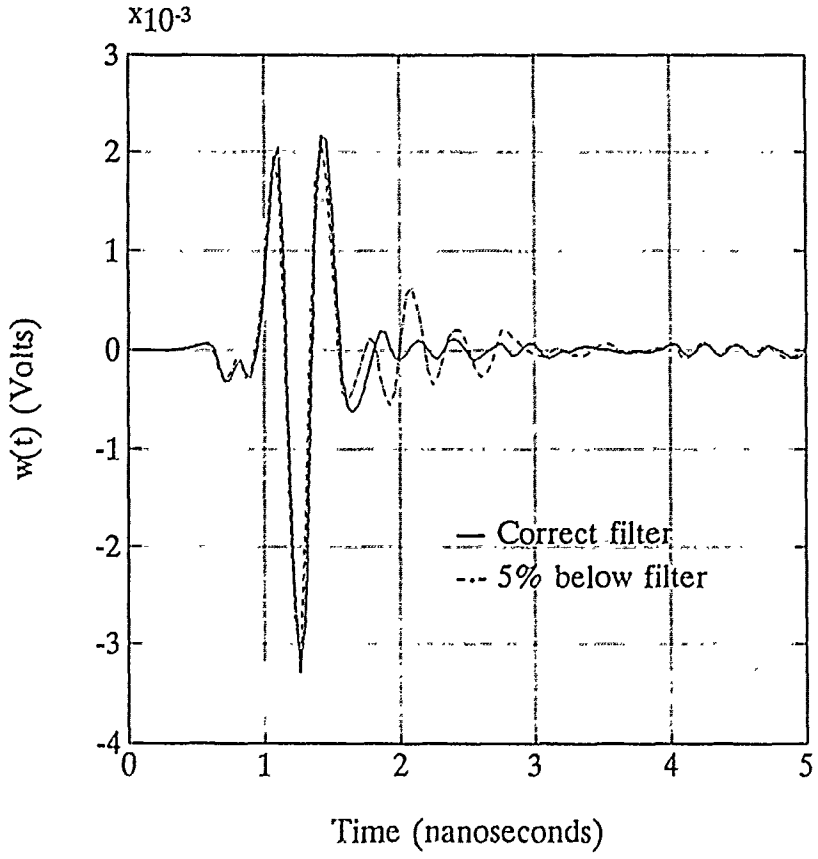

Figure 32. Measured thin-wire filter output, 30°

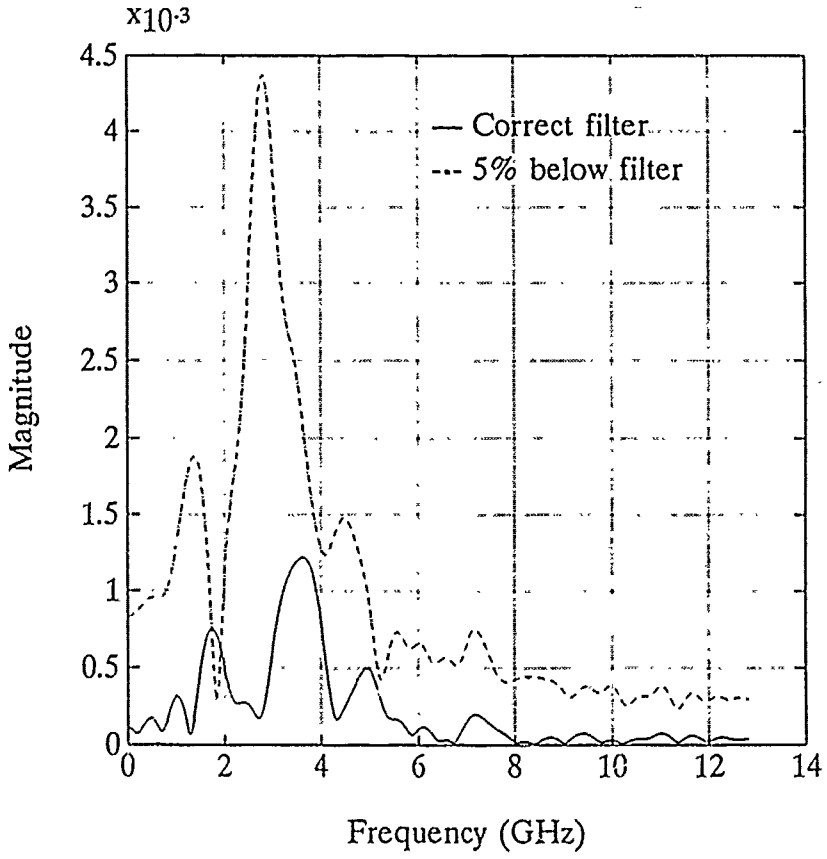

Figure 33. Spectrum of 30° measured thin-wire filter output

2 is shown in Figure 34, its spectrum, in Figure 35. The results of this test, in Table 9, show that the filter could not correctly discriminate target No. 2 from target No. 3. This problem again relates to the difficulty in extracting all the low frequency poles for each target and the similar high population of significant frequency components in this region for both targets, as discussed in Chapter III. Figure 36 shows the output waveforms for targets No. 2 and No. 3, each with nose-on incidence over the late-time energy integration period. Figure 37 shows the spectra of these output data records. Notice that a pole at approximately 2.5 GHz was not annihilated in the correct target signal. This was due to the fact that this pole was extracted for both targets, and, as such, was not included in the target No. 2 filter. At this specific aspect, however, it is excited in target No. 2 and not target No. 3, which leads to incorrect identification. Figures 38 and 39 contain the time and frequency domain plots for the best case indicated in Table 9, the planform view with the wings parallel to the electric field. Here, while the 2.5 GHz resonance seems present in both aircraft, it does not preclude correct identification. These late-time only FFT plots indicate that the effective signal-to-noise ratio in late-time is much less than that if the entire signal, including the strong early time return, is included. Generally, for all the targets examined in this thesis, the ratio of early to late-time peak power is approximately 12 to 16 dB, therefore the late-time signal-to-noise ratio is less than the early-time SNR by that much.

The observations above relate to another result encountered here, namely, a lack of frequency resolution in the K-Pulse filter algorithm was detected.

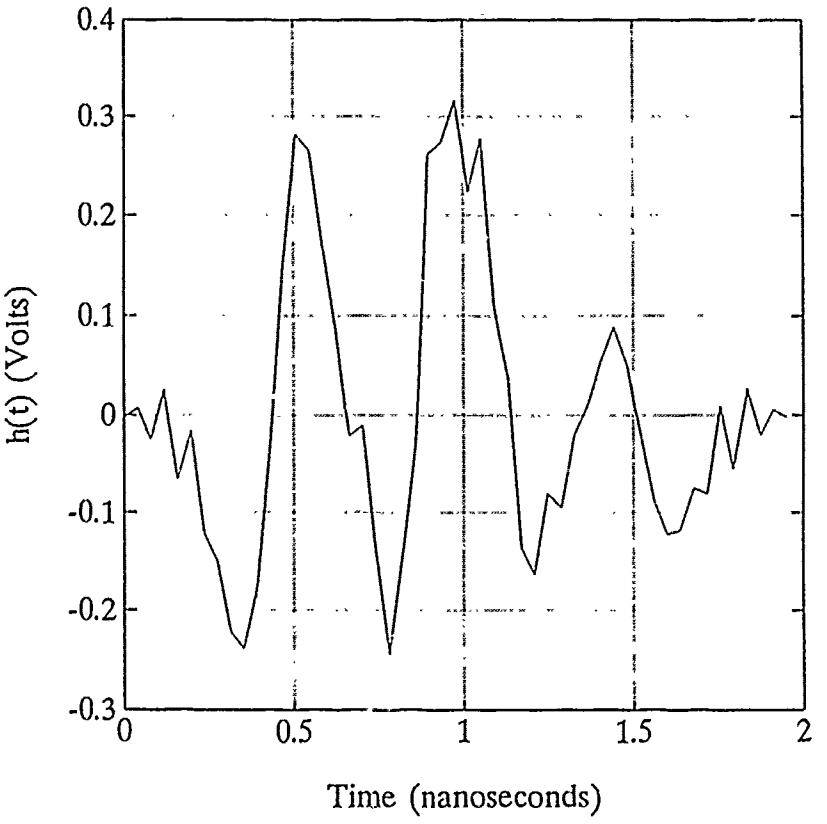

Figure 34. Smoothed K-Pulse filter, target No. 2

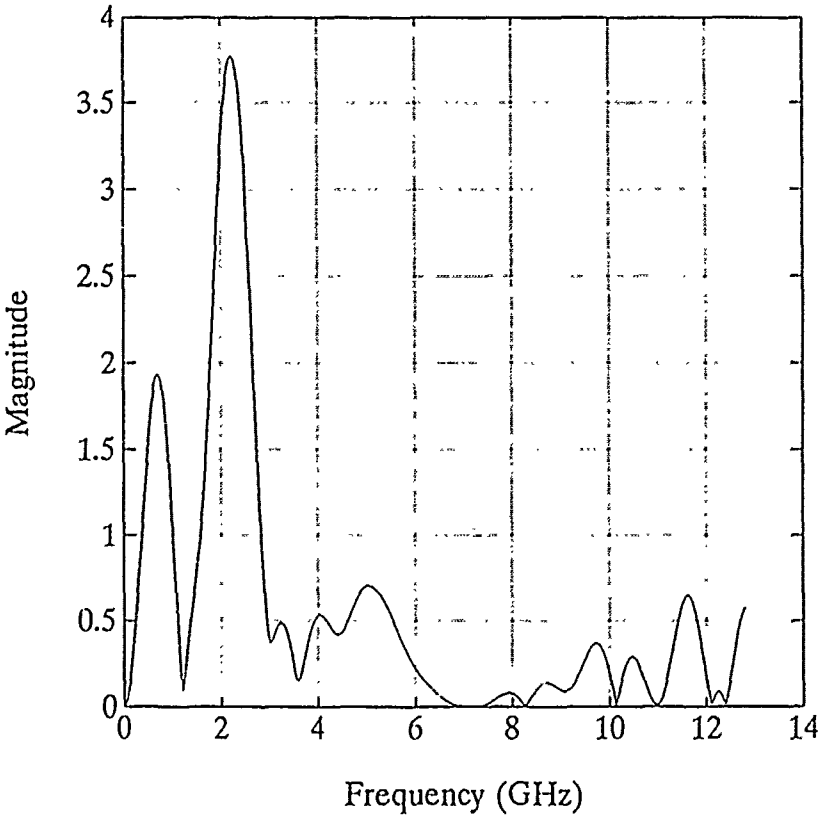

Figure 35. Spectrum of smoothed K-Pulse filter, target No. 2

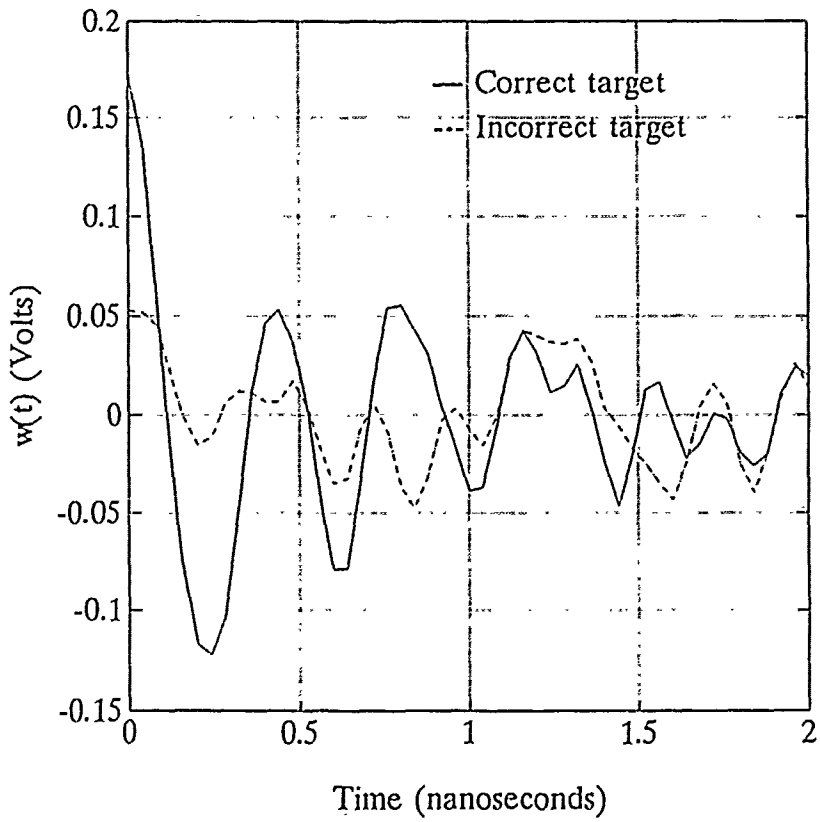

Figure 36. Late-time output of targets No. 2 and No. 3 from target No. 2 filter, nose-on

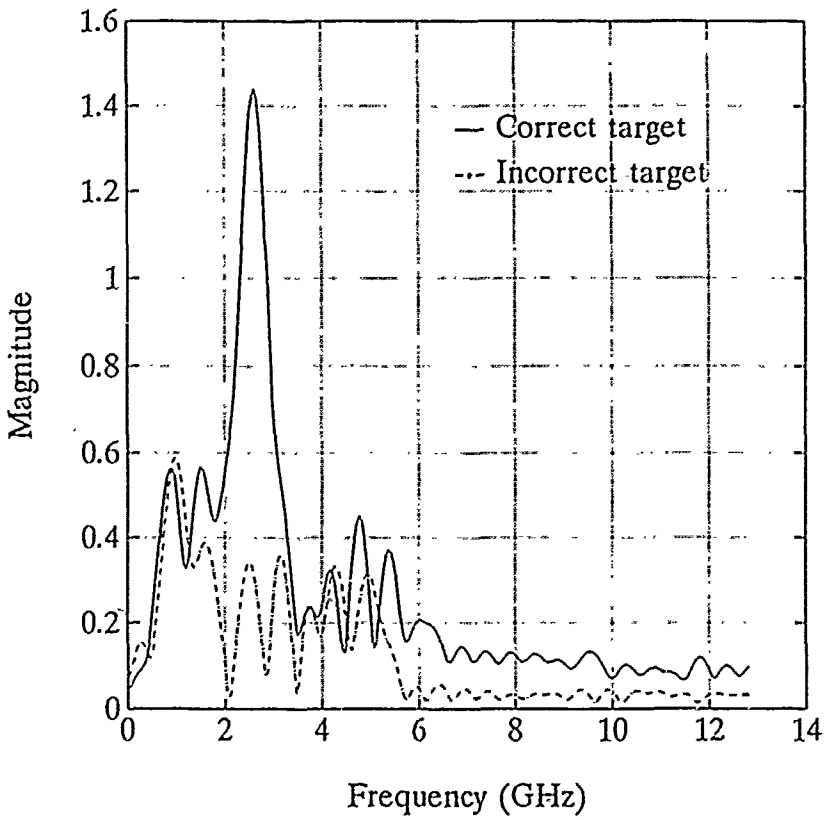

Figure 37. Spectra of output of targets No. 2 and No. 3 from target No. 2 filter, nose-on

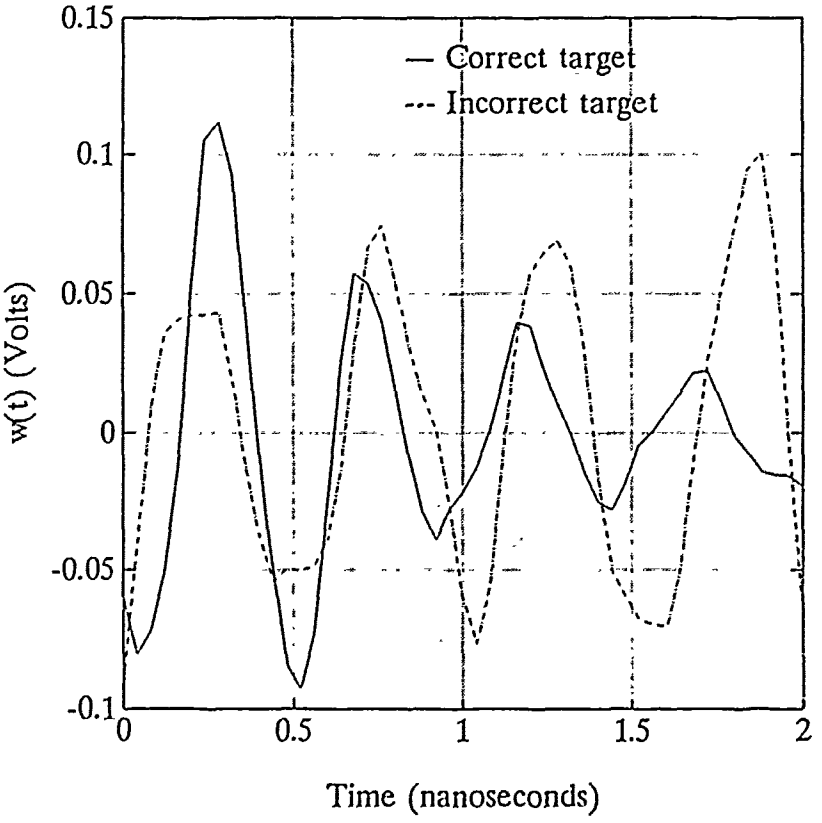

Figure 38. Late-time output of targets No. 2 and No. 3 from target No. 2 filter, wings parallel

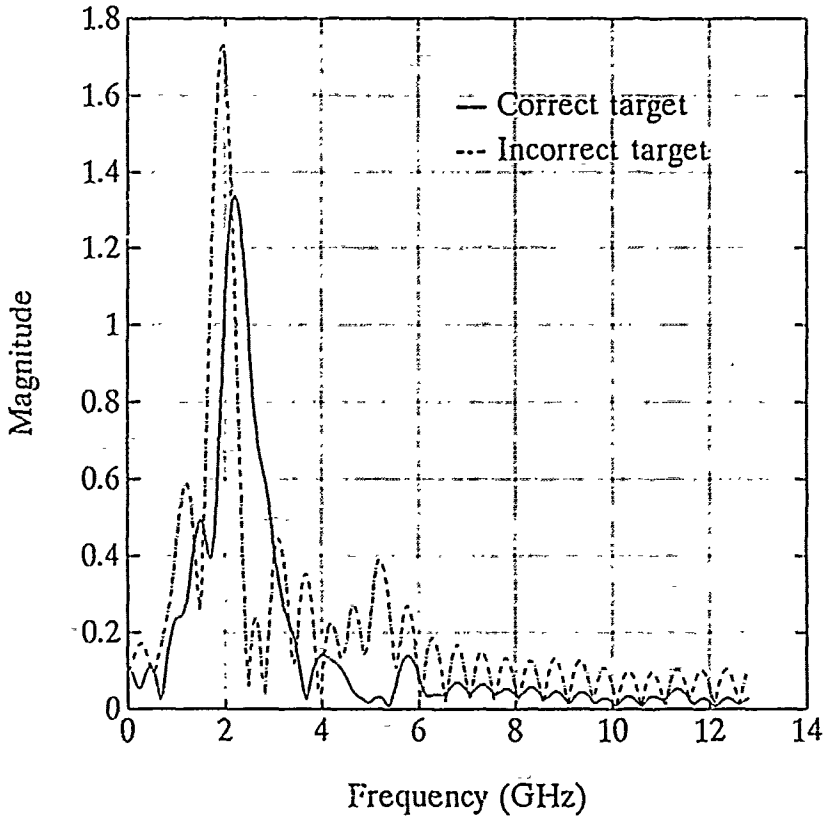

Figure 39. Spectra of output of targets No. 2 and No. 3 from target No. 2 filter, wings parallel

TABLE 9. RATIOS OF LATE-TIME ENERGIES: AIRCRAFT DATA

Target Aspect (Degrees)	Ratio (Tgt 3 LTE/Tgt 2 LTE)
Nose On	0.20
30	0.38
90	0.21
Tail On	3.33
Planform, Wings Parallel	3.38
Planform, Fuselage Parallel	1.32

These targets (targets No. 2 and No. 3) present very closely spaced poles upon extraction, as discussed in Chapter III, Section B. The target No. 2 filter used for the filtering results in Table 8 contains a zero at 1.3 and 1.5 GHz. Examination of a "zoomed-in" portion of the FFT of the unsmoothed version of this filter, Figure 40, shows that the zero corresponding to 1.5 GHz is not clearly distinguishable from that at 1.3 GHz. This means that any target with a pole in this neighborhood will have its energy annihilated, thus reducing the probability of correct discrimination. For this reason, the pole at approximately 2.5 GHz, separated between targets two and three by less than the poles discussed here, precluded incorporation of this zero into the target two filter.

e. Summary

These results are not encouraging, however, further work in the refinement of the extraction process and improvements in the annihilation filters may enable the use of this concept on real scattering data, either from models or full-scale aircraft, down to near the signal-to-noise ratios realized by the synthetic data. The

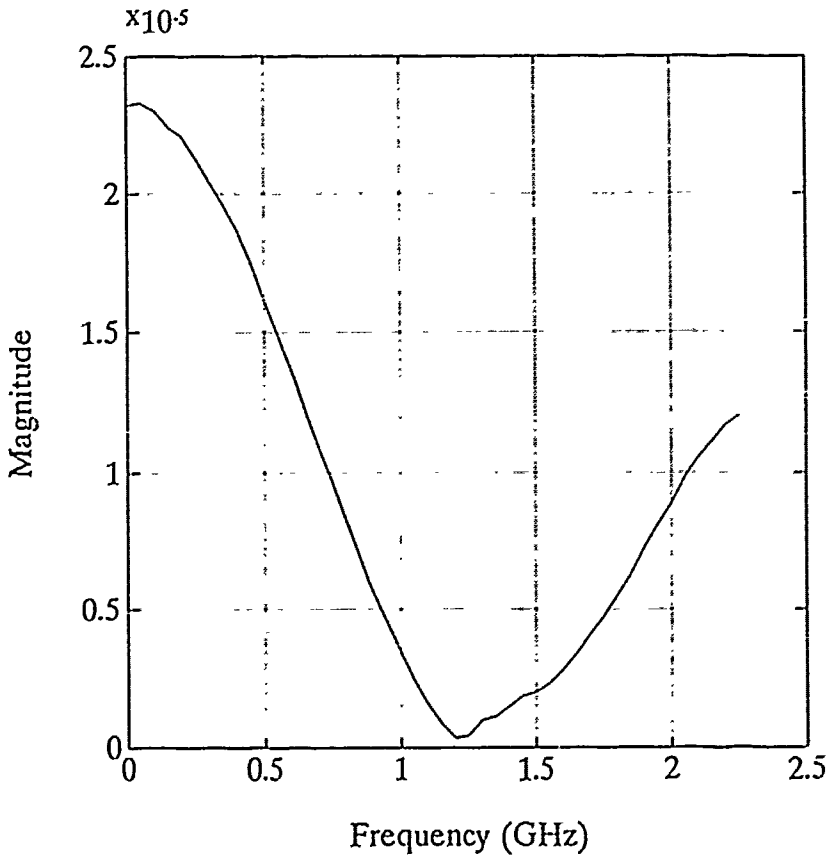

Figure 40. Close-up of FFT of target No. 2 K-Pulse filter

aircraft targets' frequency responses reveal them to be extremely complicated scatterers relative to the other, simpler models used in this thesis. Concentration on intermediate levels of target complexity will allow these algorithms to mature or other, more applicable, ones to surface. One possible avenue of investigation is reducing the bandwidth of the excitation in order to limit the number of similar poles extracted and filtered for each different target. Investigation of the frequency content of scatterers in smaller bandwidths should be conducted to discern if there is an optimum frequency range where various target frequency responses offer the maximum potential for discrimination.

4. Implementation Considerations

The relevant concerns for application of the resonance annihilation filter radar target classification method in an actual system include frequency, bandwidth, SNR required and its affect on transmit power, antenna design, clutter, electromagnetic interference, and post-filter processing and display.

a. Frequency

The transmit frequency for the annihilation filter radar must coincide with the resonances of full-scale targets - approximately 7 to 70 MHz for fighter-sized aircraft. The same considerations raised earlier for the scattering facility apply here (Chapter III, Section C), except that the option to scale the subjects to microwave frequencies no longer exists. The difficulties encountered at this frequency range include increased noise levels, the requirement for large antennas to create high gain,

a crowded spectrum of communications users, and difficult propagation properties as the bandwidth spans the middle HF region, which includes surface and sky-wave modes of propagation, to the lower VHF region, which is line-of-sight [Ref. 30, p. 529].

b. Bandwidth

In order to effect discrimination of similarly sized targets, presumably with only slightly different pole locations within a band, the system bandwidth must be sufficient to excite some number of poles, possibly two to four. As stated above, the frequencies of interest cover a 60 MHz bandwidth. Auton indicates an even wider bandwidth of 20 MHz to 1 GHz and suggests a stepped frequency system which is the most economical way of creating these wide bandwidths in this frequency range [Ref. 25]. However, as suggested above, perhaps a subset of this wide band would be an area in the frequency domain where maximum discrimination is possible among similarly sized targets. If so, this would ease the bandwidth requirements discussed here.

Pole extraction by Murphy [Ref. 6] tends to indicate that the poles of different scatterers, while different from one another, tend to reside in the same neighborhood for each successive mode. While this tends to make target discrimination more difficult, it could allow skipping all but the most relevant frequencies in a stepped frequency system such as that proposed by Auton [Ref. 25]. This skipping would save processing time and reduce interference. The transformed

transient time response could be "filled-in" with the missing frequency through fitting algorithms during the deconvolution process [Ref. 25].

Auton's resonance based target identification system specifically proposes a bank of parallel CW transmit/receive systems each operating at successive frequencies in the band of interest, each with a narrow receiver bandwidth of approximately 0.1 Hz. The system relies on a companion microwave radar to generate range-rate information to center the narrow receiver on the target doppler and avoid clutter. The return signal is processed through deconvolution, as described earlier (Chapter III, Section C). Auton then proposes a rational fitting algorithm to determine the pole locations for comparison to known locations. Here, the substitution of a Resonance Annihilation Filter bank may be made to speed the final step of the classification process. [Ref. 25]

c. Signal-to-Noise Ratio and Range

As a minimum, a late-time signal-to-noise ratio of 15 dB will be assumed for target identification via the RAF concept. Auton [Ref. 25] cites 26 dB at the end of an approximately ten second integration time. This has implications for the range equation applied to this radar. Assuming that the resonance based identification radar will be used with an accompanying microwave surveillance radar, it can be confined to operate as a surface-wave radar in the HF portion of the band and a line-of-sight VHF radar in that band. The range equation for this case (ignoring ionospheric losses) is [Ref. 30, pp. 530-531]

$$R^4 = \frac{P_{av} G_t G_r \lambda^2 \sigma T_c}{(4\pi)^3 k T F_a (S/N) L_s}, \qquad (24)$$

where R is range, P_{av} is average power, G_t and G_r are the transmit and receive antenna gains, λ is the wavelength, σ is target cross section, T_c is coherent processing time, k is Boltzmann's constant, F_a is received noise level above kTB due to other noise sources (discussed below), (S/N) is the required signal-to-noise ratio, and L_s accounts for system loss.

This frequency range, 20 to 100 MHz, is dominated in the low end by atmospheric noise and at higher frequencies, by galactic noise. Assuming a rather large system, such as this radar identification system, would be located in a rural area to avoid man-made noise, the values of F_a, in decibels above ktB, range from 32 dB at 10 MHz down to 7 dB at 90 MHz [Ref.28:p. 34.9]. Substituting these values into the range equation above yields Figure 41. Man-made suburban or urban noise levels, if included in the above calculation, would cause the power levels required to be some 20 to 30 dB higher for frequencies above 25 MHz. The other values involved in the equation are included in the figure and each is discussed below. Nominally, such a system would require approximately 250 kW average power in order to sufficiently the excite the less damped poles in the low frequency end of the resonance spectrum and to allow for increased man-made noise levels above galactic noise in the frequency region above 25 MHz. More power may be required at the lower frequencies even still to overcome the losses due to surface-wave attenuation

caused by the radar energy coupling into the ground. This phenomenon is most critical around 15 MHz and falls off with increasing frequency [Ref. 31].

The radar cross section value used above represents an average; in fact, as this is the resonance region for the targets of interest, the return signal strength can vary greatly with small changes in frequency. As the radar generates a wideband signal, the stronger resonances, used for identification, will boost the return signal. The average value indicated is derived from averaging a value at each frequency determined by approximating the actual target backscatter cross section with that of a 2:1 prolate spheroid with perpendicular electromagnetic excitation incident at 30 degrees [Ref. 32:p. 361].

d. Antenna Design

The necessity to operate over a ten-to-one bandwidth will demand much from the antenna system used for a resonance identification radar. The gain value used above, although realistic [Ref. 30:p. 532], will not remain constant over the band. As such, the antenna will represent a compromise design rather than a point design.

The polarization of the system would ideally be horizontal, as this would allow for the most coupling into the resonances of the fuselage and wingspan of the aircraft targets in level filght. However, due to the size of the arrays involved and the higher surface-wave attenuation for horizontal polarization for the lower frequency range of the system, the most suitable antenna will likely be a large array of vertical monopoles or dipoles.

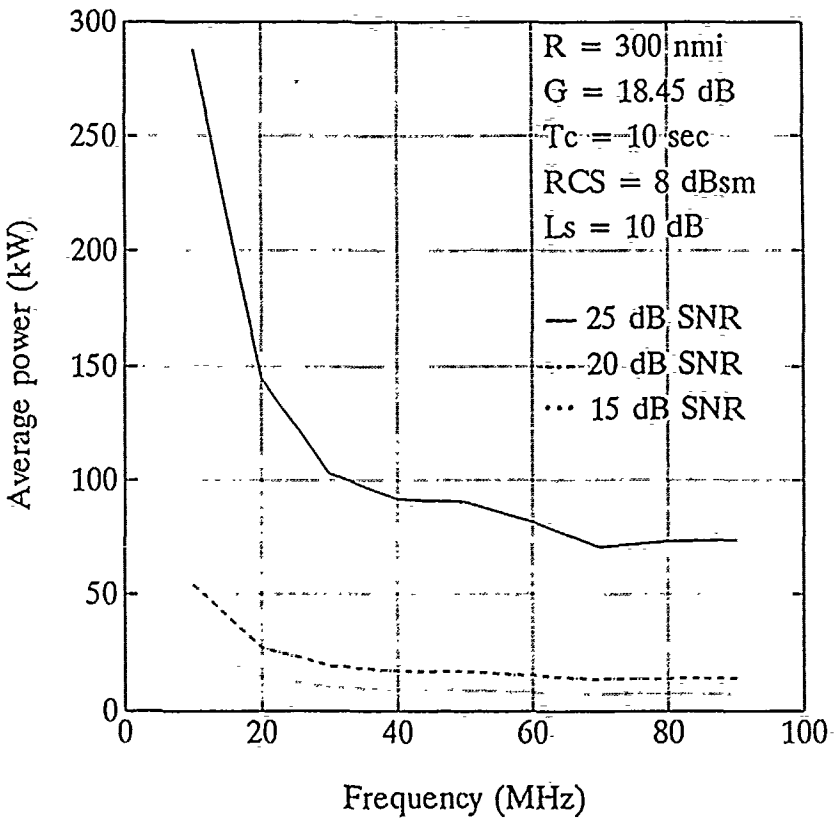

Figure 41. Average power versus frequency and SNR

In order to reduce the clutter and noise, the radar should have as narrow azimuth and elevation beamwidths as possible. However, the large antenna size will limit this: a two degree azimuth beamwidth (broadside) would require an aperture length of 1700 meters at 10 MHz or 190 meters at 90 MHz. One alternative often exploited at these low frequencies is the use of a broad, low gain transmit beamwidth generated by driving only a few elements of the array, overlaid with a number of more precise receive beamwidths. This reduces the cost and complexity and still retains some gain and resolution cell precision [Ref. 30:p. 531].

The varying propagation effects between the frequencies above and below 40 MHz may warrant two separate antenna systems tied together for wideband processing and annihilation filtering. Here, the stepped frequency nature of the system suggested by Auton [Ref. 25] may make this possible. The higher frequency resonances of the target scatterers are the most highly damped, so it may be found upon testing full-scale aircraft in actual conditions that the the higher end of the band is not cost effective.

Another consideration in the design and placement of the antenna is the interference phenomena due to multipath propagation from reflected signals at low grazing angles. The patterns which develop are highly frequency and geometry dependent. At the maximum extent of the effect, the return signal strength can be doubled or eliminated [Ref. 33:pp. 341-361]. This effect may be ameliorated by the wideband nature of the system, but may also inconsistently attenuate critical resonances required for target discrimination.

e. Clutter

The problem of clutter will be even more insidious in the resonance identification radar than in normal search or tracking radar in that the frequency content itself of the return signal is important. Auton suggests the use of narrowband, doppler tracking filters to avoid most of the clutter [Ref. 25]. Additionally, controlling the propagation and precise time-gating may reduce clutter from its various sources over the band: reflections off the surface and sky-wave reflection from the ionosphere at higher HF frequencies.

Sea clutter is, in fact lower, in the frequency region of interest than in the microwave frequencies, however, the advantage is more pronounced with horizontal polarization, which may not be an option, considering the element size. In an attempt to classify low flying targets over water, controlling the sea clutter by manipulating elevation angle may become difficult in light of the requirement to avoid multipath interference. [Ref. 30:p. 483]

The scattering data collected for this work uses a deconvolution process to remove non-target returns. This process may have application in the real world systems whereby the system could alternate the timing or direction of the information processed to allow a comparison of the target return and a non-target return via deconvolution. This processing would have to be done rapidly and may complicate the annihilation filtering process, but may be a necessary clutter rejection tactic.

f. Electromagnetic Interference

Examination of a frequency allocation chart between 7 and 70 MHz indicates a crowded spectrum of communications users filling the band [Ref. 34:p. 1.10]. Also, due to ionospheric effects, the generation of high power, wideband transmission by this system will create interference problems. Again, a stepped frequency system would allow skipping protected or overcrowded portions of the band with subsequent deconvolution and rational function fitting filling in. Additionally, during operations of this system, friendly communications may be coordinated to avoid interference.

As a victim of EMI, the system must deal with the crowded spectrum and man-made noise, as discussed earlier. This drives up the required transmit power for a given SNR, and will dictate deployment location in remote, yet, tactically significant areas. As a victim of electronic countermeasures, the system's wide bandwidth may offer some inherent jam resistance. However, the criticality of the various frequency components used to discriminate one target from another and the requirement for a greater SNR than required for mere detection systems, may make the system vulnerable. Operationally, the loss of this system to jamming is, itself, a hostile target identifier.

g. Post-filter Processing and Display

The annihilation filters operate on the decision criterion of ratios of late-time energy. In the presence of noise, these ratios are probablistic in nature. Norton conducted a rigorous analysis of the probability density function of this

process in [Ref. 4]. In order to operate as a real-time tactical or strategic decision aid the target resonance radar must quickly indicate its classification information to the operator, yet it must account for the possibilities of incorrect identification or inconclusive results. This will require high speed processing of the resonance annihilation filter outputs followed by the appropriate display. This display may take the form of a ranking of the most probable identities of the target being tracked and the confidence level of the identifications listed. Present work in artificial intelligence systems applied to imaging systems such as synthetic aperture radar offer a lead in the area of real-time man-machine interface for rapid target identification.

h. Summary

The implementation of a natural resonance target identification system represents no greater technological risk than other radar systems that have been developed in this frequency range. The most difficult implementation task will be isolating the relevant target return for identification processing from the entirety of the radar return in time and space, in order to exclude as much noise and clutter as possible and to concentrate the analysis on a single target.

C. INVERSE ARMA FILTER

1. Methodology

The inverse ARMA filter represents an extension of the K-Pulse filter concept to include canceling early-time resonance energy as well as late-time. As

such, it immediately surrenders the aspect independence property of the annihilation filter discussed earlier.

The transfer function of a scatterer is represented as a ratio of z transform polynomials

$$H_t(z) = \frac{b_0 + b_1 z^{-1} + \cdots + b_L z^{-L}}{1 + a_1 z^{-1} + \cdots + a_N z^{-N}}. \tag{25}$$

The inverse ARMA filter frequency response is formed by inverting this transfer function

$$H_{IA}(z) = \frac{(1/b_0)[1 + a_1 + \cdots + a_N z^{-N}]}{1 + \frac{b_1}{b_0} z^{-1} + \cdots + \frac{b_L}{b_0} z^{-L}} \tag{26}$$

Consider the scattered response from the target $y(t)=h_t * x(t)$, due to the interaction of the incident pulse, $x(t)$, with the target's impulse response, h_t. In the frequency domain, $Y(z)=H_t(z)X(z)$. Now, the inverse ARMA filter impulse response, h_{IA}, is derived from the inverse of the target's transfer function, so $H_{IA}=H_t^{-1}$. The filtering action is described by $w(t)=y(t)*h_{IA}$, which gives this result in the frequency domain:

$$W(z) = Y(z)H_{IA}(z) = Y(z)H_t^{-1}(z) = H_t(z)X(z)H_t^{-1}(z) = X(z). \tag{27}$$

In fact, the appropriately matched inverse ARMA filter will annihilate all early and late-time resonant energy, leaving only a replica of the incident pulse. For an inverse

ARMA filter which is not matched to the target, i.e. $H_{IA} \neq H_t$, no such cancellation will occur. [Ref. 35]

The inverse ARMA filter achieves another advantage over the K-Pulse filter in that it is, itself, an ARMA filter that inherently smoothes noisy input. As such, it requires no additional smoothing as the K-Pulse filter did. [Ref. 35] The inverse ARMA program is in Appendix H.

2. Performance

The effectiveness of the inverse ARMA was tested against the synthetic scatterer model discussed in Chapter II. This is the only available signal for which the feed-forward coefficients, b_k, were known. For actual signals, the Cadzow-Solomon algorithm would have to be modified to extract these coefficients. Presently the algorithm, particularly the bias compensation portion, is optimized to determine the a_k coefficients; the feedback coefficients which describe the target resonances. The requirement to know both the feed-forward and feedback coefficients forces the inverse ARMA identification process to be aspect dependent.

The results of the an inverse ARMA filter processing correctly matched, as well as five percent above and below, synthetic signals is summarized in Table 10. In order to allow a comparison of these results to those of the K-Pulse filter acting on these same targets, the late-time integration periods were kept the same (5.14 ns for the high Q, 1.64 ns for medium and low Q). Importantly, though, this period was slid forward in time to approximately 0.742 nanoseconds into the record, well into early-time. Comparison of Table 10 with Table 6 indicates the advantage the inverse

ARMA process realizes in discrimination using early-time energy. Figure 42 shows the inverse ARMA filter output for the 20 dB medium Q case and Figure 43 shows the output for the five percent above filter output. These results can be compared to Figures 27 and 28 for the K-Pulse filter. Notice that the correct filter output is simply a reproduction of the incident pulse; all the target return has been deconvolved out of the data. Both the high and medium Q cases show the inverse ARMA with significantly greater ratios of incorrect-to-correct filter late-time energies than the normal K-Pulse filter. In fact, the inverse ARMA performance would probably be better if the integration time were not limited to the same length as the K-Pulse filter for direct comparison.

TABLE 10. RATIOS OF OUTPUT ENERGIES FOR IARMA FILTER

Test Signal	Signal to Filter Match	SNR				
		∞	20 dB	15 dB	10 dB	7 dB
High Q[1]	5 % above	12880	57.70	18.90	6.63	3.80
	5 % below	14310	66.12	21.07	7.92	4.58
Medium Q[2]	5 % above	4420	58.12	18.75	6.42	3.63
	5 % below	4630	65.22	22.10	8.10	4.76
Low Q[2]	5 % above	417	6.08	2.43	1.35	1.13
	5 % below	422	7.56	3.25	1.81	1.45

Note 1: Integration time = 5.14 ns
Note 2: Integration time = 1.64 ns

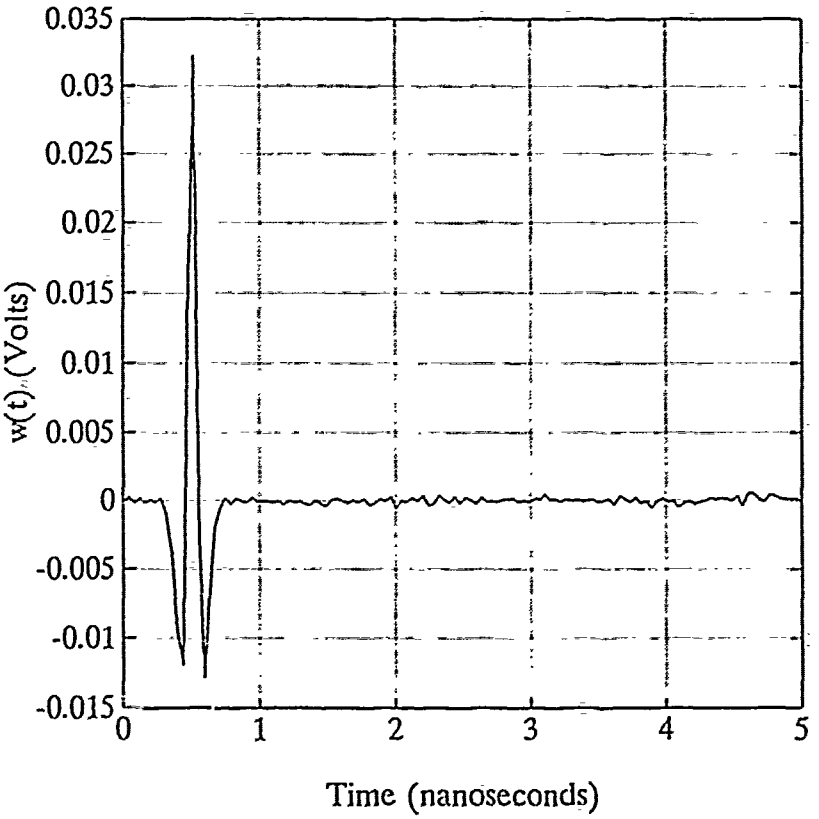

Figure 42. Correct IARMA filter output at 20 dB SNR

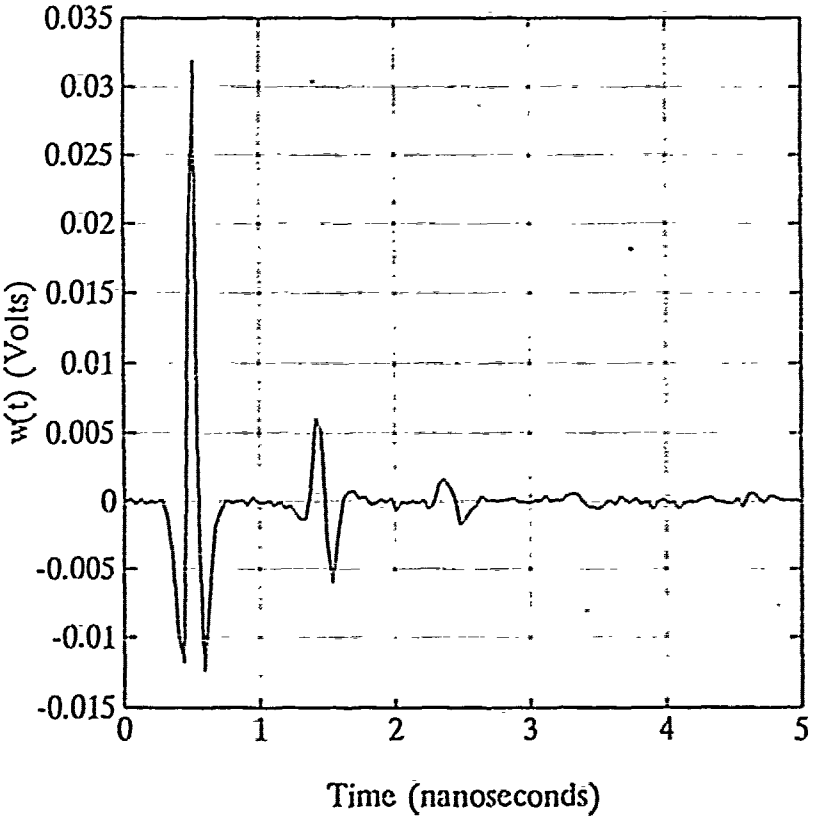

Figure 43. Five percent above IARMA filter output at 20 dB SNR

3. Implementation Considerations

The most significant change in using an inverse ARMA filter process for target identification, over the use of a K-Pulse filter system, is the fact that it is *not* an aspect independent process. Thus the feed forward coefficients of the target transfer function, the b_k's, would have to be determined for a family of target aspects of most concern for each target. The RAF concept described earlier would be much more complex, as the target aspect would have to be determined by another radar, then the response would have to be routed to a filter for that aspect for each possible target. Additionally, the number of filters required to cover the target aspects of interest (say, a 60 degree sector about the nose) would have to be determined during the extraction process. Perhaps the coefficients for certain discrete aspects within this region could be determined and some function fit to them to determine those in between. In any case, it is unlikely that the feed-forward portion of the target transfer function would be exactly matched in the IARMA filter. This would then require a closed loop, adaptive system of filters that could start with the coefficients as extracted in the filters nearest the target aspect detected. Then, the adaptive controller would dither or optimize the filter coefficients in real-time to draw out the greatest ratio of energies output from the filters. This would require much increased integration time on the target and an extremely fast and, perhaps, expert adaptive controller. [Ref. 35]

The concerns expressed above for implementation of the K-Pulse filter, such as frequency, bandwidth, and signal-to-noise ratio, remain for the inverse ARMA

concept. Considering the increased complexity due to the dependence on target aspect, practical implementation of the inverse ARMA filter process for target identification would significantly lag that of a FIR-based, aspect independent method such as the K-Pulse filter.

V. SUMMARY AND CONCLUSIONS

A. SUMMARY

This thesis has examined a resonance-based, aspect independent radar target identification system to include both major subsystems: pole extraction and annihilation filtering. Chapter I presented the theoretical analysis of electromagnetic scattering which gives rise to target resonances based solely on structure and composition, independent of incident field aspect or polarization. Chapter II discussed the four classes of signals used to evaluate the system's algorithms, namely: ARMA generated synthetic data, TDIE thin-wire data, actual measured thin-wire data, and data collected from scale model aircraft. Chapter III presented the theory of the leading candidate pole-extraction algorithm: the Cadzow-Solomon algorithm, results of its use on the target signals, and some initial implications for real world application. Chapter IV applied those extraction results in resonance annihilation filters to evaluate target discrimination and discussed relevant areas of concern for actual implementation of this portion of the system. Additionally, the inverse ARMA, an aspect *dependent* resonance-based target identification scheme was compared to the aspect independent method.

B. CONCLUSIONS

The eventual goal of application of a resonance-based target identification system is to gain early identification of non-cooperative aircraft targets. The scattering of these class of targets, as modeled by the scale aircraft used in this thesis, is extremely complex and spectrally rich, as compared with that of the more simple thin-wire targets used herein. Intermediate levels of target complexity, such as few element thin-wire structures should be investigated via these algorithms in order to refine and mature their application.

The Cadzow-Solomon pole extraction algorithm does adequately extract poles of simple, thin wire targets, both simulated and actual. It requires a signal-to-noise ratio above 20 dB and its result is sensitive to its various input parameters, especially the starting point of its input data relative to the end of early-time. The over-estimation of the system order and resultant ill-conditioning of the data matrix, while necessary to allow for noise, does introduce some bias in the extracted pole locations. The complexity of the frequency spectrum of the scattering from more complex targets, such as the model aircraft, serves as a limiting factor on the algorithm's ability to extract poles.

Implementation of a pole extraction scattering facility is feasible with the major caveat being accessibility to relevant targets for scattering analysis. The choice presented is between actual full-scale targets, which will be difficult to obtain and work with, considering their size; and scale model targets, whose resonance frequency

range is more amenable, but whose fidelity to the full-scale targets must be thoroughly evaluated before implementation.

The K-Pulse resonance annihilation filter does effectively discriminate simple targets with sets of poles separated by five percent in the presence of noise down to 10 dB SNR. However, more complicated targets present an increasingly difficult task because their pole locations are many and are closely and irregularly spaced. The K-Pulse filter, in its simplest form, has a finite limit on the frequency resolution of zeros of different targets it seeks to discriminate. This is due to the finite width of a zero null in the frequency response of the filter.

Implementation of the resonance annihilation filter radar for fighter-sized targets will require operation in the medium HF to low VHF bands: approximately 7 to 100 MHz. The design challenges here are the same as for any radar system in this regime and with the additional requirement to obtain as precise a spatial and temporal resolution as possible in order to isolate the target return from noise, clutter, and other targets. Analysis of the range equation for a system operating at 300 nautical miles indicates the requirement for 250 kW of average transmit power. These requirements are within the state-of-the-art for radar systems. The greatest technological emphasis required will be in the application of advanced computing or artificial intelligence to control the radar system precisely and assist the operator in analysis of the returns.

The inverse ARMA algorithm is superior to the K-Pulse algorithm, but is more difficult to implement in that it is *not* aspect independent. This would require a

modification of the pole extraction process to allow extraction of poles and zeros of the target's transfer function. This aspect dependence also adds the requirement to create many filters for a single target to account for aspect. This additional requirement would further emphasize high speed processing to allow tailoring of the filters to account for the feed forward, aspect and excitation-dependent portion of the target response.

C. AREAS FOR FURTHER RESEARCH

The identification of non-cooperative aircraft targets may be accomplished by other means, such as high-range resolution or synthetic aperture radars, or other target characteristics. As all these technologies mature, the relevant benefits and costs of each must be compared.

The specific algorithms discussed earlier for resonance-based identification must be refined by application to more intermediate levels of target complexity. Additionally, study of the frequency response of these less complicated targets, as well as aircraft targets, may discern the appropriate bandwidth requirements to allow the most effective target discrimination possible.

D. UTILITY

As the technology of the attacker becomes more advanced, effective, and prolific, i.e. stealth, longer range precision guided munitions, etc., the technology of NCTR becomes more imperative. Resonance-based target identification is such a technology that holds promise for development into a viable means of NCTR.

APPENDIX A. ARMA COEFFICIENT GENERATOR

A. PROGRAM DESCRIPTION

This program generates the a_k and b_k coefficients of a scatterer transfer function given by

$$H(z) = \frac{b_0 + b_1 z^{-1} + \cdots + b_L z^{-L}}{1 + a_1 z^{-1} + \cdots + a_N z^{-N}} \tag{A.1}$$

after reading a data file containing the s-plane poles for each of the N pole pairs. The program also reads in the sampling information to allow conversion of the input s-plane values to the z-plane. Additionally, the program allows input of a complex multiple of each z-plane pole pair to allow simulation of the relative amplitude and phase of the transfer function poles.

This program was written by Capt. T. J. Murphy and Capt. P. C. Reddy and uses the subroutine POLY written by Prof. M. A. Morgan.

B. PROGRAM LISTING

```
      PROGRAM HCOEF
C
      REAL*8 T, A(0:100), B(0:2),NUM1(0:100),ATMP(0:100),NUM2(0:100)
      REAL*8 SPOLR(30), SPOLI(30),PI,MAG(30),PHASE(30),C(30),D(30)
      INTEGER NPTS, NR, N
      COMPLEX*16 SPOL(30), ZPOL(30)
      CHARACTER*16 FNAME, PFNAME

      PI=3.14159265
      WRITE(*,*) 'Enter filename for s-plane poles '
      READ(*,120) PFNAME
```

```
      OPEN(1,FILE=PFNAME)
      READ(1,130) NR
      WRITE(*,*) 'Enter time interval'
      READ(*,*) T
      WRITE(*,*) 'Enter number of points'
      READ(*,*) NPTS
      DO 10 I= 1,NR
      READ(1,*) SPOLR(I)
      READ(1,*) SPOLI(I)
      SPOL(I)=DCMPLX(SPOLR(I),SPOLI(I))
      ZPOL(I)=CDEXP(DCMPLX(T/FLOAT(NPTS  ))*SPOL(I))
      write(*,*) 'z-plane pole =',zpol(i)
      WRITE(*,*) 'Enter magnitude of pole',I
      READ(*,*) MAG(I)
      WRITE(*,*) 'Enter phase (in degrees) of pole',I
      READ(*,*) PHASE(I)
      PHASE(I)=0.0
      MAG(I)=1.0
C     CONVERT MAG AND PHASE TO RECTANGULAR COORD
      C(I)=MAG(I)*COS(PHASE(I))
      D(I)=MAG(I)*SIN(PHASE(I))
10    CONTINUE
      A(0)=1.0
      A(1)=-2.0*REAL(ZPOL(1))
      A(2)=(REAL(ZPOL(1)))**2+(AIMAG(ZPOL(1)))**2
      NUM1(0)=2.0*C(1)
      NUM1(1)=-2.0*(REAL(ZPOL(1))*C(1)+AIMAG(ZPOL(1))*D(1))
      NUM1(2)=0.0
      N=2
      DO 15 I=2,NR
      NUM2(0)=2.0*C(I)
      NUM2(1)=-2.0*(REAL(ZPOL(I))*C(I)+AIMAG(ZPOL(I))*D(I))
      NUM2(2)=0.0
      B(0)=1.0
      B(1)=-2.0*REAL(ZPOL(I))
      B(2)=(REAL(ZPOL(I)))**2+(AIMAG(ZPOL(I)))**2
      DO 17 K=0,N
      ATMP(K)=A(K)
17    CONTINUE
C     CALCULATE NEW DENOMINATOR
      CALL POLY(A,B,N)
C     CALCULATE NEW NUMERATOR
      N=N-2
      CALL POLY(NUM1,B,N)
      N=N-2
      CALL POLY(ATMP,NUM2,N)
      DO 18 L=0,N
      NUM1(L)=NUM1(L)+ATMP(L)
18    CONTINUE
15    CONTINUE
```

```
      WRITE(*,*) 'Enter name of denominator coefficient output file'
      READ(*,120) FNAME
      OPEN(3,FILE=FNAME)
      WRITE(3,130) N
      DO 20 I=1,N
      WRITE(3,*) A(I)
20    CONTINUE
      CLOSE(3)
      WRITE(*,*) 'Enter name of numerator coefficient output file'
      READ(*,120) FNAME
      OPEN(3,FILE=FNAME)
      WRITE(3,130) N
      DO 21 I=0,N
      WRITE(3,*) NUM1(I)
21    CONTINUE
      CLOSE(3)
110   FORMAT(E16.10)
120   FORMAT(A)
130   FORMAT(I5)
      END
C
      SUBROUTINE POLY(A,B,N)
C
C     Multiplying  {B(0)z**2 + B(1)*z + B(2)} x
C     {A(0)z**N + A(1)*z**(N-1) + A(2)*z**(N-2) + .... + A(N)} =
C     C(0)z**(N+2) + C(1)*z**(N+1) + C(2)*z**N + ....  + C(N+2)
C
C     Computing C(n) coefficients and storing in A(n) while
C     incrementing N --> N + 2
C
      REAL*8 A(0:100),B(0:2),C(0:100)
C     A(0)=1.0
C     Initialize on first call to routine
C     IF(N.GE.2) GO TO 11
C     N=2
C     A(1)=B(1)
C     A(2)=B(2)
C     GO TO 44
11    C(0)=B(0)*A(0)
      C(1)=B(0)*A(1)+B(1)*A(0)
      DO 22 I=2,N
22    C(I)=B(0)*A(I)+A(I-1)*B(1)+A(I-2)*B(2)
      C(N+1)=A(N)*B(1)+A(N-1)*B(2)
      C(N+2)=A(N)*B(2)
      N=N+2
      DO 33 I=0,N
33    A(I)=C(I)
44    CONTINUE
      RETURN
      END
```

APPENDIX B. ARMA SIGNAL GENERATOR

A. PROGRAM DESCRIPTION

This programs generates the time response of an ARMA system via the equation

$$y(n) = \sum_{k=1}^{k=N} a_k y(n-k) + \sum_{k=0}^{k=L} b_k x(n-k) \qquad \text{(B.1)}$$

where $x(n)$ is the input excitation record, a_k and b_k are the coefficients determined by the program in Appendix A, and $y(n)$ is the output data record.

This program was written by Prof. M. A. Morgan.

B. PROGRAM LISTING

```
      Program ARMA2
C
C     Computing y[n] response for N-th order ARMA filter due to x[n]
C     input, with coefficients:
C
C              IIR  a(k) for k=1,N
C              FIR  b(k) for k=0,L
C
C     by M.A. Morgan 5/23/90
C
      REAL*8 x(0:2047),y(0:2047),a(1:30),b(0:32)
      CHARACTER*64 TITLE,TITL
      CHARACTER*16 FNAME
C     Entering D.E. Coefficients
      WRITE(*,*) 'Enter Filename For Recursive a(k):'
      WRITE(*,*) 'Use 0 for FIR Filter'
      READ(*,100) FNAME
      IF(FNAME.EQ.'0') GO TO 15
      OPEN(2,FILE=FNAME)
C     Assuming that a(k) are reversed polarity in file.
      READ(2,110) N
```

```
      write(*,*) 'Write k, a(k):'
      DO 11 k=1,N
      READ(2,*) a(k)
      a(k)=-a(k)
      write(*,*) k,a(k)
11    CONTINUE
      CLOSE(2)
15    CONTINUE
      WRITE(*,*) 'Enter Filename for Non-Recursive b(k):'
      READ(*,100) FNAME
      OPEN(2,FILE=FNAME)
      READ(2,110) L
      write(*,*) 'Write k, b(k):'
      DO 22 k=0,L
      READ(2,*) b(k)
      write(*,*) k,b(k)
22    CONTINUE
      CLOSE(2)
      WRITE(*,*) 'Enter Filename for x[n] Plot File:'
      READ(*,100) FNAME
      OPEN(2,FILE=FNAME)
      READ(2,100) TITL
      READ(2,110) NX
      READ(2,120) XQ
      READ(2,120) XQ
      write(*,*) 'Write m, x(m):'
      DO 24 m=0,NX-1
      READ(2,120) x(m)
      write(*,*) m,x(m)
24    CONTINUE
      CLOSE(2)
C     Setting up Plot File for y[n]
      WRITE(*,*) 'Enter Number of Points: (.le. 2048)'
      READ(*,*) NY
      WRITE(*,*) 'Enter time interval (nanoseconds)'
      READ(*,*) Tmax
      Tmin=0.0
      WRITE(*,*) 'Enter filename for y[n] response output'
      READ(*,100) FNAME
      TITLE= 'ARMA Filter y[n] Response'
      OPEN(1,FILE=FNAME)
      WRITE(1,100) TITLE
      WRITE(1,110) NY
      WRITE(1,120) Tmin
      WRITE(1,120) Tmax
C     Initializing then iterating to form y[m]
      y(0)=b(0)*x(0)
      write(1,120) y(0)
      DO 44 m=1,NY-1
      y(m)=0.0
```

```
      Lmax=MIN(m,L)
      DO 27 k=0,Lmax
27    y(m)=y(m)+b(k)*x(m-k)
      Nmax=MIN(m,N)
      DO 33 k=1,Nmax
33    y(m)=y(m)+a(k)*y(m-k)
      write(*,*) y(m)
      WRITE(1,120) y(m)
44    CONTINUE
      WRITE(*,*) 'Thats All Folks !'
      CLOSE(1)
100   FORMAT(A)
110   FORMAT(I5)
120   FORMAT(E12.6)
      STOP
      END
```

APPENDIX C. NOISE POLLUTION GENERATOR

A. PROGRAM DESCRIPTION

This program reads in a data file and computes the signal power. After inputing a seed between zero and one, it uses a routine from the FORTRAN Scientific Libraray called STRNUM to generate numbers under a zero mean uniform distribution. This routine is called 1000 times for each additive noise point corresponding to each point of the input record, in order to drive the random number to a zero-mean Gaussian distribution. The variance of the random noise generated is scaled to accomodate a user input signal-to-noise ratio.

This program is based on a signal generator originally written by Prof. M. A. Morgan, modified successively by Lt. L. A. Cheeks, Lt. M. S. Simon, and Capt. T. J. Murphy.

B. PROGRAM LISTING

```
      PROGRAM NPLUS.FOR
C
C     PROGRAM NOTES:
C       1) GAUSSIAN NOISE ADDITION TO SYN SIGNAL OPTION
C       2) PROGRAM REQUIRES 8087 MATH CO-PROCESSOR TO RUN
C       3) ORIGINAL SYNGEN PROGRAM WRITTEN IN BASIC
C          BY DR. M. A. MORGAN
C       4) STWO87FOR PROGRAM WRITTEN IN MSFORTRAN 77
C          BY L. A. CHEEKS
C       5) UPDATE AUG89 BY LT M.S. SIMON
C       6) UPDATE MAR90 BY CAPT T. J. MURPHY
C
C     ***DECLARATIONS***
```

```
C
      REAL T9,T0,A,C9,PI,X0SUM,GSUM,GSUMPRM,R,CDB,X0(1024),R0(100),I0(10
     +0),A0(100),P0(100),G(1024),X1(1024),P,TZ/0.0/,DT1,DT,L2,X02SUM,X02
     +(1024),GADJ,GMEAN
      INTEGER N,Z,I9,I1,NCOUNT
      CHARACTER FN*16,TITLE*16,ANS*1,HEADER*64
      DATA PI/3.1415927/
C
C     ***MAIN BODY OF PROGRAM***
C
C     ***DATA INPUT ROUTINE***
C
170   WRITE(*,*) 'ENTER NAME OF DATA FILE TO BE CORRUPTED'
      READ (*,280) TITLE
      OPEN(1,FILE=TITLE)
      READ (1,260) HEADER
      READ (1,240) NPTS
      READ (1,250) TBEGIN
      READ (1,250) TEND
C
      DO 190 I=1,NPTS
      READ (1,250) X0(I)
190   CONTINUE
      CLOSE(1)
C
      WRITE(*,*)'DONE READING FILE'
C
      X0SUM=0.0
      DO 80 I=1,NPTS
      X0SUM=X0SUM+(X0(I)**2)
80    CONTINUE
C
C     X0SUM/NPTS IS AVERAGE POWER
      X0SUM=X0SUM/NPTS
C
C     ***ROUTINE TO ADD GAUSSIAN NOISE TO SIGNAL***
C
      GSUM=0.0
      GADJ=0.0
      GMEAN=0.0
120   WRITE(*,*)'ENTER SEED FOR RANDOM NUMBER GENERATION FOR NOISE'
      WRITE(*,*)'(0 < R < 1.0)  0.21289 GENERATES A GOOD DISTRIBUTION'
      READ(*,250) R
      DO 130 I=1,NPTS
      CALL CLMT(R,P)
      G(I)=P
      GADJ=GADJ+G(I)
130   CONTINUE
C     ADJUST DISTRIBUTION SO MEAN IS 0
      GMEAN=GADJ/FLOAT(NPTS)
```

```
      DO 135 I=1,NPTS
      G(I)=G(I)-GMEAN
      GSUM=GSUM+(G(I)**2)
135   CONTINUE
C     GSUM/NPTS IS AVERAGE POWER OF GAUSSIAN SIGNAL
      GSUM=GSUM/NPTS
      WRITE(*,*) 'ENTER DESIRED SIGNAL TO NOISE RATIO IN DB'
      READ(*,*) DB
      GSUMPRM=X0SUM/(10.0**(DB/10.0))
      CDB=10.0*ALOG10(X0SUM/GSUMPRM)
      WRITE(*,*) 'CHECK DB =',CDB
      RATIO=SQRT(GSUMPRM/GSUM)
      DO 140 I=1,NPTS
      G(I)=RATIO*G(I)
140   CONTINUE
      DO 150 I=1,NPTS
      X0(I)=X0(I)+G(I)
150   CONTINUE
C
C     ***ROUTINE TO NORMALIZE SYN GEN SIGNAL***
C
155   X02SUM=0.0
      DO 156 I=1,NPTS
      X02(I)=X0(I)**2
      X02SUM=X02SUM+X02(I)
156   CONTINUE
      L2=SQRT(X02SUM)
      DO 160 I=1,NPTS
      X0(I)=X0(I)/L2
160   CONTINUE
C
C
C     ***ROUTINE TO STORE SYN GEN SIGNAL DATA IN DATA FILE***
C

      WRITE(*,*) 'ENTER NAME OF DATA FILE TO CONTAIN CORRUPTED SIGNAL'
      READ (*,280) FN
      WRITE(*,*) 'STORING CORRUPTED SIGNAL DATA IN DATA FILE'
      OPEN(1,FILE=FN)
      WRITE(1,260) HEADER
      WRITE(1,240) NPTS
      WRITE(1,250) TBEGIN
      WRITE(1,250) TEND
C
      DO 17 I=1,NPTS
      WRITE(1,250) X0(I)
17    CONTINUE
      CLOSE(1)
C
240   FORMAT(I5)
```

```
250   FORMAT(E12.6)
260   FORMAT(A64)
270   FORMAT(A8)
280   FORMAT(A16)
      WRITE(*,*) 'CHECK NEW FILE(S)'
      GO TO 170
      STOP
      END
C
C     ***SUBROUTINES***

      SUBROUTINE CLMT(R,P)
C
C     THIS SUBROUTINE IS BASED ON THE CENTRAL LIMIT THEOREM AND
C     GENERATES A SEQUENCE OF INDEPENDANT NUMBERS WHICH ARE
C     NORMALLY DISTRIBUTED ABOUT THE INTERVAL 0 TO 1
C
      REAL P,R
C
      P=0.0
      DO 170 I=1,1000
      CALL STRNUM(R)
      P=P+R
170   CONTINUE
      P=P/1000.0
      RETURN
      END
C
      SUBROUTINE STRNUM(R)
C
C     THIS SUBROUTINE GENERATES A SEQUENCE OF NUMBERS WHICH ARE
C     RANDOMLY AND UNIFORMLY DISTRIBUTED OVER THE UNIT INTERVAL.
C     REF: P. 280 OF FORTRAN: Scientific Subroutine Library
C
C     NOTES:
C     1) R = 0.21289 GENERATES A GOOD UNIFORM DISTRIBUTION
C
      BB=1.0
      P1=R*317.0
      R=AMOD(P1,BB)
      RETURN
      END
```

APPENDIX D. K-PULSE GENERATOR

A. PROGRAM DESCRIPTION

This program creates an K-Pulse filter impulse response after reading a file containing the *s*-plane poles to be annihilated. This program allows scaling of the filter impulse response as well as integer delays bewteen filter weights, each to allow additional degrees of freedom in the filter design. In this thesis, these parameters were set to one.

This program was written by Prof. M. A. Morgan, with susequent modifications by Lt. M. S. Simon and Capt. P. C. Reddy.

B. PROGRAM LISTING

```
      PROGRAM KP
C
C     PROGRAM NOTES
C        1) PROGRAM GENERATES KILL PULSES
C        2) KEYBOARD INPUTS:  POLES/REAL,IMAG
C        3) OUTPUT TO DATA FILE:  K-PULSE TIME SERIES
C        4) PROGRAM REQUIRES 8087 MATH CO-PROCESSOR
C        5) PROGRAM WRITTEN IN MSFORTRAN BY PROF. M.A. MORGAN
C        6) INTERACTIVE MODS BY LT M.S. SIMON
C        7) ADDITONAL MOS BY CAPT P.C. REDDY
C
C     K-Pulse Generation Using Z-Transform Product Non-Recursive
C     Filter Design Approach by M.A. Morgan 8/24/89.
C
      REAL SR(20),SI(20),A(0:100),B(2),H(401),SF
      CHARACTER FNAME*16,TITLE*64,ANS*1,PFNAME*16
      WRITE(*,*) '*** K-PULSE GENERATOR ***'
      WRITE(*,*)
1     WRITE(*,*) 'ENTER NUMBER OF POLE PAIRS (<=50):'
      WRITE(*,*) 'ENTER SCALE FACTOR'
      READ(*,*) SF
```

```
      WRITE(*,*) 'ENTER TIME WINDOW (NANOSEC):'
      READ(*,*) T0
      WRITE(*,*) 'ENTER NUMBER OF TIME POINTS:'
      READ(*,*) NT
      DT=T0/(NT-1.0)
      WRITE(*,*) 'ENTER TIME-STEPS BETWEEN FILTER WEIGHTS (>=1):'
      READ(*,*) KS
      WRITE(*,*) 'ENTER FILENAME OF SPLANE POLES'
      READ(*,100) PFNAME
      OPEN(2,FILE=PFNAME)
      READ(2,*) NP
      DO 11 N=1,NP
      READ(2,*) SR(N)
      READ(2,*) SI(N)
11    CONTINUE
      CLOSE(2)
C
C     INPUT DATA CHECK
C
      WRITE(*,*) ' '
      WRITE(*,*)'INPUT DATA CHECK'
      WRITE(*,*)'NUMBER OF POLE PAIRS IS ',NP
      WRITE(*,*)'SCALE FACTOR IS ',SF
      WRITE(*,*)'TIME WINDOW IS ',T0,' NANOSEC'
      WRITE(*,*)'NUMBER OF TIME POINTS IS ',NT
      WRITE(*,*)'NUMBER OF TIME STEPS BETWEEN FILTER WEIGHTS IS ',KS
      WRITE(*,*)' '
      DO 12 N=1,NP
      WRITE(*,*)'SIGMA ',N,' = ',SR(N)
      WRITE(*,*)'OMEGA ',N,' = ',SI(N)
      PAUSE
12    CONTINUE
13    WRITE(*,*)'IS DATA CORRECT?'
      READ(*,200)ANS
      IF((ANS.EQ.'Y').OR.(ANS.EQ.'y'))THEN
      WRITE(*,*)'DATA CORRECT'
      GO TO 14
      ELSEIF((ANS.EQ.'N').OR.(ANS.EQ.'n'))THEN
      WRITE(*,*)'DATA ERRORS. START AGAIN'
      GO TO 1
      ELSE
      WRITE(*,*)'TRY AGAIN! Y OR N'
      GO TO 13
      ENDIF
C
C     SCALING POLES
C
14    DO 15 N=1,NP
      SR(N)=SR(N)/SF
      SI(N)=SI(N)/SF
```

```
15    CONTINUE
C
C     CALCULATIONS
C
      MP=0
      DO 22 N=1,NP
      E=EXP(KS*SR(N)*DT)
      C=COS(KS*SI(N)*DT)
      B(1)=-2.0*E*C
      B(2)=E*E
      CALL POLY(A,B,MP)
22    CONTINUE
      WRITE(*,*)
      WRITE(*,*) 'UN-NORMALIZED K-PULSE FILTER WEIGHTS:'
      WRITE(*,*)
      DO 33 M=0,MP
      WRITE(*,*) M,A(M)
33    CONTINUE
            PAUSE
C
C     NORMALIZE K-PULSE TO UNIT ENERGY
C
      ENERGY=A(0)**2
      M1=KS*MP+1
      DO 44 M=1,MP
44    ENERGY=ENERGY+A(M)**2
      RMS=SQRT(ENERGY)
C
C     DEFINING UNIT SAMPLE RESPONSE
C
      H(1)=A(0)/RMS
      I=1
      DO 55 N=1,MP
      M=0
50    M=M+1
      I=I+1
      IF(M.GE.KS) GO TO 55
      H(I)=0.0
      GO TO 50
55    H(I)=A(N)/RMS
C
C     STORING K-PULSE IN DATA FILE
C
      TS=0.0
      TF=KS*MP*DT
      WRITE(*,*) 'STORING K-PULSE IN DATA FILE'
      WRITE(*,*)
      WRITE(*,*) 'ENTER OUTPUT FILE (<= 16 CHAR):'
      READ(*,100) FNAME
      WRITE(*,*) 'ENTER HEADER FOR OUTPUT FILE (<= 64 Char):'
```

```
      READ(*,100) TITLE
      OPEN(1,FILE=FNAME)
      WRITE(1,100) TITLE
      WRITE(1,110) M1
      WRITE(1,120) TS
      WRITE(1,120) TF
      DO 66 N=1,M1
      WRITE(1,120) H(N)
66    CONTINUE
88    WRITE(*,*)'K-PULSE GENERATOR PROGRAM COMPLETE'
      WRITE(*,*)'CHECK NEW FILE'
100   FORMAT(A)
110   FORMAT(I5)
120   FORMAT(E12.6)
200   FORMAT(A1)
      STOP
      END
C
      SUBROUTINE POLY(A,B,N)
C
C     MULTIPLYING  {z**2 + B(1)*z + B(2)} x
C     {z**N + A(1)*z**(N-1) + A(2)*z**(N-2) + .... + A(N)} =
C     z**(N+2) + C(1)*z**(N+1) + C(2)*z**N + ....  + C(N+2)
C
C     COMPUTING C(N) COEFFICIENTS AND STORING INTO A(N) WHILE
C     INCREMENTING N --> N + 2
C
      REAL A(0:100),B(2),C(0:100)
      A(0)=1.0
C     INITIALIZE ON FIRST CALL TO ROUTINE
      IF(N.GE.2) GO TO 11
      N=2
      A(1)=B(1)
      A(2)=B(2)
      GO TO 44
11    C(1)=A(1)+B(1)
      DO 22 I=2,N
22    C(I)=A(I)+A(I-1)*B(1)+A(I-2)*B(2)
      C(N+1)=A(N)*B(1)+A(N-1)*B(2)
      C(N+2)=A(N)*B(2)
      N=N+2
      DO 33 I=1,N
33    A(I)=C(I)
44    CONTINUE
      RETURN
      END
```

APPENDIX E. DOUBLE GAUSSIAN SMOOTHING FUNCTION GENERATOR

A. PROGRAM DESCRIPTION

This program creates a double Gaussian smoothing function used to allow the use of the difference equation based K-Pulse filter in the presence the noise. The program uses input values of the ten percent height of the low and high frequency ends of the double Gaussian frequency response to determine the pulse widths in the time domain. The user defines a threshold value to truncate the tails of the double Gaussian function to limit its temporal extent. The program uses the PLTSUB subroutine written by Prof. M. A. Morgan, which uses the Grafmatics FORTRAN graphics package, to create a plot of the result.

This program was originally written by Prof. M. A. Morgan and was modified by Capt. P. C. Reddy.

B. PROGRAM LISTING

```
      PROGRAM DGSMF
C
C     Adaptive Double-Gaussian Smoothing Function Generator
C     By M.A. Morgan 2/22/90; Modified by P.C. Reddy 8/1/90
C
      REAL Y1(1024),DT,T1,T2,F1,F2,TMIN,TMAX,TMAX1,THR
      REAL*8 Y(1024),E1,E2,F(1024),A1,A2,ALFA1,ALFA2,C1,C2
      INTEGER NPTS, N
      CHARACTER*1 YN
      CHARACTER*64 FNAME,TITLE
      WRITE(*,*) 'Enter No. Time Points '
      READ(*,*) NPTS
      TMIN=0.0
      WRITE(*,*)
```

```
      WRITE(*,*) 'Enter Time Window in NSec:  '
      READ(*,*) TMAX
      DT=TMAX/FLOAT(NPTS-1)
44    CONTINUE
      WRITE(*,*) 'Enter Upper 10% Freq Rolloff in GHz  '
      READ(*,*) F1
      T1=1.47/F1
      WRITE(*,*) 'Narrow 10% Pulse Width in NSec:= ',T1
      WRITE(*,*) 'Enter Lower 10% Freq Rolloff in GHz '
      READ(*,*) F2
      WRITE(*,*)
      T2=.31/F2
      WRITE(*,*) 'Wide 10% Pulse Width in NSec:= ',T2
      WRITE(*,*)
      WRITE(*,*) 'Are These Pulse Widths OK ? (Y/N) '
      READ(*,100) YN
      IF(YN.EQ.'N'.OR.YN.EQ.'n') GO TO 44
      WRITE(*,*) 'Enter THRESHOLD '
      READ(*,*) THR
      ALFA1=4*DLOG(10)/T1**2
      ALFA2=4*DLOG(10)/T2**2
      A1=DSQRT(ALFA1)/(DSQRT(ALFA1)-DSQRT(ALFA2))
      A2=A1-1.0
      I=0
      DO 10 K=1,NPTS
      T=(K-1.0-(NPTS/2))*DT
      C1=ALFA1*T**2
      C2=ALFA2*T**2
      IF(C1.GT.THR)THEN
      E1=0.0
      ELSE
      E1=A1*EXP(-C1)
      ENDIF
      IF(C2.GT.THR)THEN
      F(K)=0.0
      GO TO 10
      ELSE
      E2=A2*EXP(-C2)
      ENDIF
      F(K)=E1-E2
9     IF(F(K).NE.0.0)THEN
      I=I+1
      Y(I)=F(K)
      Y1(I)=SNGL(Y(I))
      N=I
      ENDIF
10    CONTINUE
      TMAX1=DT*N
C     EGA Assumed:
      NS=1
```

```
C     Impact Printer Assumed:
      NFD=1
C
      TITLE='DOUBLE-GAUSSIAN SMOOTHING FUNCTION'
      CALL PLTSUB(TITLE,N,TMIN,TMAX1,Y1,NS,NFD)
      WRITE(*,*) 'Do You Want to Store These Results ? (Y/N) '
      READ(*,100) YN
      IF(YN.EQ.'N'.OR.YN.EQ.'n') GO TO 99
      WRITE(*,*) 'Enter File Name for Plot Data Storage: '
      READ(*,100) FNAME
      OPEN(3,FILE=FNAME)
      WRITE(3,100) TITLE
      WRITE(3,110) N
      WRITE(3,120) TMIN
      WRITE(3,120) TMAX1
      DO 88 I=1,N
      WRITE(3,120) Y(I)
88    CONTINUE
      CLOSE(3)
99    CONTINUE
      WRITE(*,*) 'Program Completed'
100   FORMAT(A)
110   FORMAT(I5)
120   FORMAT(E12.6)
      STOP
      END
```

APPENDIX F. SMOOTHED K-PULSE GENERATOR

A. PROGRAM DESCRIPTION

This program is an adapataion of a linear convolution program written by Prof. M. A. Morgan. This program reads two data files and convolves them and normalizes the output waveform energy before depositing the result in user specified data file.

B. PROGRAM LISTING

```
      PROGRAM CVN
C
C     Convolution of PLOT Format Data Files X(n)*Y(n) to Produce
C     Z(n). Provides Local Plotting and PLOT Output File.
C     By M. Morgan, 8/21/89. Modified by P. Reddy, 8/25/90.
C
      REAL X(1024),Y(1024),Z(2048),Z1(2048),TLATE
      CHARACTER*1 ANS, BELL
      CHARACTER*8 FNX,FNY,FNZ
      CHARACTER*64 TITX,TITY,TITZ
C
      BELL=CHAR(7)
C
C     DATA FILE INPUT
C
10    CONTINUE
      WRITE(*,*) 'THIS PROGRAM CONVOLVES X(n) * Y(n) = Z(n)'
      WRITE(*,*) 'AND PLACES Z(n) IN USER SPECIFIED OUTPUT FILE'
      WRITE(*,*)
      WRITE(*,100) BELL
      WRITE(*,*) 'ENTER NAME OF X(n) INPUT FILE'
      WRITE(*,*)
      READ(*,100) FNX
      WRITE(*,*)
      WRITE(*,*) 'X(n) INPUT FILE IS ',FNX
      WRITE(*,*)
      WRITE(*,100) BELL
      WRITE(*,*) 'ENTER NAME OF Y(n) INPUT FILE'
```

```
      WRITE(*,*)
      READ(*,100) FNY
      WRITE(*,*)
      WRITE(*,*) 'Y(n) INPUT FILE IS ';FNY
      WRITE(*,*)
C
C     READING INPUT FILES
C
      OPEN(1,FILE=FNX)
      OPEN(2,FILE=FNY)
      READ(1,100) TITX
      READ(1,120) NX
      READ(1,130) TX1
      READ(1,130) TX2
      DO 20 I=1,NX
      READ(1,130) X(I)
20    CONTINUE
      WRITE(*,*) 'X(t) FILE READ'
      READ(2,100) TITY
      READ(2,120) NY
      READ(2,130) TY1
      READ(2,130) TY2
      DO 30 I=1,NY
      READ(2,130) Y(I)
30    CONTINUE
      WRITE(*,*) 'Y(t) FILE READ'
      WRITE(*,*)
      CLOSE(1)
      CLOSE(2)
C
C     CONVOLUTION ALGORITHM WITHOUT ZERO PADDING
C     Written by M.A. Morgan 5/19/89
C
      WRITE(*,*) 'CONVOLUTION IN PROGRESS'
      WRITE(*,*)
      DO 50 N=1,NY
      Z(N)=0.0
      M2=MIN0(N,NX)
      DO 40 M=1,M2
      Z(N)=Z(N)+X(M)*Y(N-M+1)
40    Z1(N)=Z(N)
50    CONTINUE
      N1=NY+1
      N2=NX+NY-1
      DO 70 N=N1,N2
      Z(N)=0.0
      M1=N+1-NY
      M2=MIN0(N,NX)
      DO 60 M=M1,M2
60    Z(N)=Z(N)+X(M)*Y(N-M+1)
```

```
70    CONTINUE
C
      TZ1=TX1+TY1
      TZ2=TX2+TY2
      ENERGY=0.0
      DO 90 N=1,N2
90    ENERGY=ENERGY+Z(N)*Z(N)
      DO 92 N=1,N2
      Z(N)=Z(N)/SQRT(ENERGY)
92    Z1(N)=Z(N)
      WRITE(*,*)
      PAUSE
C
C     *** Plotting Z(n) ***
      TITZ='Convolution Z(n)=X(n)*Y(n)'
      CALL PLTSUB(TITZ,N2,TZ1,TZ2,TZ1,TZ2,Z1,1,1,0)
C
      WRITE(*,100) BELL
      WRITE(*,*) 'ENTER NAME OF Z(n) FILE'
      WRITE(*,*)
      READ(*,100) FNZ
      WRITE(*,*)
      WRITE(*,*) 'OUTPUT FILE IS ',FNZ
      OPEN(3,FILE=FNZ)
      WRITE(*,*)
      WRITE(*,100) BELL
      WRITE(*,*) 'ENTER HEADER TITLE FOR Z(n) FILE'
      WRITE(*,*)
      READ(*,100) TITZ
      WRITE(*,*)
      WRITE(*,*) 'SAVING Z(t) TO OUTPUT DATA FILE'
      WRITE(3,100) TITZ
      WRITE(3,120) N2
      WRITE(3,130) TZ1
      WRITE(3,130) TZ2
      DO 80 I=1,N2
      WRITE(3,130) Z(I)
80    CONTINUE
      CLOSE(3)
C     QUERY TO DO ANOTHER RUN
C
95    CONTINUE
      WRITE(*,*)
      WRITE(*,100) BELL
      WRITE(*,*) 'DO YOU WISH TO CONVOLVE ADDITIONAL WAVEFORMS?'
      WRITE(*,*)
      READ(*,100) ANS
      IF((ANS.EQ.'Y').OR.(ANS.EQ.'y')) THEN
      GO TO 10
      ELSEIF((ANS.EQ.'N').OR.(ANS.EQ.'n')) THEN
```

```
      GO TO 99
      ELSE
      WRITE(*,*) 'TRY AGAIN! "Y" OR "N".'
      GO TO 95
      ENDIF
99    CONTINUE
      WRITE(*,100) BELL
      WRITE(*,*) 'CONVOLUTION PROGRAM IS OVER.  CHECK NEW FILE(S)'
100   FORMAT(A)
120   FORMAT(I5)
130   FORMAT(E12.3)
STOP
END
```

APPENDIX G. K-PULSE CONVOLUTION PROGRAM

A. PROGRAM DESCRIPTION

This program is an adapataion of a linear convolution program wriiten by Prof. M. A. Morgan. This program reads two data files and convolves them and calculates the average energy over a specified time of the output record. The program plots the result and deposits it in a user specified data file. This program was modified by Capt. P. C. Reddy.

B. PROGRAM LISTING

```
      PROGRAM CV2
C
C     Convolution of PLOT Format Data Files X(n)*Y(n) to Produce
C     Z(n).   Provides Local Plotting and PLOT Output File Along
C     With Late-Time Energy Calculation.
C     By M. Morgan, 8/21/89.  Modified by P. Reddy, 8/25/90.
C
      REAL X(1024),Y(1024),Z(2048),Z1(2048),TLATE
      CHARACTER*1 ANS, BELL
      CHARACTER*8 FNX,FNY,FNZ
      CHARACTER*64 TITX,TITY,TITZ
C
      BELL=CHAR(7)
C
C     DATA FILE INPUT
C
10    CONTINUE
      WRITE(*,*) 'THIS PROGRAM CONVOLVES X(n) * Y(n) = Z(n)'
      WRITE(*,*) 'AND PLACES Z(n) IN USER SPECIFIED OUTPUT FILE'
      WRITE(*,*)
      WRITE(*,100) BELL
      WRITE(*,*) 'ENTER NAME OF X(n) INPUT FILE'
      WRITE(*,*)
      READ(*,100) FNX
      WRITE(*,*)
      WRITE(*,*) 'X(n) INPUT FILE IS ',FNX
```

```
      WRITE(*,*)
      WRITE(*,100) BELL
      WRITE(*,*) 'ENTER NAME OF Y(n) INPUT FILE'
      WRITE(*,*)
      READ(*,100) FNY
      WRITE(*,*)
      WRITE(*,*) 'Y(n) INPUT FILE IS ',FNY
      WRITE(*,*)
C
C     READING INPUT FILES
C
      OPEN(1,FILE=FNX)
      OPEN(2,FILE=FNY)
      READ(1,100) TITX
      READ(1,120) NX
      READ(1,130) TX1
      READ(1,130) TX2
      DO 20 I=1,NX
      READ(1,130) X(I)
20    CONTINUE
      WRITE(*,*) 'X(t) FILE READ'
      READ(2,100) TITY
      READ(2,120) NY
      READ(2,130) TY1
      READ(2,130) TY2
      DO 30 I=1,NY
      READ(2,130) Y(I)
30    CONTINUE
      WRITE(*,*) 'Y(t) FILE READ'
      WRITE(*,*)
      CLOSE(1)
      CLOSE(2)
C
C     CONVOLUTION ALGORITHM WITHOUT ZERO PADDING
C     Written by M.A. Morgan 5/19/89
C
      WRITE(*,*) 'CONVOLUTION IN PROGRESS'
      WRITE(*,*)
      DO 50 N=1,NY
      Z(N)=0.0
      M2=MIN0(N,NX)
      DO 40 M=1,M2
      Z(N)=Z(N)+X(M)*Y(N-M+1)
40    Z1(N)=Z(N)
50    CONTINUE
      N1=NY+1
      N2=NX+NY-1
      DO 70 N=N1,N2
      Z(N)=0.0
      M1=N+1-NY
```

```
      M2=MIN0(N,NX)
      DO 60 M=M1,M2
      Z(N)=Z(N)+X(M)*Y(N-M+1)
60    Z1(N)=Z(N)
70    CONTINUE
C
C     CALCULATING LATE-TIME ENERGY
C
83    TZ1=TX1+TY1
      TZ2=TX2+TY2
      WRITE(*,*)
      WRITE(*,*) 'ENTER TL (Nsec) FOR LATE-TIME ENERGY CALCULATION'
      WRITE(*,*)
      READ(*,*) TLATE
      WRITE(*,*) 'ENTER TZ3 (Nsec) FOR END OF'
      WRITE(*,*) 'LATE-TIME ENERGY CALCULATION'
      WRITE(*,*)
      READ(*,*) TZ3
      NLATE=NINT(TLATE*N2/(TZ2-TZ1))+1
      N3=NINT(TZ3*N2/(TZ2-TZ1))+1
      IF(NLATE.LT.N2) GO TO 85
      WRITE(*,100) BELL
      WRITE(*,*) 'TLATE TOO LARGE - TRY AGAIN'
      GO TO 83
85    CONTINUE
      IF(NLATE.GE.1) GO TO 87
      WRITE(*,100) BELL
      WRITE(*,*) 'TLATE TOO SMALL - TRY AGAIN'
      GO TO 83
87    CONTINUE
      ENERGY=0.0
      DO 90 N=NLATE,N3
90    ENERGY=ENERGY+Z(N)*Z(N)
      ENERGY=ENERGY/(N3-NLATE+1)
      WRITE(*,*)
      WRITE(*,*) 'LATE TIME ENERGY =', ENERGY
      PAUSE
C
C     *** Plotting Z(n) ***
      TITZ='Convolution Z(n)=X(n)*Y(n)'
      CALL PLTSUB(TITZ,N2,TZ1,TZ2,TZ1,TZ2,Z1,1,1,0)
C
      WRITE(*,100) BELL
      WRITE(*,*) 'ENTER NAME OF Z(n) FILE'
      WRITE(*,*)
      READ(*,100) FNZ
      WRITE(*,*)
      WRITE(*,*) 'OUTPUT FILE IS ',FNZ
      OPEN(3,FILE=FNZ)
      WRITE(*,*)
```

```
      WRITE(*,100) BELL
      WRITE(*,*) 'ENTER HEADER TITLE FOR Z(n) FILE'
      WRITE(*,*)
      READ(*,100) TITZ
      WRITE(*,*)
      WRITE(*,*) 'SAVING Z(t) TO OUTPUT DATA FILE'
      WRITE(3,100) TITZ
      WRITE(3,120) N2
      WRITE(3,130) TZ1
      WRITE(3,130) TZ2
      DO 80 I=1,N2
      WRITE(3,130) Z(I)
80    CONTINUE
      CLOSE(3)
C     QUERY TO DO ANOTHER RUN
C
95    CONTINUE
      WRITE(*,*)
      WRITE(*,100) BELL
      WRITE(*,*) 'DO YOU WISH TO CONVOLVE ADDITIONAL WAVEFORMS?'
      WRITE(*,*)
      READ(*,100) ANS
      IF((ANS.EQ.'Y').OR.(ANS.EQ.'y')) THEN
      GO TO 10
      ELSEIF((ANS.EQ.'N').OR.(ANS.EQ.'n')) THEN
      GO TO 99
      ELSE
      WRITE(*,*) 'TRY AGAIN! "Y" OR "N".'
      GO TO 95
      ENDIF
99    CONTINUE
      WRITE(*,100) BELL
      WRITE(*,*) 'CONVOLUTION PROGRAM IS OVER.  CHECK NEW FILE(S)'
100   FORMAT(A)
120   FORMAT(I5)
130   FORMAT(E12.6)
      STOP
      END
```

APPENDIX H. INVERSE ARMA PROGRAM

A. PROGRAM DESCRIPTION

This program implements an inverse ARMA aspect dependent annihilation filter. As such, it is an adaptation of the ARMA signal generator in Appendix B. It requires input of the a_k and b_k coefficients for the target transfer function it is intended to annihilate. It then creates the inverse impulse response and convolves it with an input data record. Finally, it computes the average energy over a user specified time period in the output.

This program was written by Prof. M. A. Morgan and modified by Capt. P. C. Reddy.

B. PROGRAM LISTING

```
      Program IARMA
C
C     Reading N-th order ARMA filter with coefficients:
C
C           IIR  a(k) for k=1,N
C           FIR  b(k) for k=0,L
C
C     Processing y[n] using the inverse ARMA filter with output
C     z[n].  Inverse ARMA has coefficients:
C
C           IIR  ai(k)=-b(k)/b(0) for k=1,L
C           FIR  bi(k)=-a(k)/b(0) for k=1,N
C              bi(0)=  1.0/b(0)
C
C     by M.A. Morgan 5/24/90
C     Modified by P.C. Reddy 5/27/90
C
      REAL*8 y(0:2047),z(0:2047)
      REAL*8 a(1:30),b(0:32),ai(1:30),bi(0:30)
```

```
      CHARACTER*64 TITLE,TITL
      CHARACTER*16 FNAME
C     Entering D.E. Coefficients
      WRITE(*,*) 'Enter Filename For Recursive a(k):'
      WRITE(*,*) 'Use 0 for FIR Filter'
      READ(*,100) FNAME
      IF(FNAME.EQ.'0') GO TO 15
      OPEN(2,FILE=FNAME)
C     Assuming that a(k) are reversed polarity in file.
      READ(2,110) N
      write(*,*) 'Write k, a(k):'
      DO 11 k=1,N
      READ(2,*) a(k)
      a(k)=-a(k)
C     write(*,*) k,a(k)
11    CONTINUE
      CLOSE(2)
15    CONTINUE
      WRITE(*,*) 'Enter Filename for Non-Recursive b(k):'
      READ(*,100) FNAME
      OPEN(2,FILE=FNAME)
      READ(2,110) L
C     write(*,*) 'Write k, b(k):'
      DO 22 k=0,L
      READ(2,*) b(k)
C     write(*,*) k,b(k)
22    CONTINUE
      CLOSE(2)
      WRITE(*,*) 'Enter Filename for y[n] Plot File:'
      READ(*,100) FNAME
      OPEN(2,FILE=FNAME
      READ(2,100) TITL
      READ(2,110) NY
      READ(2,120) XQ
      READ(2,120) XQ
      DO 24 m=0,NY-1
      READ(2,120) y(m)
24    CONTINUE
      CLOSE(2)
      WRITE(*,*)
C     Setting up Plot File for z[n]
      WRITE(*,*) 'Enter Number of Points for z[n]: (.le. 2048)'
      READ(*,*) NZ
      WRITE(*,*) 'Enter time interval (nanoseconds)'
      READ(*,*) Tmax
      Tmin=0.0
      WRITE(*,*) 'Enter filename for z[n] response output'
      READ(*,100) FNAME
      TITLE= 'Inverse ARMA Filter z[n] Response'
      OPEN(1,FILE=FNAME)
```

```
      WRITE(1,100) TITLE
      WRITE(1,110) NZ
      WRITE(1,120) Tmin
      WRITE(1,120) Tmax
C     Generating Inverse Filter Coefficients
C     Assuming b(0) .ne. 0 !!!
      Li=N
      Ni=L
      DO 50 k=1,Ni
50    ai(k)=-b(k)/b(0)
      bi(0)=1.0D00/b(0)
      DO 55 k=1,Li
55    bi(k)=-a(k)/b(0)
      WRITE(*,*)
C     Initializing then iterating to form z[m]
      z(0)=bi(0)*y(0)
      write(1,120) z(0)
      DO 77 m=1,NZ-1
      z(m)=0.0
      Lmax=MIN(m,Li)
      DO 60 k=0,Lmax
      IF((m-k).GE.NY) GO TO 60
      z(m)=z(m)+bi(k)*y(m-k)
60    Continue
      Nmax=MIN(m,Ni)
      DO 66 k=1,Nmax
66    z(m)=z(m)+ai(k)*z(m-k)
C     write(*,*) z(m)
      WRITE(1,120) z(m)
77    CONTINUE
      CLOSE(1)
C
C     CALCULATING LATE-TIME ENERGY
C

      WRITE(*,*) 'ENTER TL (Nsec) FOR LATE-TIME ENERGY CALCULATION'
      WRITE(*,*)
      READ(*,*) TLATE
      WRITE(*,*) 'ENTER TE (Nsec) FOR LATE-TIME ENERGY CALCULATION'
      WRITE(*,*)
      READ(*,*) TE
      NLATE=NINT((TLATE/Tmax)*NZ)+1
      NE=NINT((TE/Tmax)*NZ)+1
      ENERGY=0.0
      DO 90 N=NLATE,NE
90    ENERGY=ENERGY+Z(N)*Z(N)
      ENERGY=ENERGY/(NE-NLATE+1)
      WRITE(*,*)
      WRITE(*,*) 'LATE TIME ENERGY =', ENERGY
      WRITE(*,*) 'Thats All Folks !'
```

```
100   FORMAT(A)
110   FORMAT(I5)
120   FORMAT(E12.6)
      STOP
      END
```

LIST OF REFERENCES

1. C. E. Baum, "On the singularity expansion method for the solution of electromagnetic interaction problems," Air Force Weapons Laboratory Interaction Note 88, December 1971.

2. D. L. Moffat and R. K. Mains, "Detection and discrimination of radar targets," *IEEE Transactions on Antennas and Propagation*, Vol. AP-23, May 1975, pp. 358-367.

3. Michael A. Morgan, "Singularity expansion representations of fields and currents in transient scattering," *IEEE Transactions on Antennas and Propagation*, Vol. AP-32, No. 5, May 1984, pp 466-473.

4. Scott A. Norton, "Radar target classification by natural resonances: signal processing algorithms," Engineer's thesis, Naval Postgraduate School, Monterey, California, 1988.

5. King Wai Jean, "Radar target identification by natural resonance cancellation," Master's thesis, Naval Postgraduate School, Monterey, California, 1984.

6. Timothy J. Murphy, "Natural resonance extraction and annihilation filtering methods for radar target identification," Master's thesis, Naval Postgraduate School, Monterey, California, September, 1990.

7. M. A. Morgan, "Scatterer discrimination based upon natural resonance annihilation," *Journal of Electromagnetic Waves and Applications*, Vol. 2, No. 5/6, 1988, pp. 481-502.

8. Barbara L. Merchant, *et al.*, "Complex pole patterns of the scattering amplitude for conducting spheroids and finite-length cylinders," *IEEE Transactions on Antennas and Propagation*, Vol. 36, No. 12, December 1988, pp. 1769-1778.

9. Peter David Larison, "Evaluation of system identification algorithms for aspect-independent radar target classification," Master's thesis, Naval Postgraduate School, Monterey, California, 1989.

10. Martin S. Simon, "A comparison of the K-Pulse and E-Pulse techniques for aspect independent radar target identification," Master's thesis, Naval Postgraduate School, Monterey, California, 1989.

11. Frederick M. Tesche, "On the analysis of scattering and antenna problems using the Singularity Expansion technique," *IEEE Transactions on Antennas and Propagation*, Vol. AP-21, No. 1, January, 1973, pp. 53-62.

12. Michael L. Van Blaricum and Raj Mittra, "A technique for extracting the poles and residues of a system directly from its transient response," *IEEE Transactions on Antennas and Propagation*, Vol. AP-23, No. 6, November 1975, pp. 777-781.

13. Michael L. Van Blaricum and Raj Mittra, "Problems and solutions with Prony's method for processing transient data," *IEEE Transactions on Antennas and Propagation*, Vol. AP-26, No. 1, January 1978, pp. 174-182.

14. Choong Y. Chong, "Investigation of non-linear estimation of natural resonances in target identification," Master's thesis, Naval Postgraduate School, Monterey, California, 1983.

15. Ramdas Kumaresan and Donald W. Tufts, "Estimating the parameters of exponentially damped sinusoids and pole-zero modeling in noise," *IEEE Transactions on Acoustics, Speech, and Signal Processing*, Vol. ASSP-30, No. 6, December, 1982, pp. 833-840.

16. James A. Cadzow and Otis M. Solomon, Jr., "Algebraic approach to system identification," *IEEE Transactions on Acoustics, Speech, and Signal Processing*, Vol. ASSP-34, No. 3, June 1986, pp. 462-469.

17. James B. Dunavin, "Identification of scatterers based on annihilation of complex natural resonances," Master's thesis, Naval Postgraduate School, Monterey, California, 1985.

18. Edward M. Kennaugh, "The K-Pulse concept," *IEEE Transactions on Antennas and Propagation*, Vol. AP-29, No. 2, March, 1981, pp. 327-331.

19. Kun-Mu Chen, *et al.*, "Radar target discrimination by convolution of radar return with Extinction-Pulses and single-mode extraction signals," *IEEE Transactions on Antennas and Propagation*, Vol. AP-34, No. 7, July, 1986, pp. 896-904.

20. Michael A. Morgan, *Time-Domain Thin-Wire Integral Equation Program*, Naval Postgraduate School, Monterey, California, 1989.

21. Norman J. Walsh, "Bandwidth and signal-to-noise ratio enhancement of the NPS Transient Electromagnetic Scattering Laboratory," Master's thesis, Naval Postgraduate School, Monterey, California, 1989.

22. Robert D. Strum and Donald E. Kirk, *First Principles of Discrete Systems and Digital Signal Processing*, Addison-Wesley, Reading, Massachusetts, 1989.

23. John W. R. Taylor, ed., *Jane's All the World's Aircraft 1962/63*, p. 296, Sampson Low, Martson & Co. Ltd, London, 1963.

24. John W. R. Taylor, ed., *Jane's All the World's Aircraft 1988/89*, pp. 244, 426, 429, Jane's Information Group, Inc., Alexandria, Virginia, 1989.

25. J. R. Auton, "Resonance-based target identification systems," Preliminary draft, March 1990 (unpublished).

26. Michael A. Morgan, Unpublished notes, 1990.

27. Michael A. Morgan and Brent W. McDaniel, "Transient electromagnetic scattering: data acquisition and signal processing," *IEEE Transactions on Instrumentation and Measurement*, Vol. 37, No. 2, June 1988, pp. 263-267.

28. Wilbur R. Vincent, "Radio noise and interference," in *Reference Data for Engineers: Radio, Electronics, Computer, and Communications*, Edward C. Jordan, ed., pp. 34.2–34.13, Howard W. Sams & Company, Indianapolis, 1989.

29. Michael A. Morgan, Unpublished notes, 1989.

30. Merrill I. Skolnik, *Introduction to Radar Systems*, McGraw-Hill, New York, 1980.

31. George H. Millman and Gary R. Nelson, "Surface Wave HF radar for Over-the-Horizon detection," *IEEE International Radar Conference*, pp. 106-112, IEEE, 1980.

32. G. T. Ruck, "Ellipsoids and Ogives," in *Radar Cross Section Handbook*, George T. Ruck, and others, eds., Plenum Press, New York, 1970.

33. Robert E. Collin, *Antennas and Radiowave Propagation*, McGraw-Hill, New York, 1985.

34. Douglass D. Crombie, "Frequency Data" in *Reference Data for Engineers: Radio, Electronics, Computer, and Communications*, Edward C. Jordan, ed., Howard W. Sams & Company, Indianapolis, 1989.

35. Michael A. Morgan, Unpublished notes, 1990.

INITIAL DISTIBUTION LIST

		No. Copies
1.	Defense Technical Information Center Cameron Station Alexandria, Virginia 22304-6145	2
2.	Library, Code 52 Naval Postgraduate School Monterey, California 93943-5002	2
3.	Department Chairman, Code EC Department of Electrical and Computer Engineering Naval Postgraduate School Monterey, California 93943-5000	1
4.	Professor Joseph Sternberg, Code NS/Sn Electronic Warfare Academic Group Naval Postgraduate School Monterey, California 93943-5100	1
5.	Professor Michael A. Morgan, Code EC/Mw Department of Electrical and Computer Engineering Naval Postgraduate School Monterey, California 93943-5000	5
6.	Commandant of the Marine Corps Code TE 06 Headquarters, U. S. Marine Corps Washington, D. C. 20380-0001	1

7. Dr. Rabiner Madan — 1
Code 1114SE
Office of Naval Research
800 N. Quincy Street
Arlington, Virginia 22217

8. Dr. John Entzminger — 1
Director, Tactical Technology Office
Defense Advanced Research Projects Agency
1400 Wilson Blvd.
Arlington, Virginia 22209

9. Dr. Bill Pala — 1
Code 5316
Naval Research Laboratory
4555 Overlook Ave., N. W.
Washington, D. C. 20375

10. Joint Electronic Warfare Center — 1
Code SE
Kelly AFB
San Antonio, Texas 78243-5000

11. Capt. Peter C. Reddy, USMC — 1
20 Wells Rd.
Stafford, Virginia 22554